Supporting Information for:

Spin Orbit Charge Transfer Intersystem Crossing (SOCT-ISC) in Bodipy-Phenoxazine Dyads: Effect of the Chromophore Orientation and Conformation Restriction On the Photophysical Properties

Yu Dong [†§] *Andrey A. Sukhanov,* [¶§] *Jianzhang Zhao* [*,†,‡] *Ayhan Elmali,* [⊥] *Xiaolian Li,* [†,*] *Bernhard Dick,* [*,#] *Ahmet Karatay* [*,⊥] *and Violeta K. Voronkova* [*,¶]

[†] State Key Laboratory of Fine Chemicals, School of Chemical Engineering, Dalian University of Technology, E-208 West Campus, 2 Ling Gong Road, Dalian 116024, P. R. China. E-mail: zhaojzh@dlut.edu.cn (J.Z.) xlianli@dlut.edu.cn (X. L.)

[¶] Zavoisky Physical-Technical Institute, FRC Kazan Scientific Center of Russian Academy of Sciences, Kazan 420029, Russia. E-mail: vio@kfti.knc.ru

[‡] School of Chemistry and Chemical Engineering, and Key Laboratory of Energy Materials Chemistry, Institute of Applied Chemistry, Xinjiang University, Urumqi 830046, China.

[#] Lehrstuhl für Physikalische Chemie, Institut für Physikalische und Theoretische Chemie, Universität Regensburg, Universitätsstr. 31, D-93053 Regensburg, Germany. E-mail: Bernhard.Dick@chemie.uni-regensburg.de

[⊥] Department of Engineering Physics, Faculty of Engineering, Ankara University, 06100 Beşevler, Ankara, Turkey. Email: Ahmet.Karatay@eng.ankara.edu.tr

[§] Y. D. and A. A. S. contributed equally to this work.

Index

1. Synthesis Procedures

*Synthesis of Compound **1***.[S1] *n*-C_4H_9Br (247.0 mg, 1.80 mmol), phenoxazine (300.0 mg, 1.64 mmol) and KOH (137 mg, 2.46 mmol) were dissolved in dry DMSO (20 mL) and the mixture were stirred at RT for 12 h under N_2 atmosphere. Then DCM was added and the mixture was washed with water, the organic layer was isolated, dried over anhydrous Na_2SO_4 and concentrated under reduced pressure. The crude product was purified by column chromatography (silica gel, PE/DCM = 10/1, v/v) to give **1** as colorless oil (235.0 mg, yield: 60%). ^1H NMR (400 MHz, $CDCl_3$): δ = 7.44–7.42 (m, 1H), 6.81–6.47 (m, 8H), 3.51 (s, 2H), 1.69–1.62 (m, 2H), 1.50–1.41 (m, 2H), 1.02 (t, 3H, J = 6.0 Hz). ESI–HRMS: *m/z* $[M]^+$ Calcd for $C_{16}H_{18}NO^+$: 240.1389, found: 240.1373.

*Synthesis of Compound **2***.[S1] Under N_2 atmosphere, DMF (220.0 mg, 3.0 mmol) was added dropwise to phosphorus oxychloride (837 mg, 5.47 mmol) at 0 °C, the mixture was stirred for 0.5 h. Solution of compound **1** (500 mg, 2.09 mmol) in dichloromethane (20 mL) was added dropwise into the reaction mixture at 0 °C. Then the mixture was slowly warmed to RT and stirred for 2 h. 1.0 M NaOH aqueous solution was added slowly into the mixture to bring the pH value to 7. The mixture was extracted with DCM, the organic layers were combined, dried over anhydrous Na_2SO_4 and concentrated under reduced pressure. The crude product was purified by column chromatography (silica gel, PE/DCM = 2/1, v/v) to give compound **2** as yellow oil (360.0 mg, yield: 65%). ^1H NMR (400 MHz, $CDCl_3$): δ = 9.66 (s, 1H), 7.31 (dd, 1H, J = 4.0 Hz), 7.08 (d, 2H, J = 4.0 Hz), 6.84–6.80 (m, 1H), 6.75–6.71 (m, 1H), 6.67–6.64 (m, 1H), 6.55–6.50 (m, 2H), 3.54 (t, 2H, J = 8.0 Hz), 1.71–1.63 (m, 2H), 1.52–1.43 (m, 2H), 1.03 (t, 3H, J = 8.0 Hz). ESI–HRMS: *m/z* $[M]^+$ Calcd for $C_{17}H_{18}NO_2^+$: 268.1338, found: 268.1336.

*Synthesis of Compound **3***.[S2] Phenoxazine (183.0 mg, 1.0 mmol) was dissolved in THF (10 mL). Solution of *N*-bromosuccinimide (NBS. 126.0 mg, 1.0 mmol) in THF (10 mL) was added dropwise into the above solution at 0 °C under N_2 atmosphere. The reaction progress was monitored by TLC, after completion of the reaction, water was added into the mixture to quench the reaction. The solvent was removed under reduced pressure and the crude product was purified by column chromatography (silica gel, PE/EA = 10/1, v/v) to give compound **3** as light green solid (78.6 mg, yield: 30%). ^{1}H NMR (400 MHz, $CDCl_3$): δ = 6.82–6.75 (m, 7H). ESI–HRMS: *m/z* $[M+H]^+$ Calcd for $C_{12}H_8BrNO^+$: 260.9789, found: 260.9786.

*Synthesis of Compound **4***.[S1] Compound **4** was prepared with the method similar to that of compound **1**, 339 mg, yield: 65%. ^{1}H NMR (400 MHz, $CDCl_3$): δ = 6.87 (dd, 1H, J = 8.0 Hz), 6.82–6.78 (m, 1H), 6.74 (s, 1H), 6.62–6.60 (m, 2H), 6.47 (d, 1H, J = 8.0 Hz), 6.30 (d, 1H, J = 8.0 Hz), 3.45 (s, 2H), 1.66–1.58 (m, 2H), 1.48–1.39 (m, 2H), 1.00 (t, 3H, J = 6.0 Hz). ESI–HRMS: *m/z* $[M+H]^+$ Calcd for $C_{16}H_{17}BrNO^+$: 318.0494, found: 318.0438.

*Synthesis of Compound **5***. [S2] Compound **4** (317 mg, 1 mmol), bis(pinacolato)diboron (559 mg, 2.2 mmol), potassium acetate (490 mg, 5 mmol) and $Pd(PPh_3)_2Cl_2$ (35 mg, 0.05 mmol) were dissolved in toluene (20 mL) under N_2, then the mixture was refluxed for 8 h. The mixture was cooled to RT and the solvent was removed under reduced pressure. The mixture was extracted with DCM, the organic layers were combined, dried over anhydrous Na_2SO_4 and concentrated under reduced pressure. The crude product was purified by column chromatography (silica gel, PE/DCM = 1/1, v/v) to give compound **5** as green oil (190.0 mg, yield: 52%). ^{1}H NMR (400 MHz, DMSO-d_6): δ = 7.15 (dd, 1H, J = 8.0 Hz), 6.85–6.78 (m, 2H), 6.70–6.61 (m, 4H), 3.55 (t, 2H, J = 8.0 Hz), 1.56–1.48 (m, 2H), 1.45–1.36 (m, 2H), 1.26 (s, 12H), 0.94 (t, 3H, J = 8.0 Hz). ^{13}C NMR (100 MHz, DMSO-d_6): δ = 144.69, 143.93, 136.31, 134.85, 132.70, 131.78, 124.50, 121.77,

120.39, 115.59, 112.72, 111.91, 83.82, 43.04, 26.95, 25.10, 19.8, 14.24. ESI–HRMS: *m/z* $[M+H]^+$ Calcd for $C_{22}H_{29}BN_6O_3^+$: 366.2241, found: 366.2235.

Synthesis of Compound ***6***.[S3] Compound **BDP-1** (324 mg, 1 mmol) was dissolved in DCM (50 mL). *N*-iodosuccinimide (NIS. 225 mg, 1 mmol) was dissolved in THF (10 mL) and the solution was added dropwise into the mixture at 0 °C under N_2. Water was added into the mixture after 10 min. THF was removed under reduced pressure and the mixture was extracted with DCM, the organic layers were combined, dried over anhydrous Na_2SO_4 and concentrated under reduced pressure. The crude product was purified by column chromatography (silica gel, PE/DCM = 2/1, v/v) to give compound **6** as red solid (234 mg, yield: 52%). ^{1}H NMR (400 MHz, $CDCl_3$): δ = 7.52–7.48 (m, 3H), 7.27–7.25 (m, 3H), 6.04 (s, 1H), 2.63 (s, 3H), 2.57 (s, 3H), 1.38 (s, 6H). TOF–HRMS: *m/z* $[M]^+$ Calcd for $C_{19}H_{18}BF_2N_2I^+$: 450.0576, found: 450.0575.

Synthesis of Compound 7. Compound **BDP-2** (134 mg, 0.5 mmol) was dissolved in DCM/MeOH (50 mL, 1/1, v/v). Under N_2, iodine monochloride (ICl. 82 mg, 0.5 mmol) was dissolved in MeOH (10 mL) and the solution was added dropwise into the reaction mixture at 0 °C. Then the reaction was under 0 °C for 1 h and $Na_2S_2O_4$ solution was added into the system. MeOH was removed under reduced pressure and the mixture was extracted with DCM, the organic layers were combined, dried over anhydrous Na_2SO_4 and concentrated under reduced pressure. The crude product was purified by column chromatography (silica gel, PE/DCM = 2/1, v/v) to give compound **7** as red solid (124 mg, yield: 63%). ^{1}H NMR (400 MHz, $CDCl_3$): δ = 8.00 (s, 1H), 7.85 (s, 1H), 7.63–7.52 (m, 5H), 7.02–7.01 (m, 2H), 6.01 (d, 1H, J = 4.0 Hz). ^{13}C NMR (100 MHz, $CDCl_3$): δ = 146.79, 146.59, 145.99, 136.16, 135.19, 133.36, 133.20, 130.45, 128.63, 119.66, 119.37. TOF–HRMS: *m/z* $[M]^+$ Calcd for $C_{15}H_{10}BF_2N_2I^+$: 393.9950, found: 393.9957.

Synthesis of Compound ***8***.[S4,S5] Compound phenoxazine (549.0 mg, 3 mmol), 4-bromobenzaldehyde (617 mg, 3.38 mmol), Cs_2CO_3 (2.44 g, 14.6 mmol), tri-tert-butylphosphine (TTBP, 0.7 mL, 2.98 mmol) and $Pd(OAc)_2$ (50 mg) were dissolved in toluene under N_2. Then the reaction mixture was refluxed for 12 h. The reaction mixture was cooled to RT and toluene was removed under reduced pressure, the residual was extracted with DCM, the organic layers were combined, dried over anhydrous Na_2SO_4 and concentrated under reduced pressure. The crude product was purified by column chromatography (silica gel, PE/DCM = 2/1, v/v) to give compound **8** as yellow solid (575 mg, yield: 66%). ^{1}H NMR (400 MHz, $CDCl_3$): δ = 10.11 (s, 1H), 8.12 (d, 2H, J = 8.0 Hz), 7.56 (d, 2H, J = 8.0 Hz), 6.74–6.88 (m, 4H), 6.64–6.60 (m, 2H), 5.96 (d, 2H, J = 8.0 Hz). ESI–HRMS: *m/z* $[M+H]^+$ Calcd for $C_{19}H_{14}NO_2^+$: 288.1025, found: 288.1018.

Synthesis of ***BDP-PXZ-3***. Compound **6** (100 mg, 0.22 mmol), **5** (120 mg, 0.33 mmol), $Pd(PPh_3)_4$ (26 mg, 0.022 mmol) and K_2CO_3 (138 mg, 1 mmol) were dissolved in mixed solvent toluene/EtOH/H_2O (25 mL, 2:1:1, v/v) under N_2 atmosphere. Then the mixture was refluxed for 4 h and the solution was concentrated under reduced pressure and dissolved in DCM and washed by water (3×100 mL). The organic layers were combined, dried over anhydrous Na_2SO_4 and concentrated under reduced pressure. The crude product was purified by column chromatography (silica gel, PE/DCM = 3/1, v/v) to give **BDP-PXZ-3** as red solid (124 mg, yield: 88%). M.p. 208.6–210.9 °C. ^{1}H NMR (400 MHz, $CDCl_3$): δ = 7.49–7.47 (m, 3H, J = 8.0 Hz), 7.31 (d, 2H, J = 8.0 Hz), 6.78–6.43 (m, 7H), 5.99 (s, 1H), 3.54 (s, 2H), 2.58–2.55 (m, 6H), 1.64 (s, 2H), 1.48–1.42 (m, 2H), 1.38 (s, 3H), 1.31 (s, 3H), 1.01 (t, 3H, J = 6.0 Hz). ^{13}C NMR (100 MHz, $CDCl_3$): δ = 155.27, 135.27, 129.15, 128.95, 128.04, 125.26, 121.20, 121.89, 110.97, 20.18, 14.60, 14.38, 13.90, 12.73. ESI–HRMS: *m/z* [M+H]+ Calcd for $C_{35}H_{35}BF_2N_3O$+: *m/z* = 562.2842, found: *m/z* = 562.2830.

*Synthesis of **BDP-PXZ-4**.* **BDP-PXZ-4** was prepared by similar method to that used for **BDP-PXZ-3**. Dark green solid was obtained (15.4 mg, yield: 12%). M.p. 221.8–222.8 °C. ^{1}H NMR (400 MHz, $CDCl_3$): δ = 8.20 (s, 1H), 7.91 (s, 1H), 7.63–7.53 (m, 5H), 6.98–6.90 (m, 3H), 6.81–6.77 (m, 2H), 6.66–6.59 (m, 2H), 6.54–6.52 (m, 1H), 6.49–6.44 (m, 2H), 3.49 (t, 2H, J = 8.0 Hz), 1.68–1.62 (m, 2H), 1.49–1.42 (m, 2H), 1.01 (t, 3H, J = 6.0 Hz). ^{13}C NMR (100 MHz, $CDCl_3$): δ = 146.18, 143.31, 142.33, 135.79, 133.92, 130.82, 130.69, 130.49, 128.51, 124.08, 123.76, 120.60, 118.08, 115.39, 111.42, 20.16, 13.89. MALDI–TOF–HRMS: *m/z* [M]+ Calcd for $C_{31}H_{26}BF_2N_3O$+: *m*/*z* = 505.2137, found: *m*/*z* = 505.2154.

*Synthesis of **BDP-PXZ-5**.* **BDP-PXZ-5** was prepared by a method similar to that of **BDP-PXZ-1**. Orange solid was obtained (141 mg, yield: 14%). M.p. > 250 °C. ^{1}H NMR (500 MHz, $CDCl_3$): δ = 7.54 (dd, 4H, J = 10.0 Hz), 6.73–6.72 (m, 2H), 6.70–6.66 (m, 2H), 6.63–6.59 (m, 2H), 6.05 (s, 2H), 5.91–5.90 (m, 2H), 2.58 (s, 6H), 1.56 (s, 6H). ^{13}C NMR (100 MHz, $CDCl_3$): δ = 155.99, 144.00, 142.65, 140.38, 139.65, 135.47, 133.94, 131.99, 131.15, 123.30, 121.73, 121.63, 115.74, 112.87, 14.65, 14.56. MALDI–TOF–HRMS: *m/z* [M]+ Calcd for $C_{31}H_{26}BF_2N_3O$+: *m*/*z* = 505.2137, found: *m*/*z* = 505.2390.

*Synthesis of **BDP-PXZ-6**.* **BDP-PXZ-6** was prepared by a method similar to that of **BDP-PXZ-2**. Green solid was obtained (98.8 mg, yield: 22%). M.p. > 250 °C. ^{1}H NMR (400 MHz, $CDCl_3$): δ = 7.99 (s, 2H), 7.81 (d, 2H, J = 8.0 Hz), 7.55 (d, 2H, J = 8.0 Hz), 7.03 (d, 2H, J = 4.0 Hz), 6.76–6.60 (m, 8H), 6.01 (d, 2H, J = 8.0 Hz). ^{13}C NMR (100 MHz, $CDCl_3$): δ = 145.90, 144.66, 144.09, 141.75, 134.81, 133.80, 133.13, 131.48, 131.02, 123.34, 121.98, 118.88, 115.83, 113.29. ESI–HRMS: *m/z* [M]+ Calcd for $C_{27}H_{18}BF_2N_3O$+: *m*/*z* = 449.1511, found: *m*/*z* = 449.1505.

2.0 NMR and HR-MS Spectra

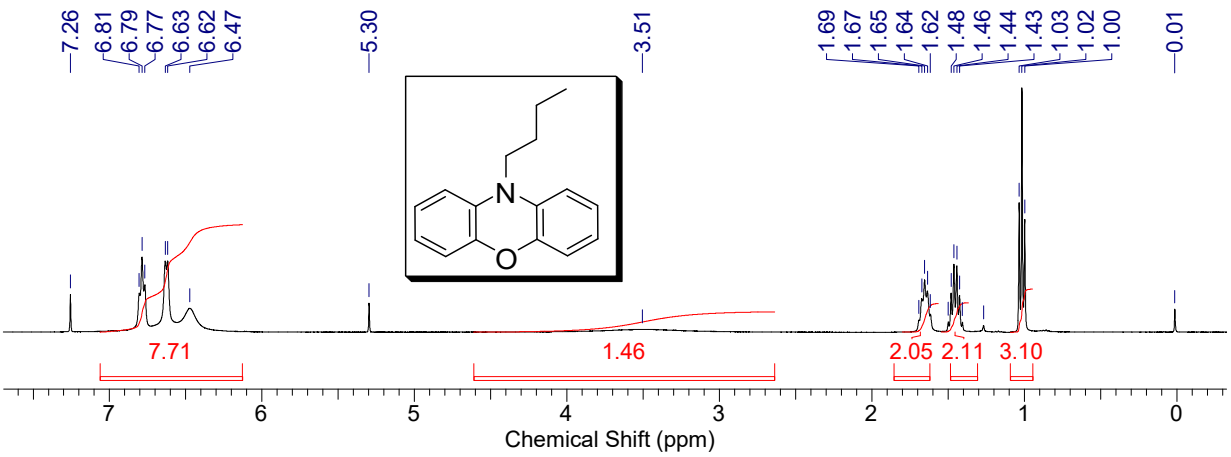

Figure S1. ^{1}H NMR spectrum of **1** (400 MHz, $CDCl_3$).

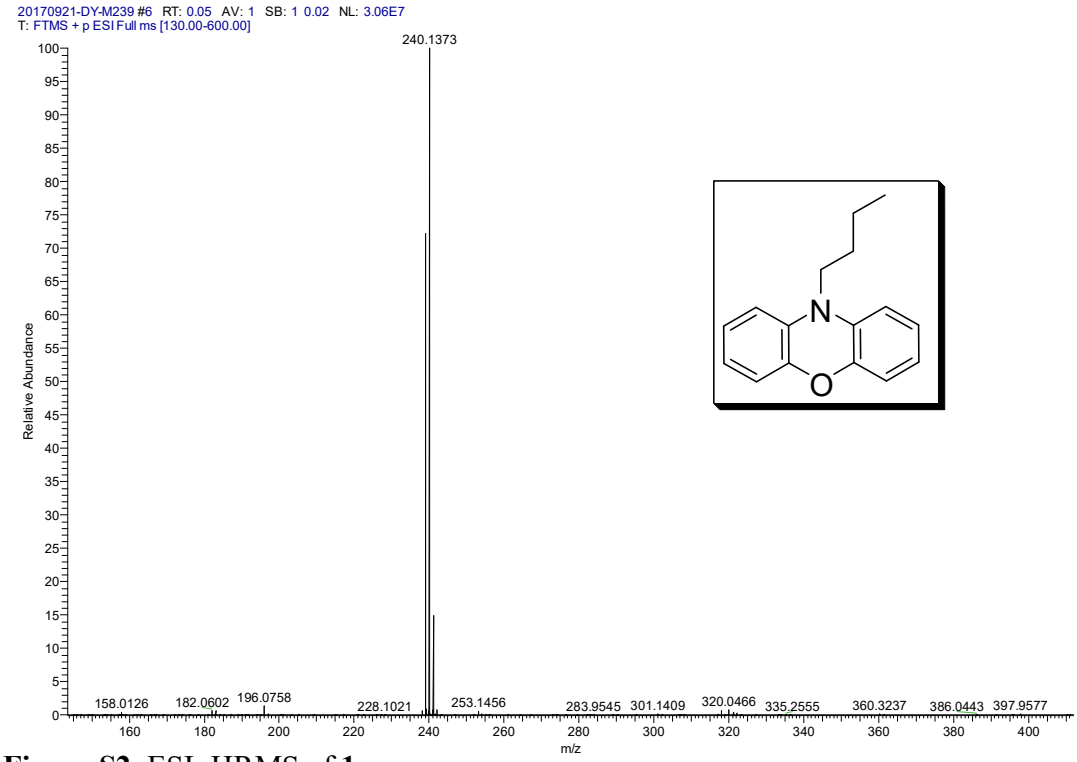

Figure S2. ESI–HRMS of **1**.

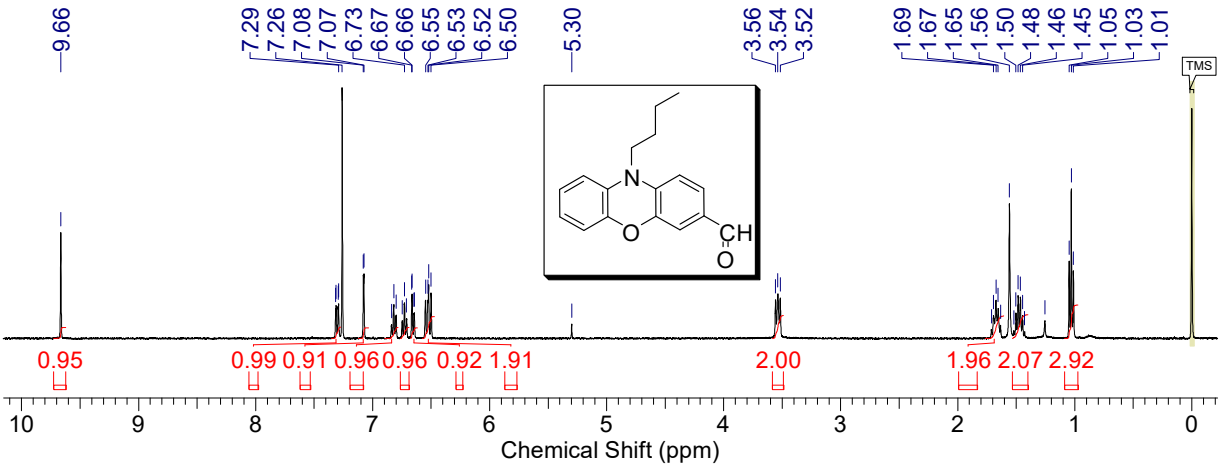

Figure S3. ^{1}H NMR spectrum of **2** (400 MHz, $CDCl_3$).

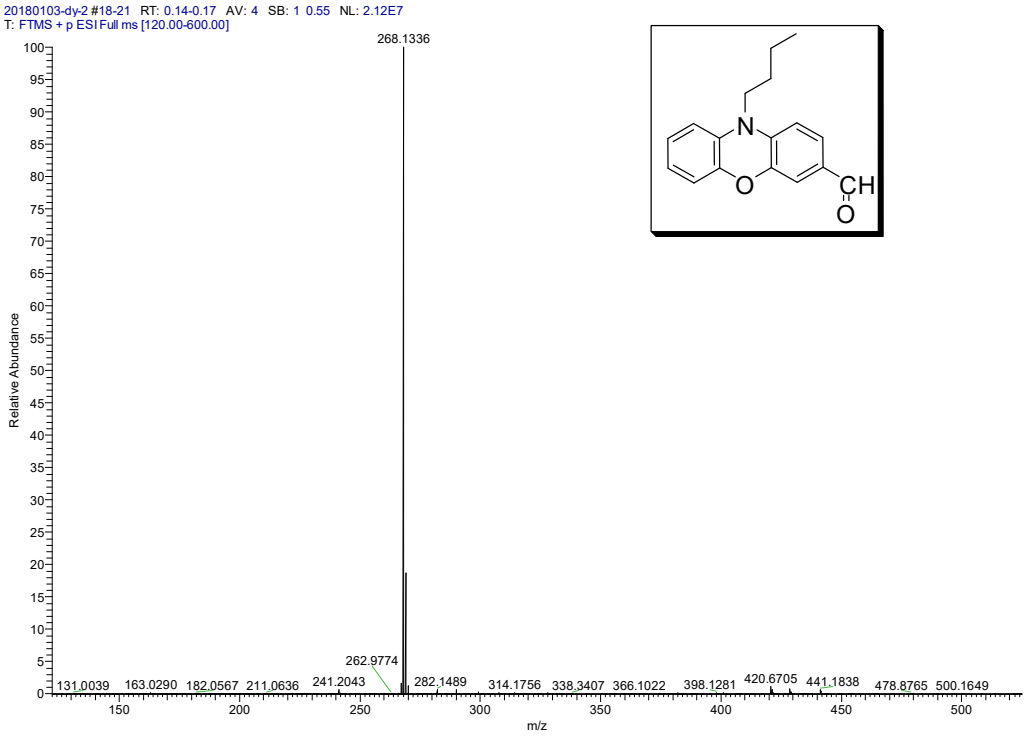

Figure S4. ESI–HRMS of **2**.

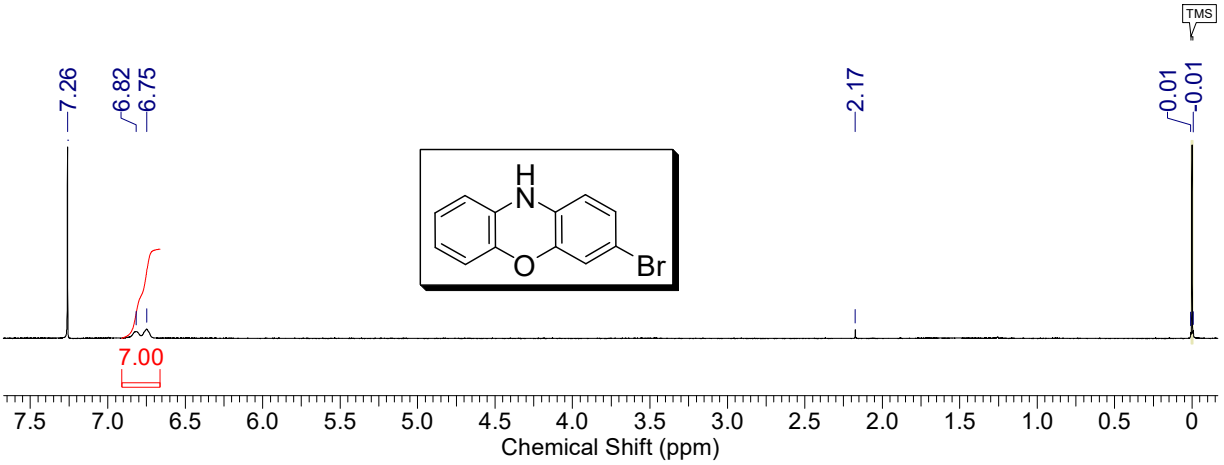

Figure S5. ^{1}H NMR spectrum of **3** (400 MHz, $CDCl_3$).

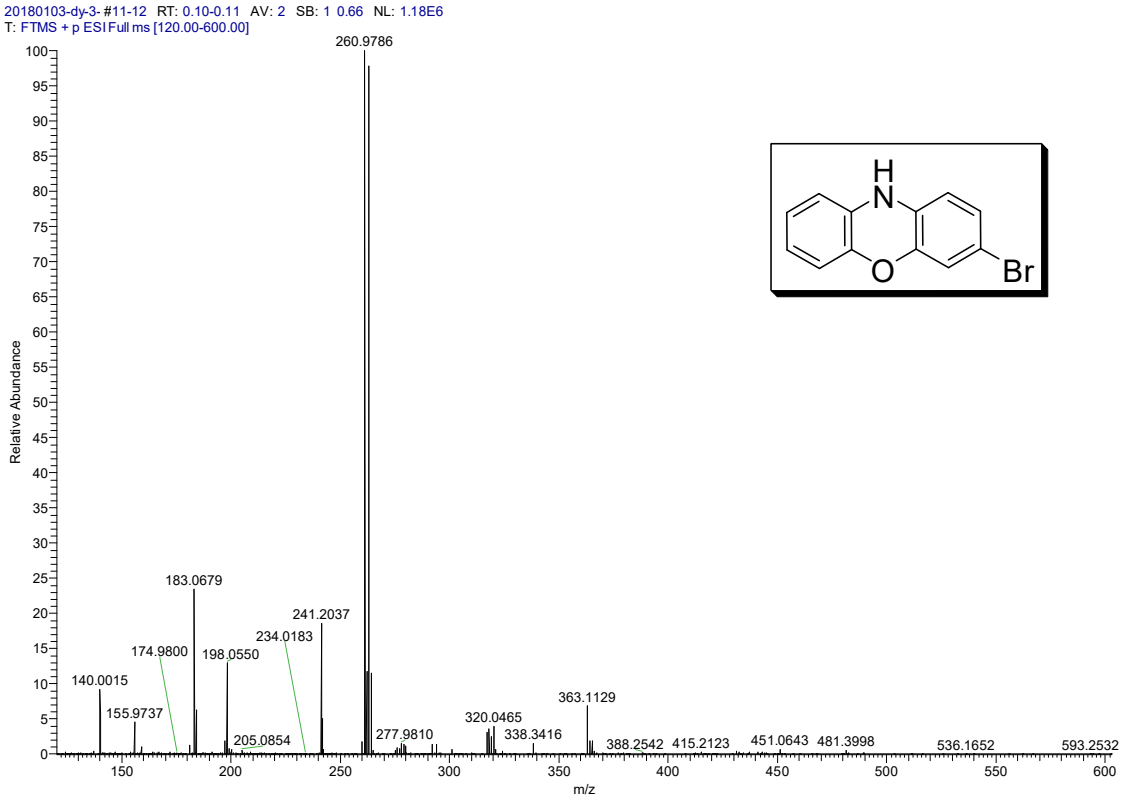

Figure S6. ESI–HRMS of **3**.

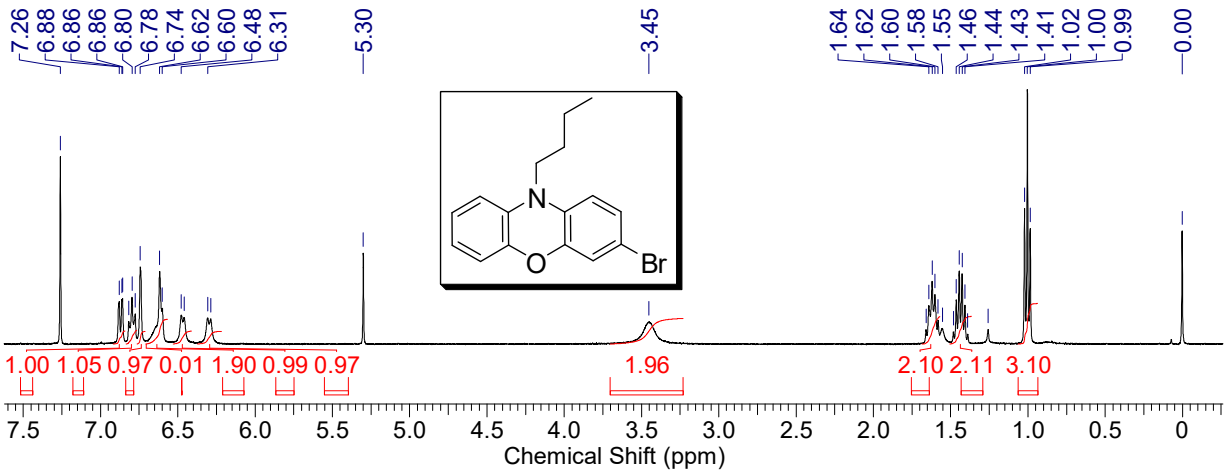

Figure S7. ^{1}H NMR spectrum of **4** (400 MHz, $CDCl_3$).

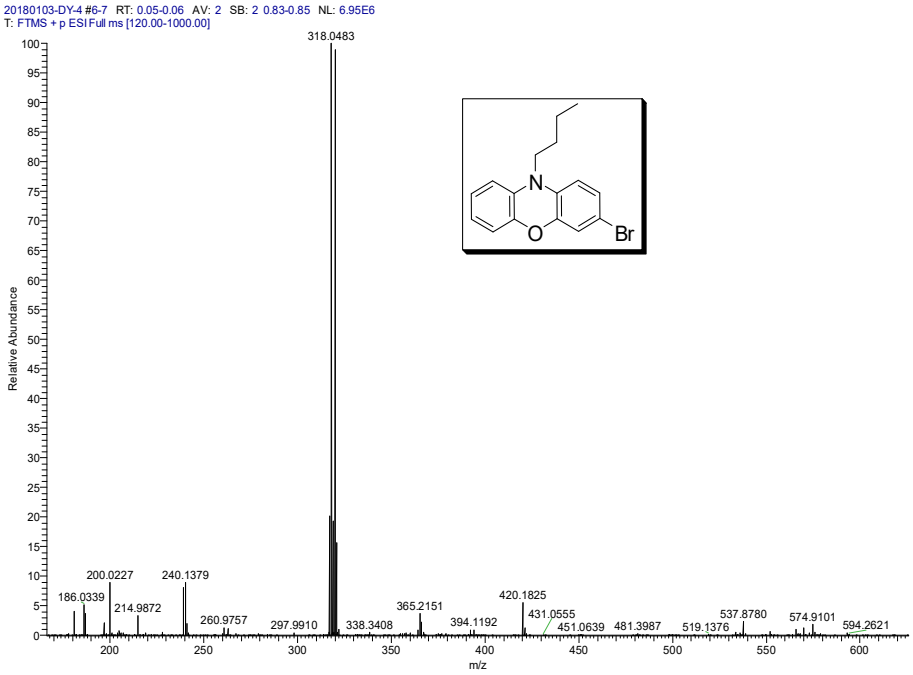

Figure S8. ESI–HRMS of **4**.

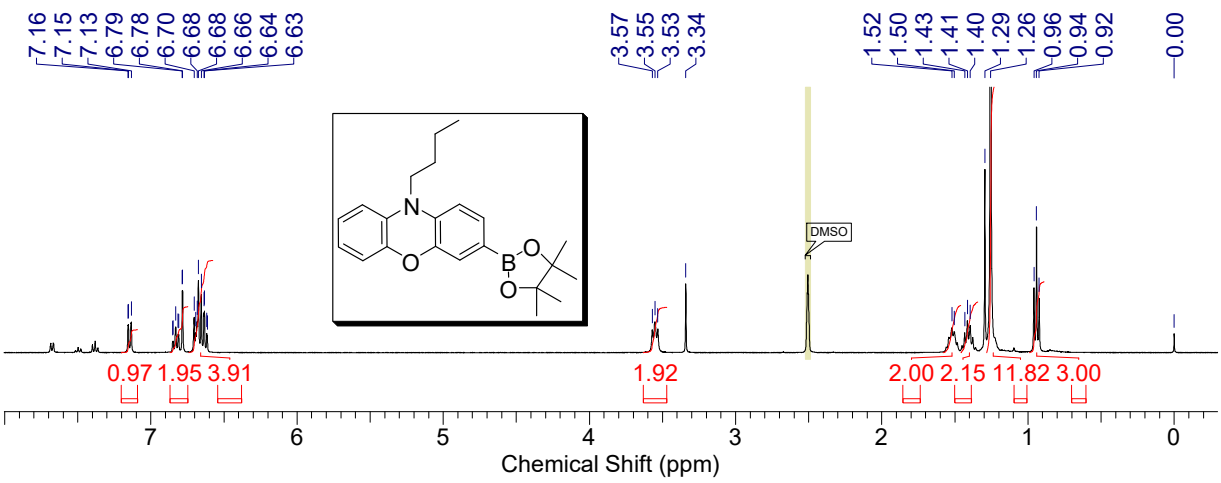

Figure S9. ^{1}H NMR spectrum of **5** (400 MHz, DMSO-d_6).

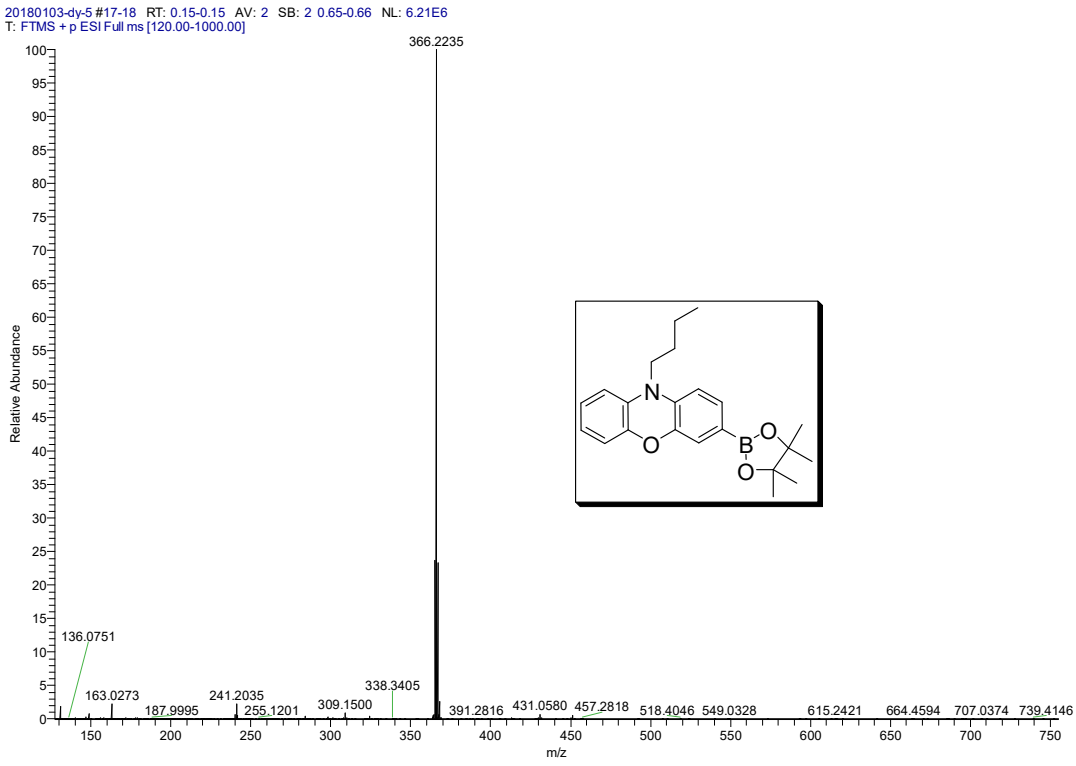

Figure S10. ESI–HRMS of **5**.

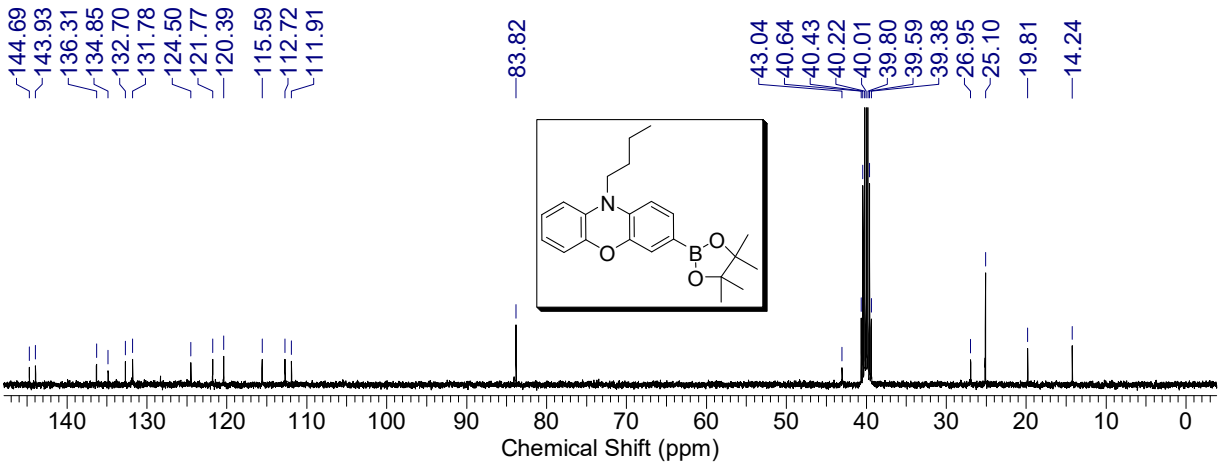

Figure S11. ^{13}C NMR spectrum of **5** (100 MHz, $CDCl_3$).

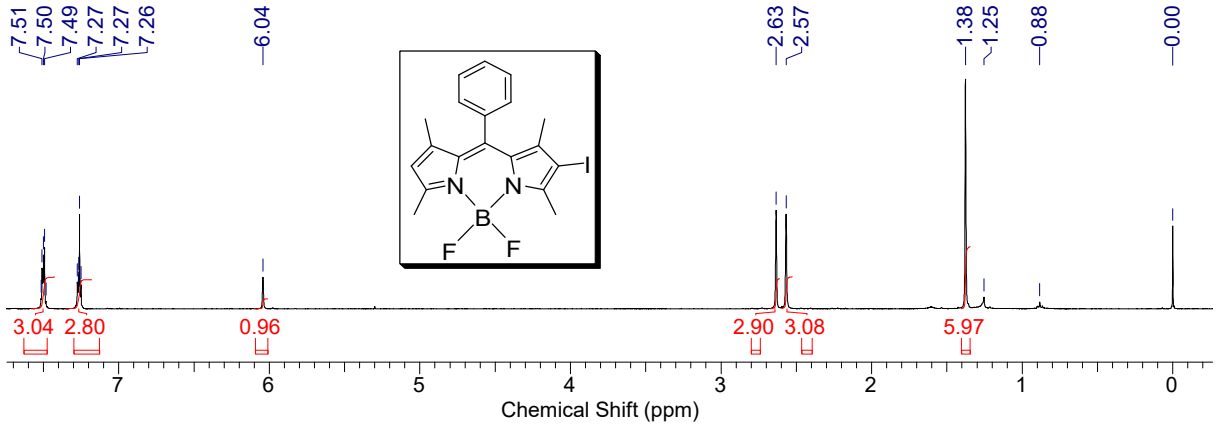

Figure S12. ^{1}H NMR of **6** (400 MHz, $CDCl_3$).

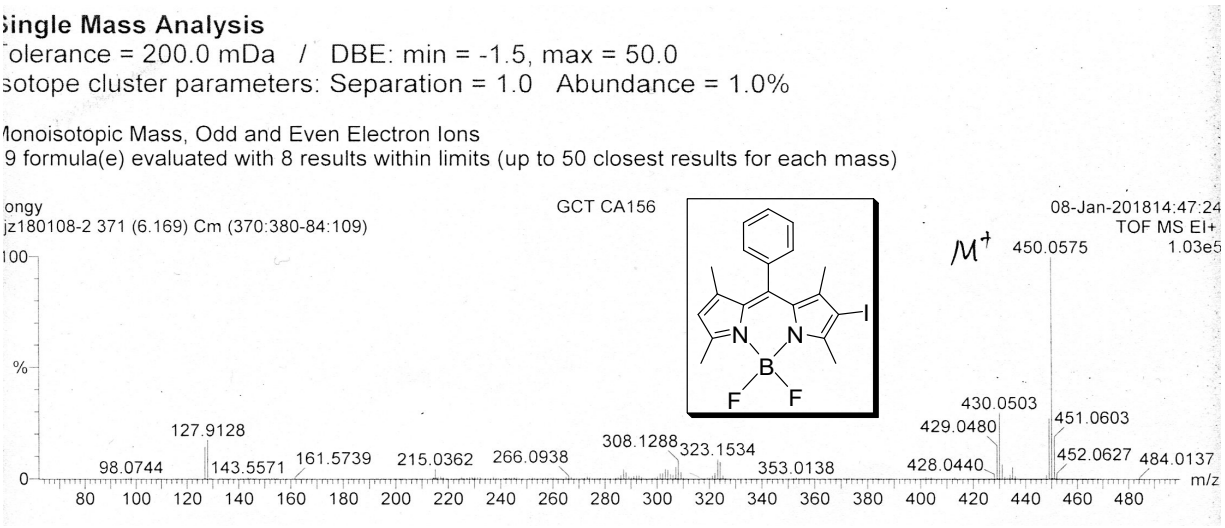

Figure S13. TOF–HRMS of **6**.

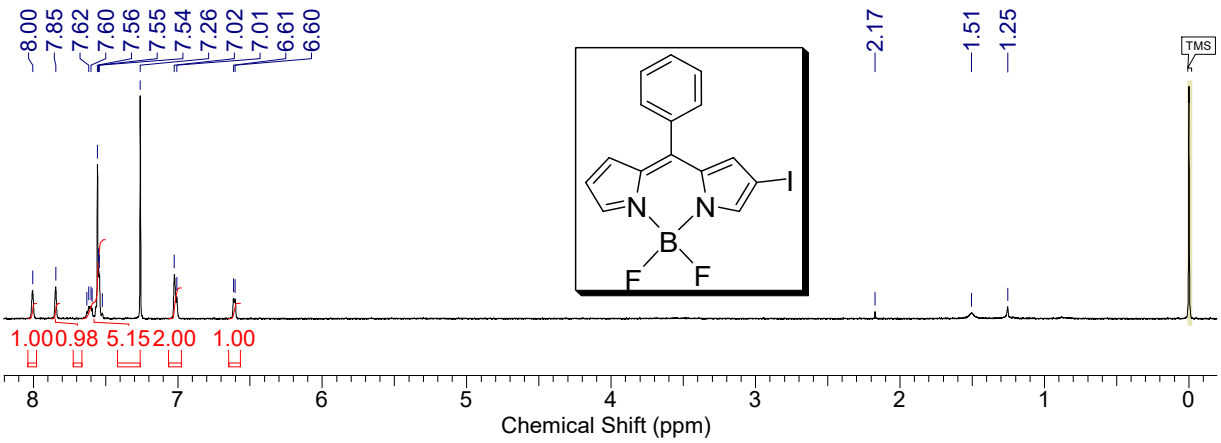

Figure S14. ^{1}H NMR spectrum of **7** (400 MHz, $CDCl_3$).

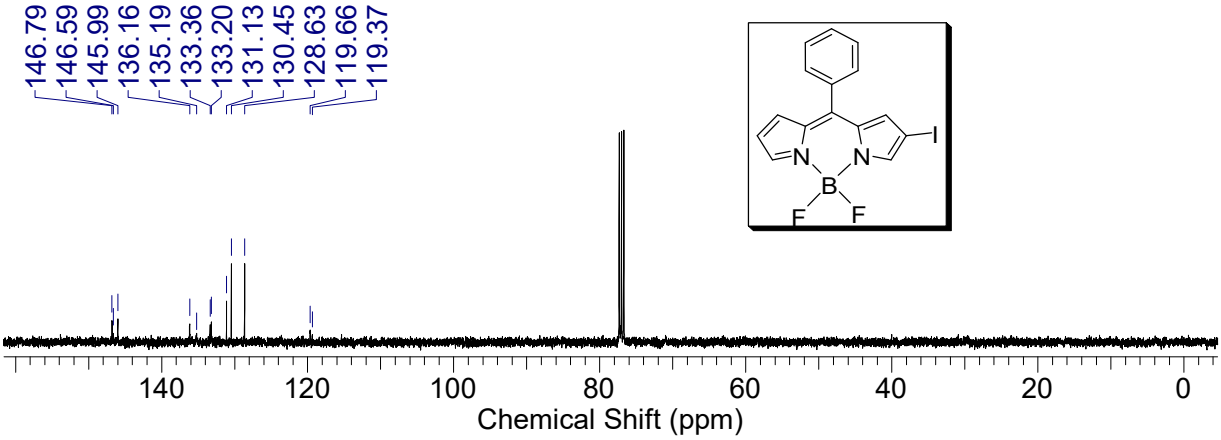

Figure S15. ^{13}C NMR spectrum of **7** (100 MHz, $CDCl_3$).

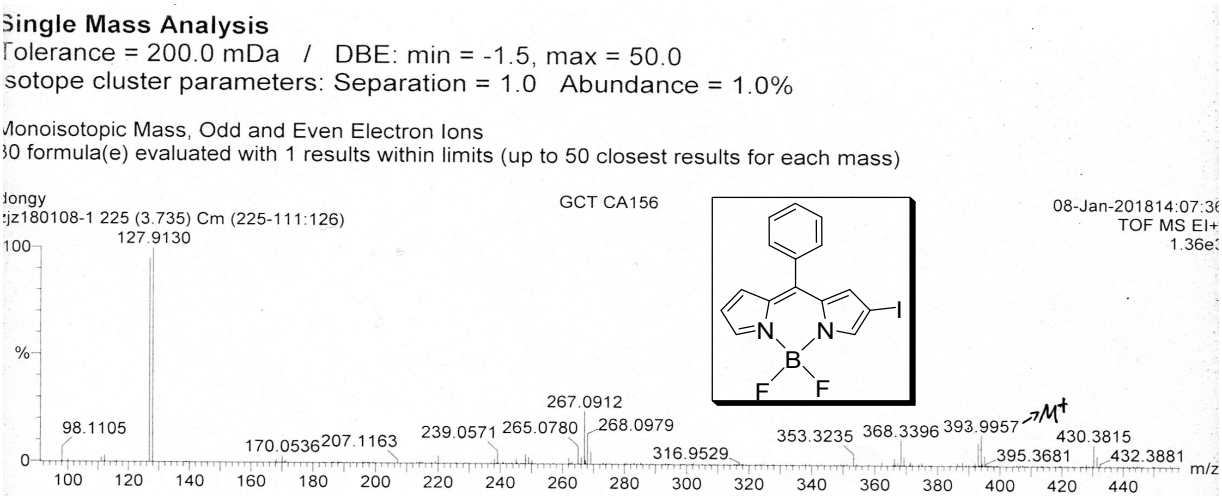

Figure S16. ESI–HRMS of **7**.

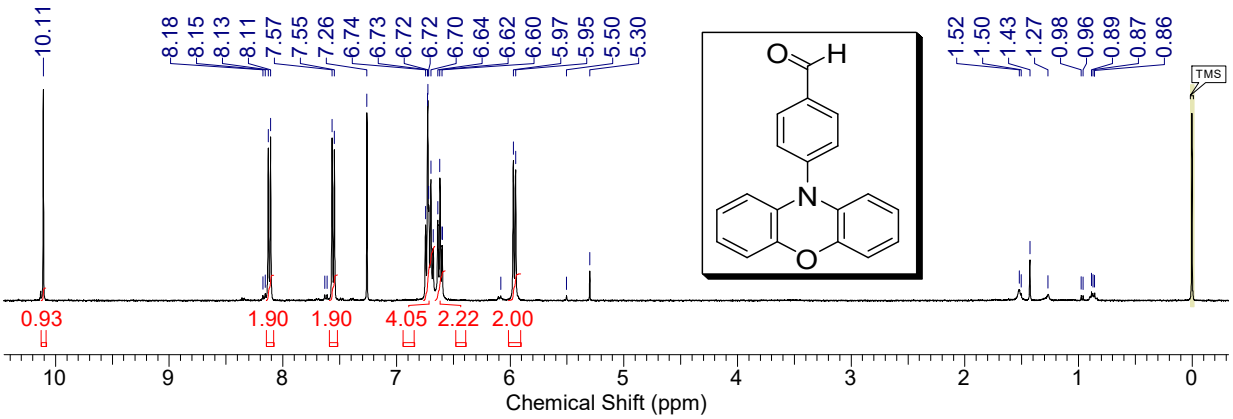

Figure S17. ^{1}H NMR spectrum of **8** (400 MHz, $CDCl_3$).

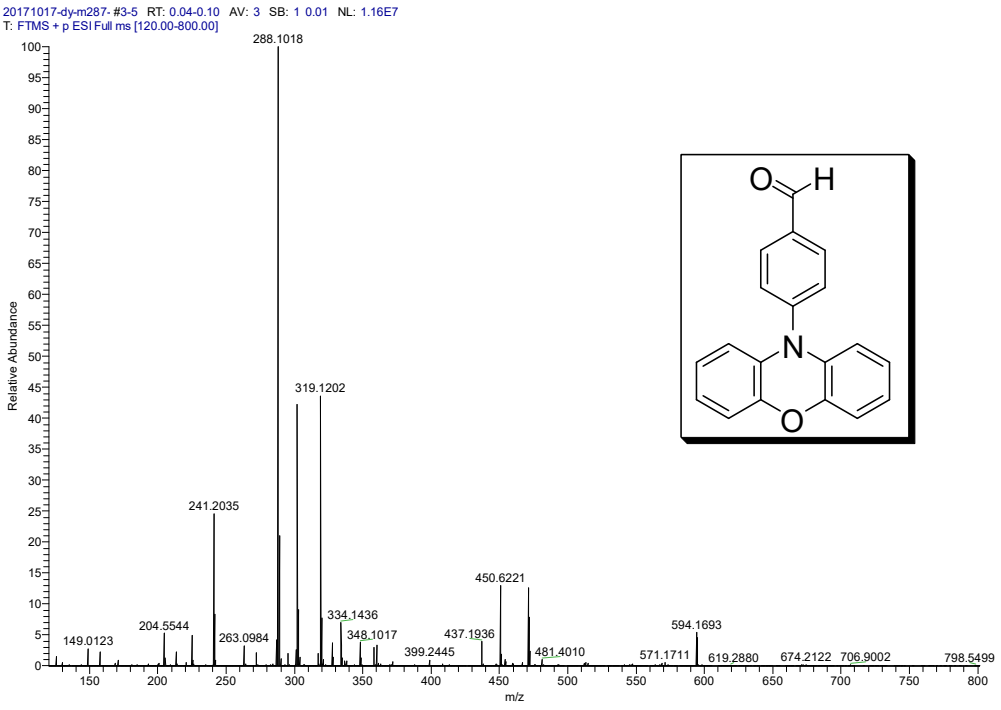

Figure S18. ESI–HRMS of **8**.

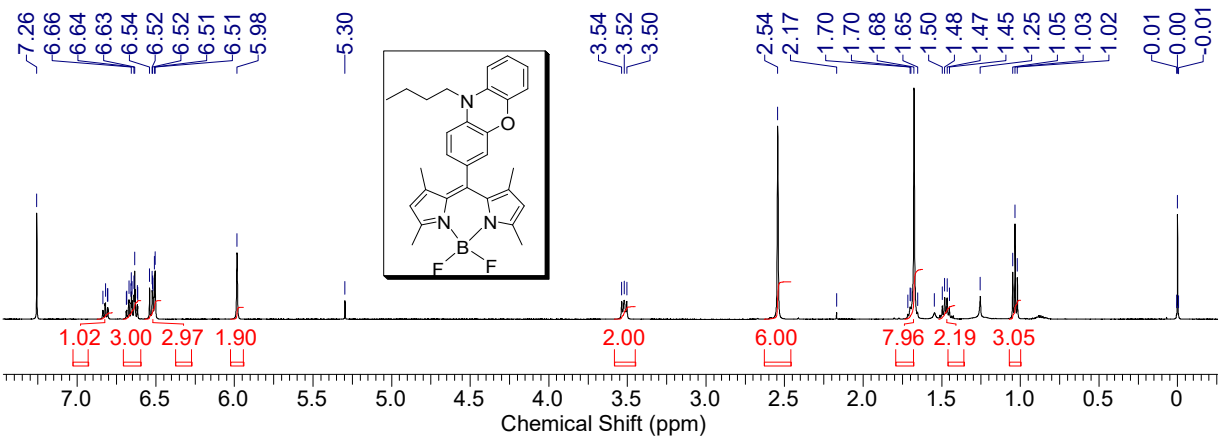

Figure S19. ^{1}H NMR spectrum of **BDP-PXZ-1** (400 MHz, $CDCl_3$).

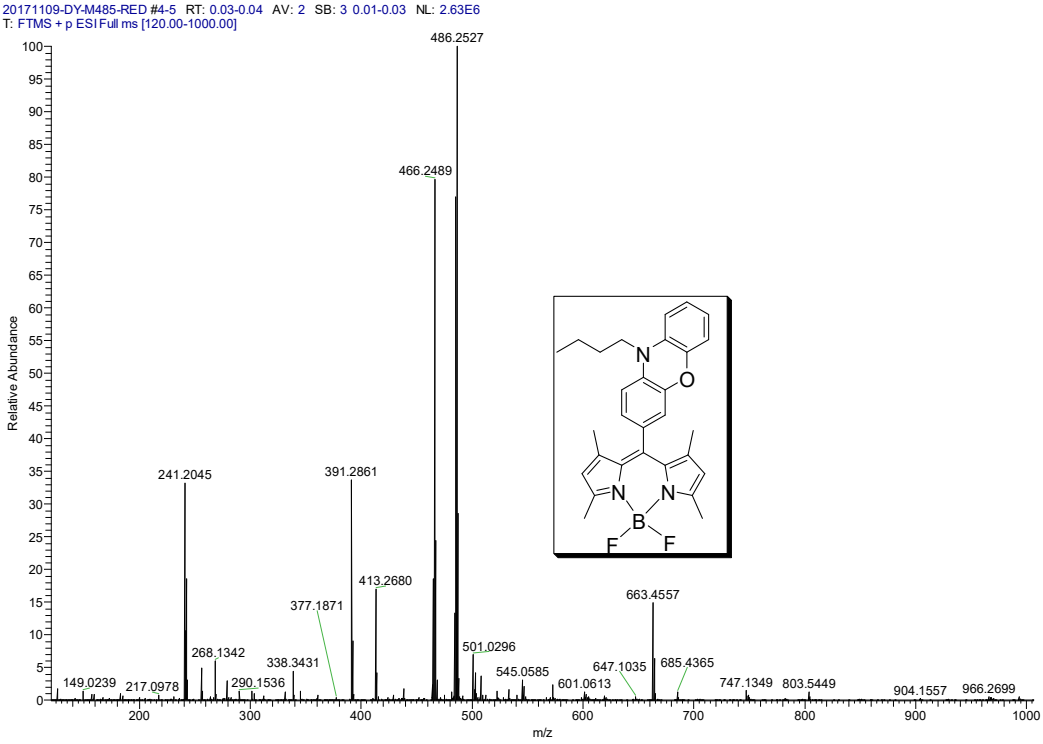

Figure S20. ESI–HRMS of **BDP-PXZ-1**.

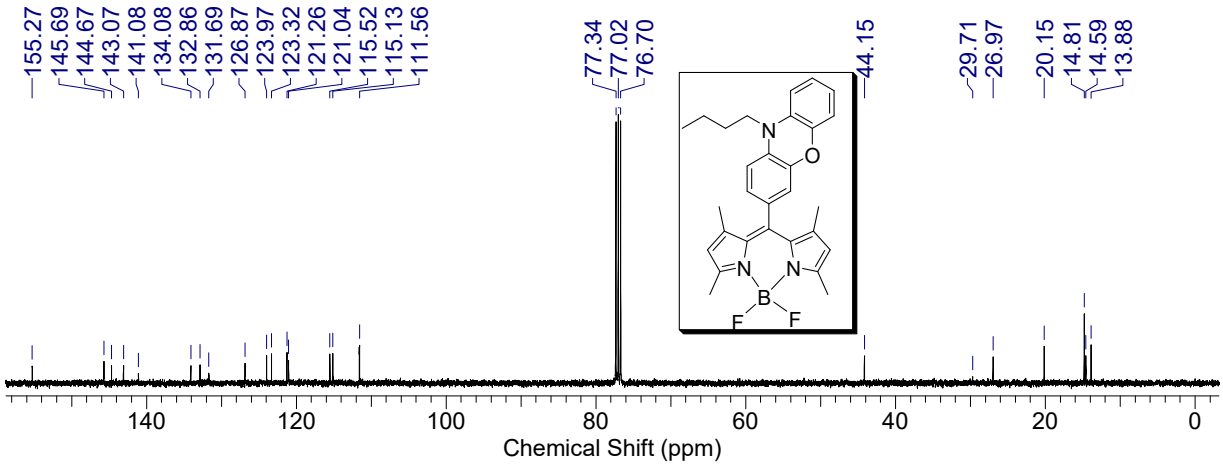

Figure S21. ^{13}C NMR spectrum of **BDP-PXZ-1** (100 MHz, $CDCl_3$).

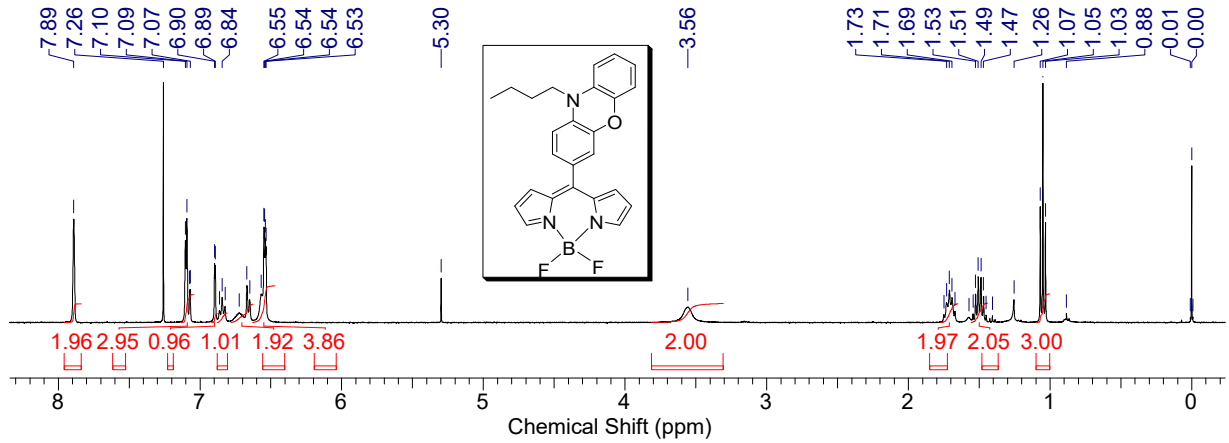

Figure S22. ^{1}H NMR spectrum of **BDP-PXZ-2** (400 MHz, $CDCl_3$).

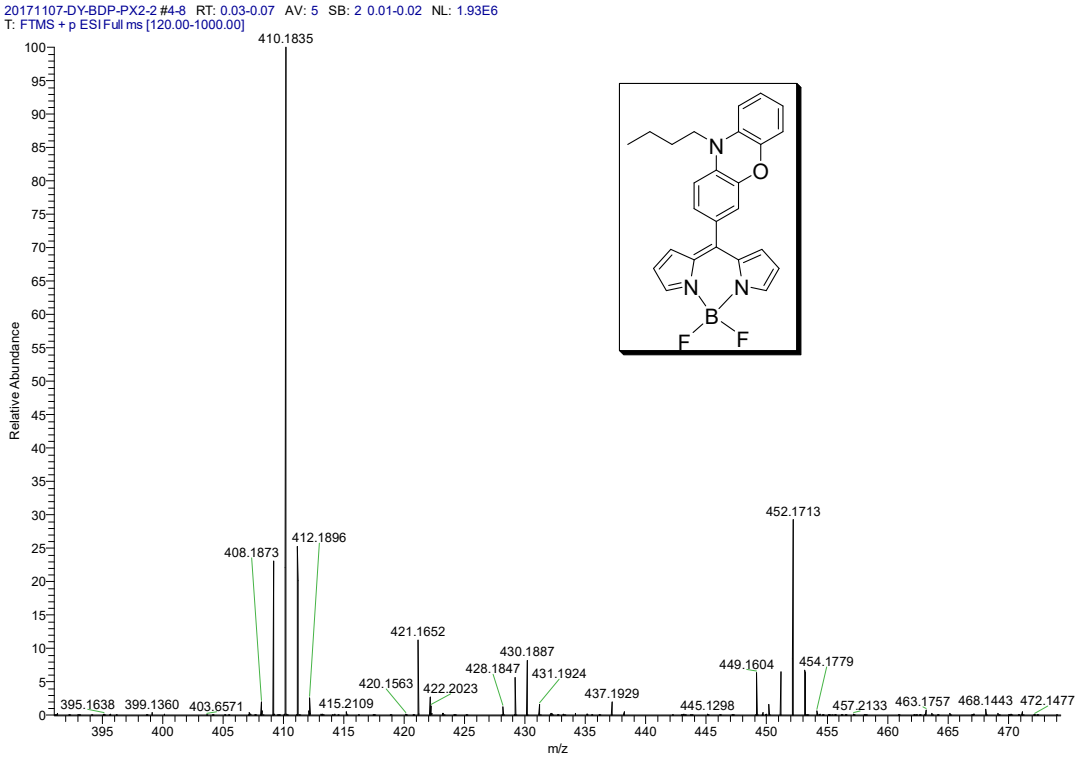

Figure S23. ESI–HRMS of **BDP-PXZ-2**.

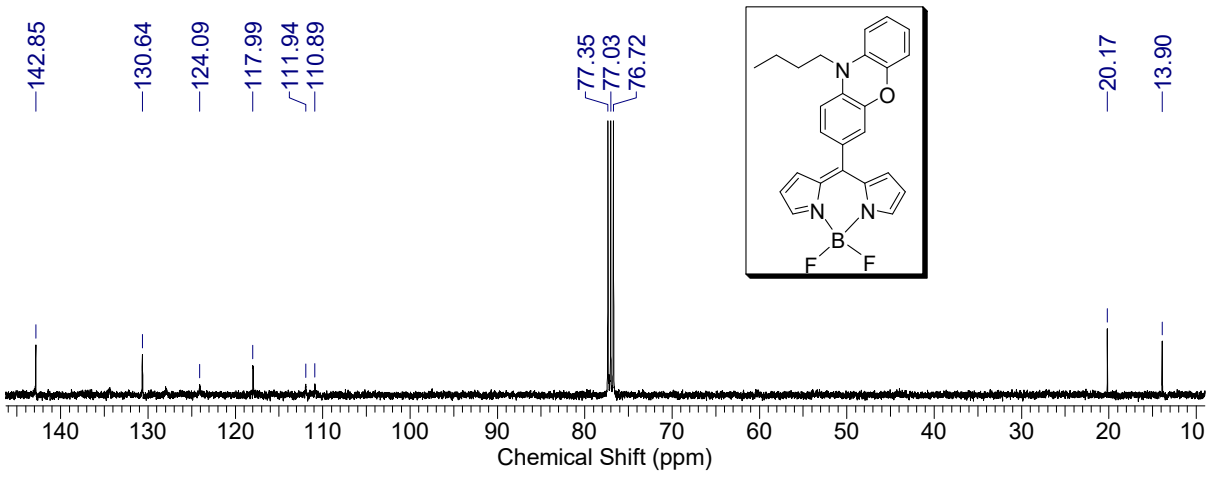

Figure S24. ^{13}C NMR spectrum of **BDP-PXZ-2** (100 MHz, $CDCl_3$).

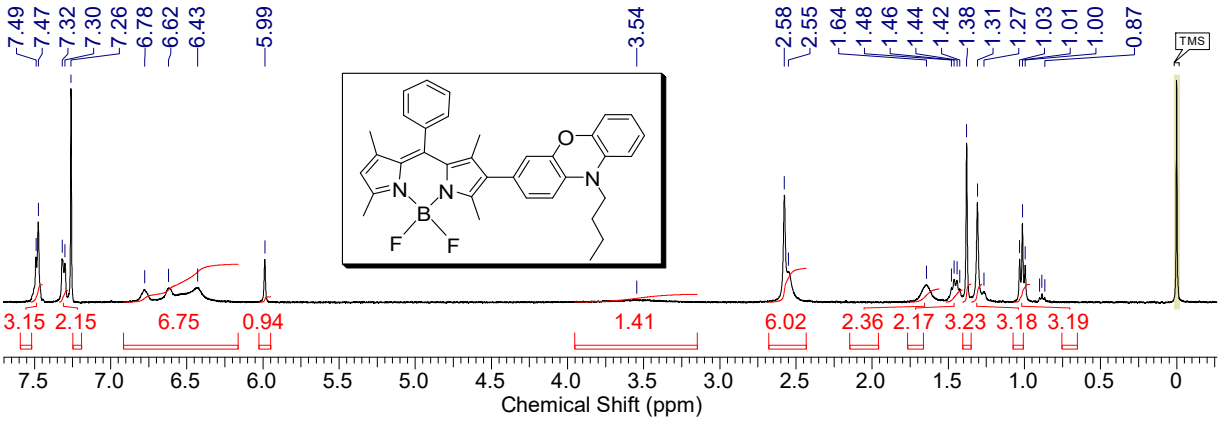

Figure. S25. ^{1}H NMR spectrum of **BDP-PXZ-3** (400 MHz, $CDCl_3$).

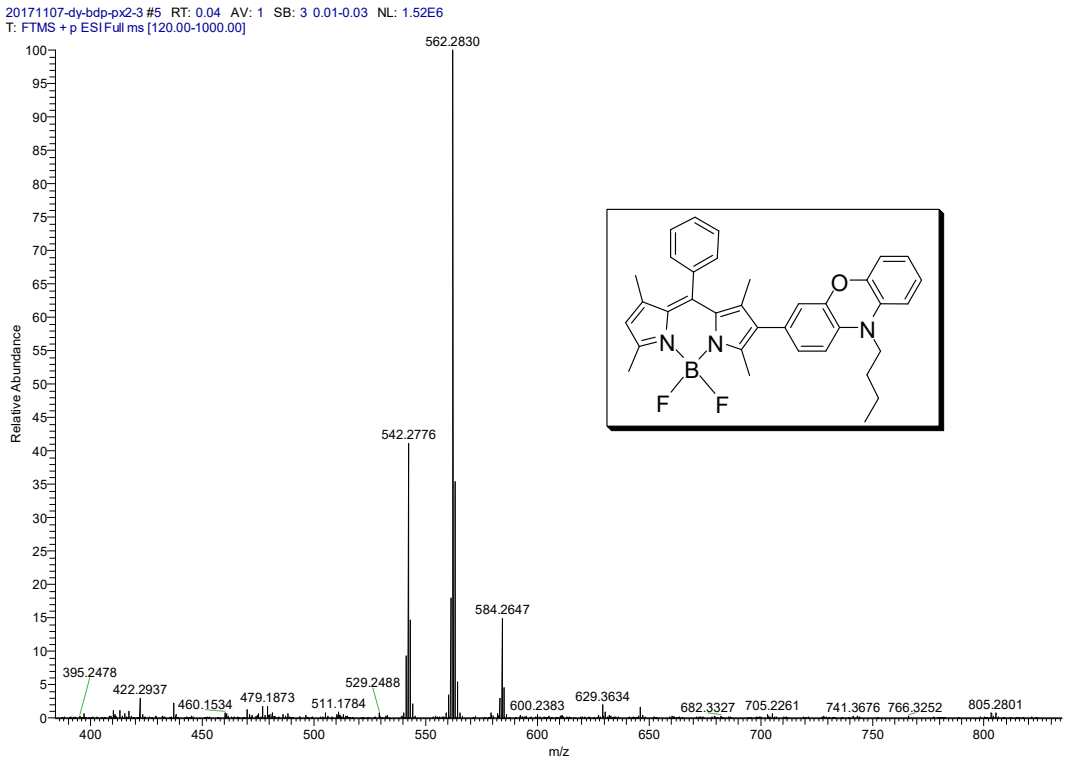

Figure S26. ESI–HRMS of **BDP-PXZ-3**.

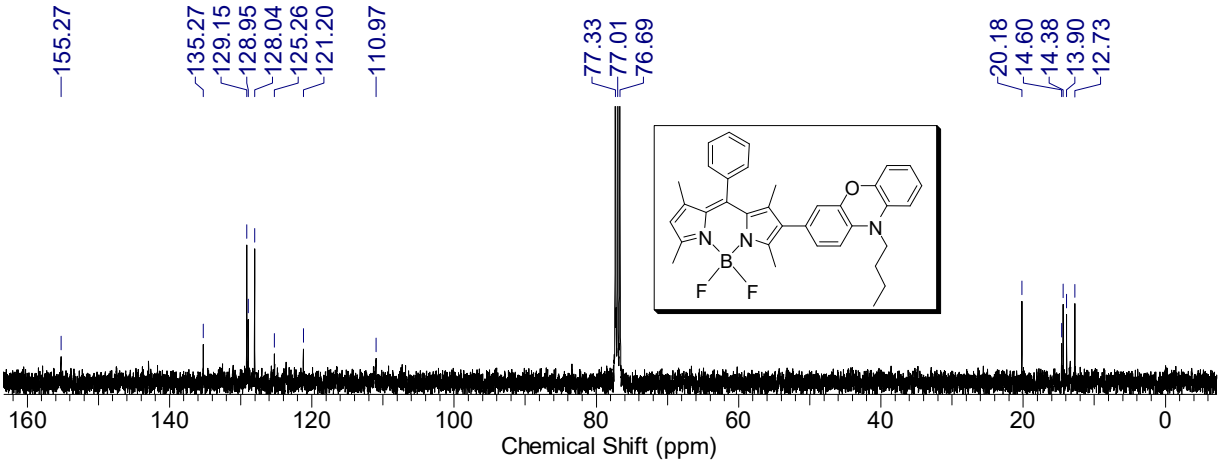

Figure S27. ^{13}C NMR spectrum of **BDP-PXZ-3** (100 MHz, $CDCl_3$).

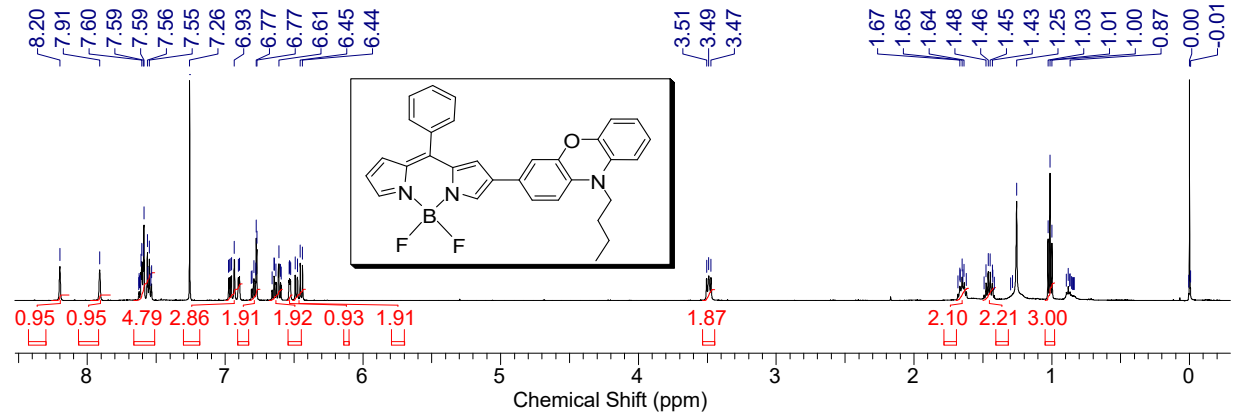

Figure S28. ^{1}H NMR spectrum of **BDP-PXZ-4** (400 MHz, $CDCl_3$).

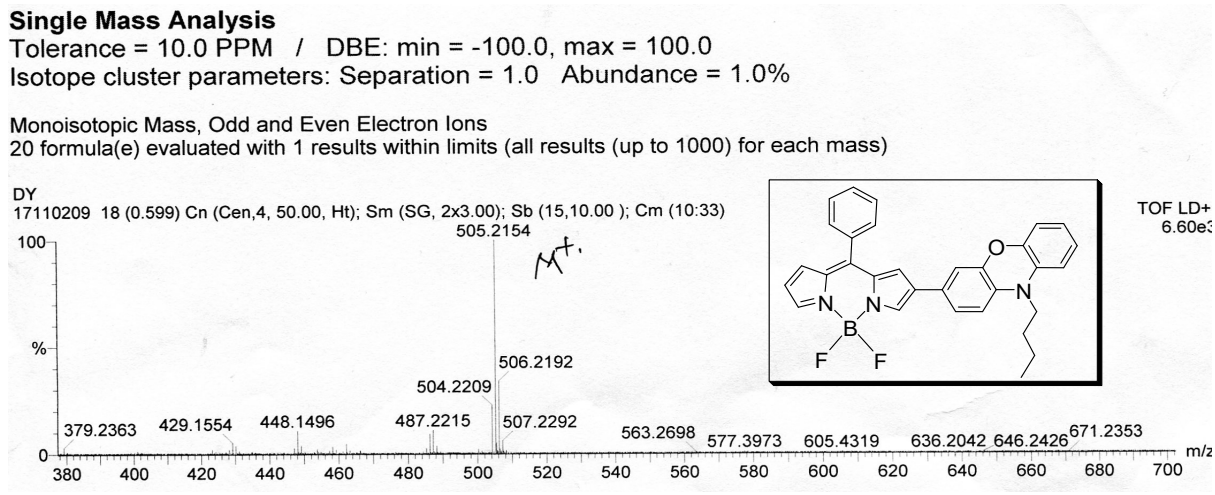

Figure S29. MALDI–TOF–HRMS of **BDP-PXZ-4**.

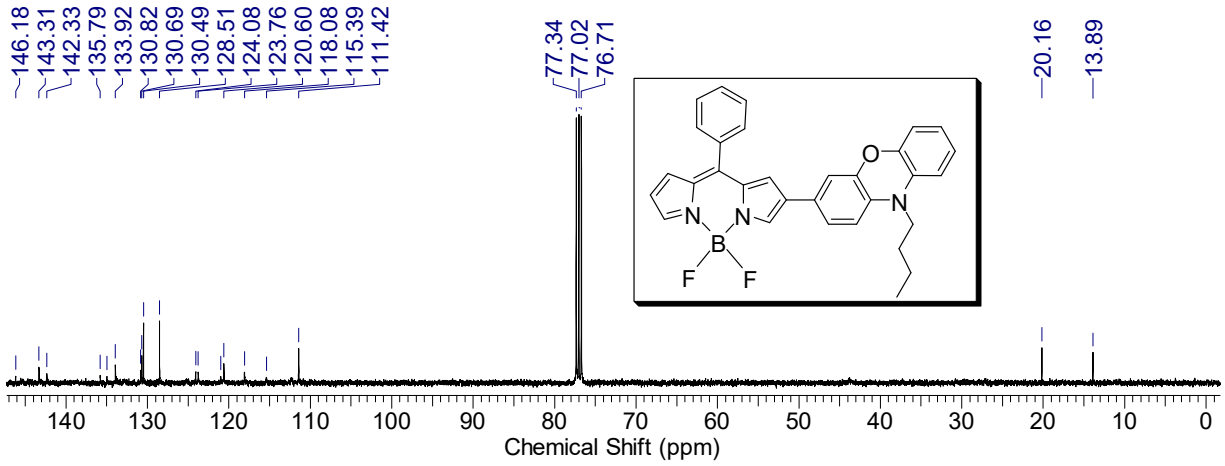

Figure S30. ^{13}C NMR spectrum of **BDP-PXZ-4** (100 MHz, $CDCl_3$).

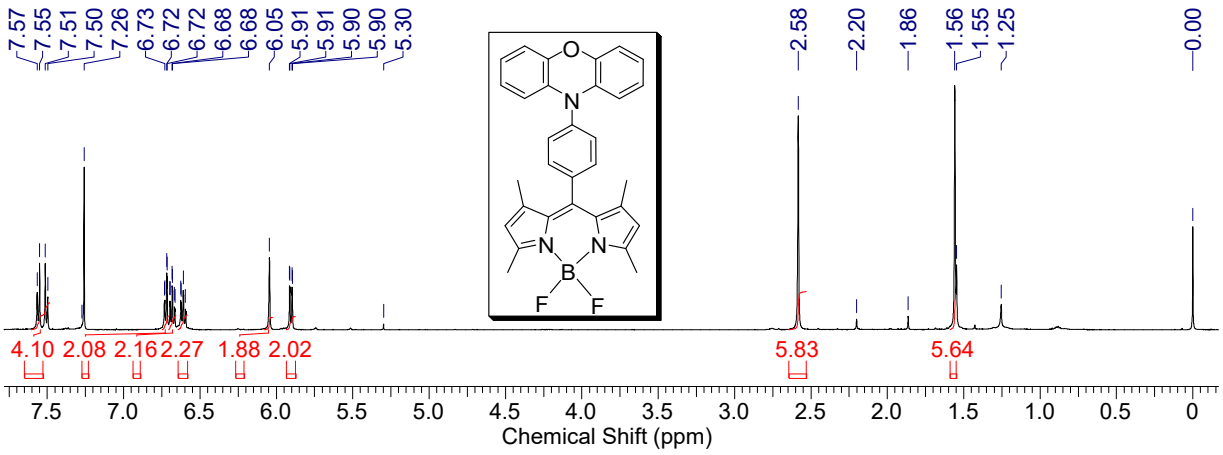

Figure S31. ^{1}H NMR spectrum of **BDP-PXZ-5** (500 MHz, $CDCl_3$).

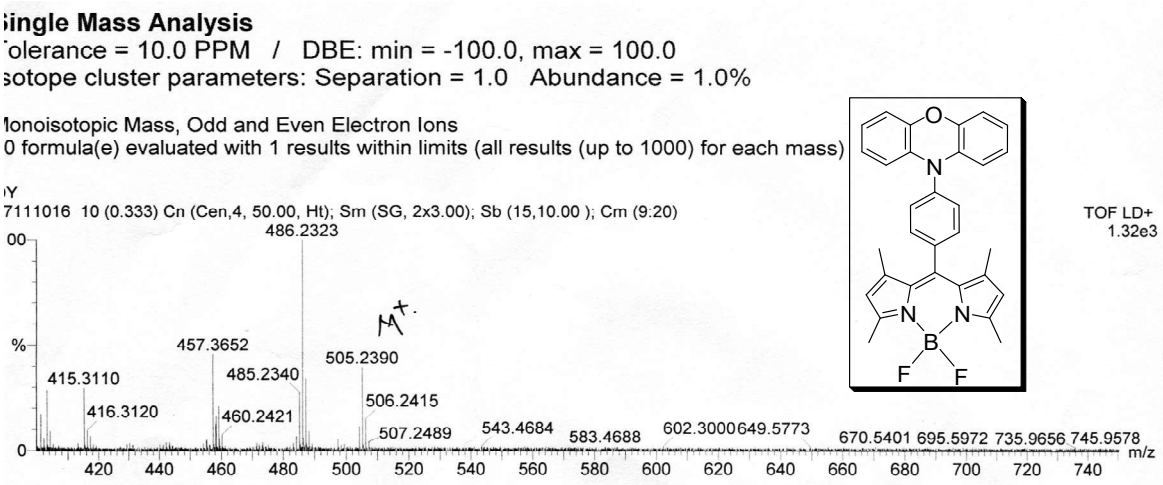

Figure S32. MALDI–TOF–HRMS of **BDP-PXZ-5**.

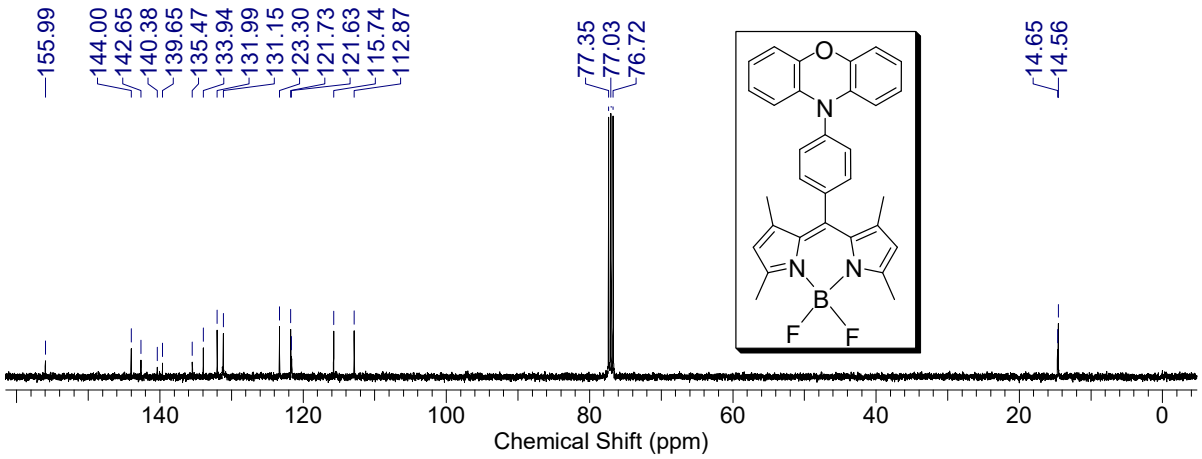

Figure S33. ^{13}C NMR spectrum of **BDP-PXZ-5** (100 MHz, $CDCl_3$).

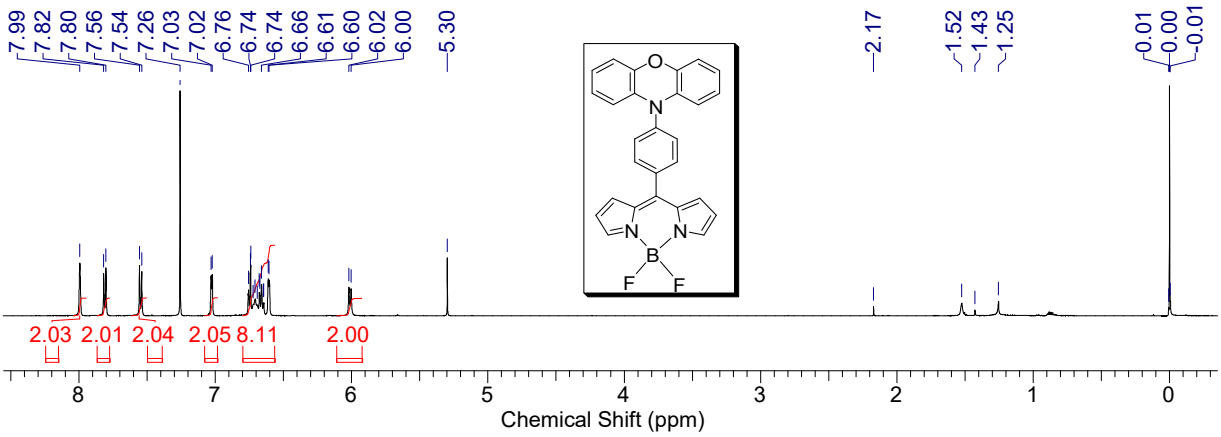

Figure S34. ^{1}H NMR spectrum of **BDP-PXZ-6** (400 MHz, $CDCl_3$).

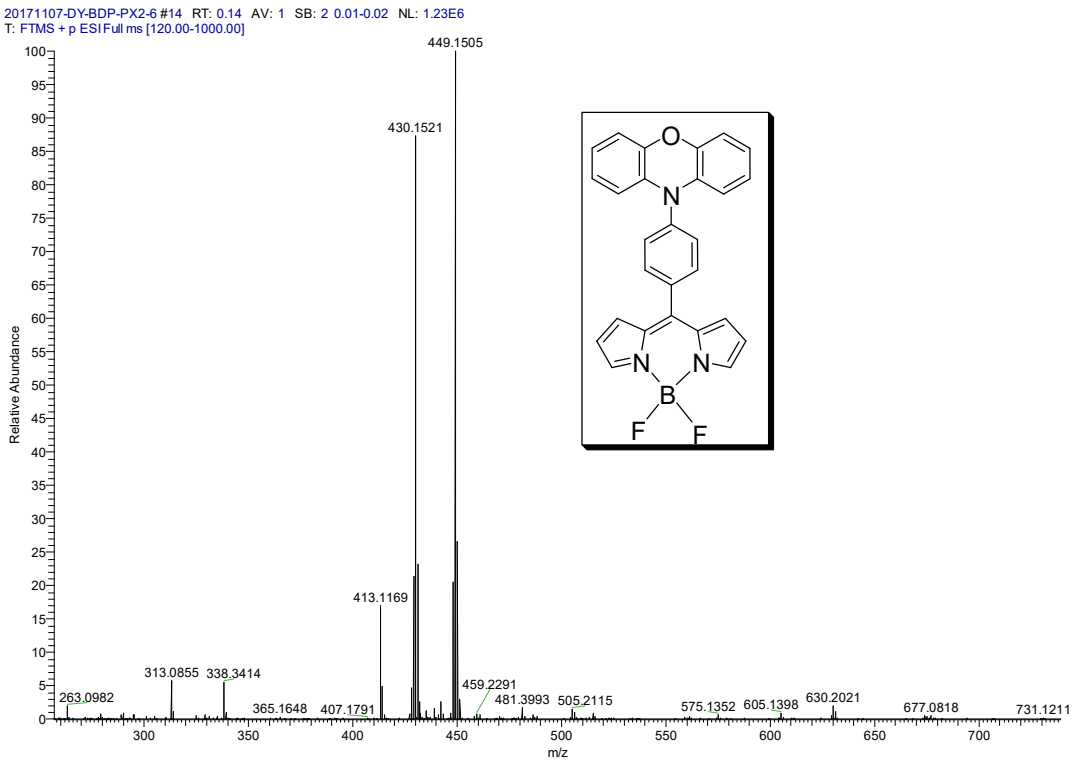

Figure S35. ESI–HR MS of **BDP-PXZ-6**.

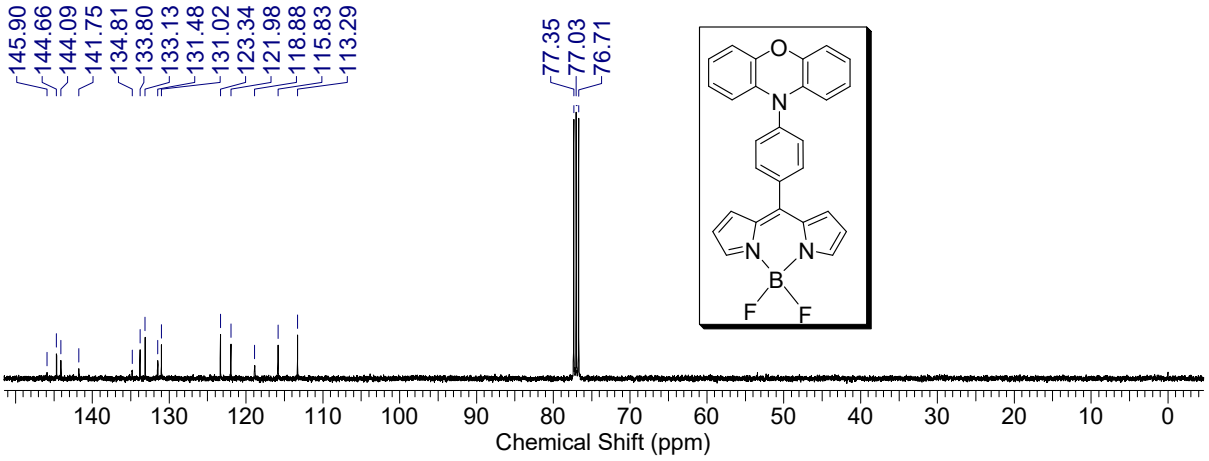

Figure S36. ^{13}C NMR spectrum of **BDP-PXZ-6** (100 MHz, $CDCl_3$).

3.0 UV-Vis Absorption Spectra.

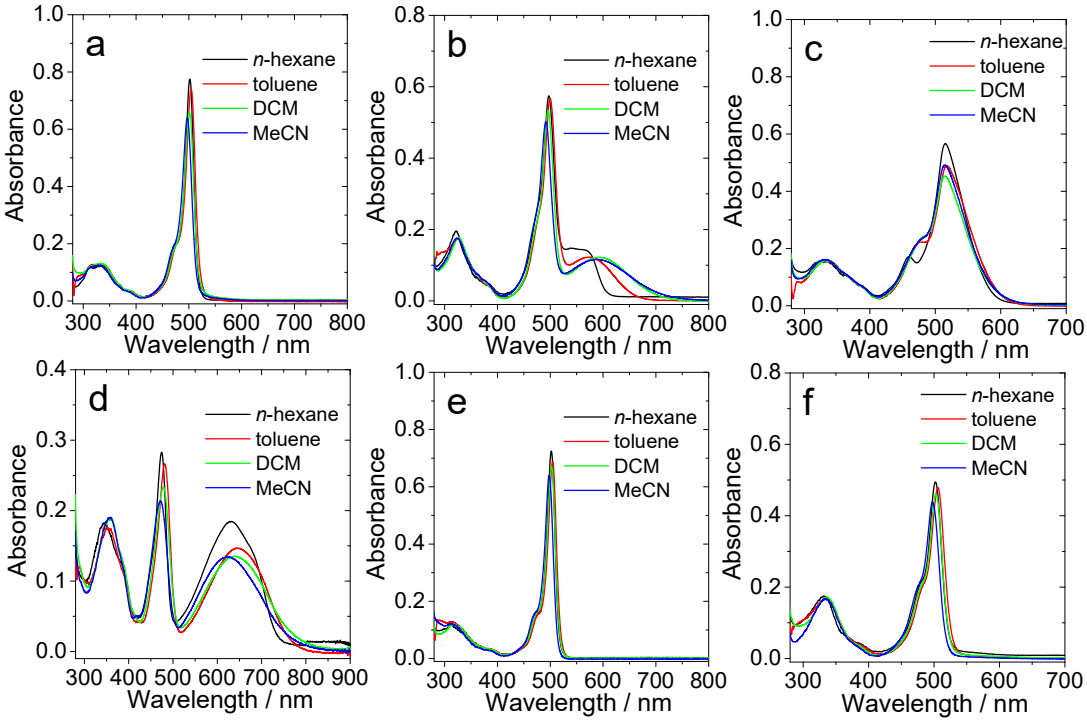

Figure S37. UV−Vis absorption spectra of the compounds in different solvents. (a) **BDP-PXZ-1**; (b) **BDP-PXZ-2**; (c) **BDP-PXZ-3**; (d) **BDP-PXZ-4**; (e) **BDP-PXZ-5** and (f) **BDP-PXZ-6**. c =1.0 × 10^{-5} M. 20 °C.

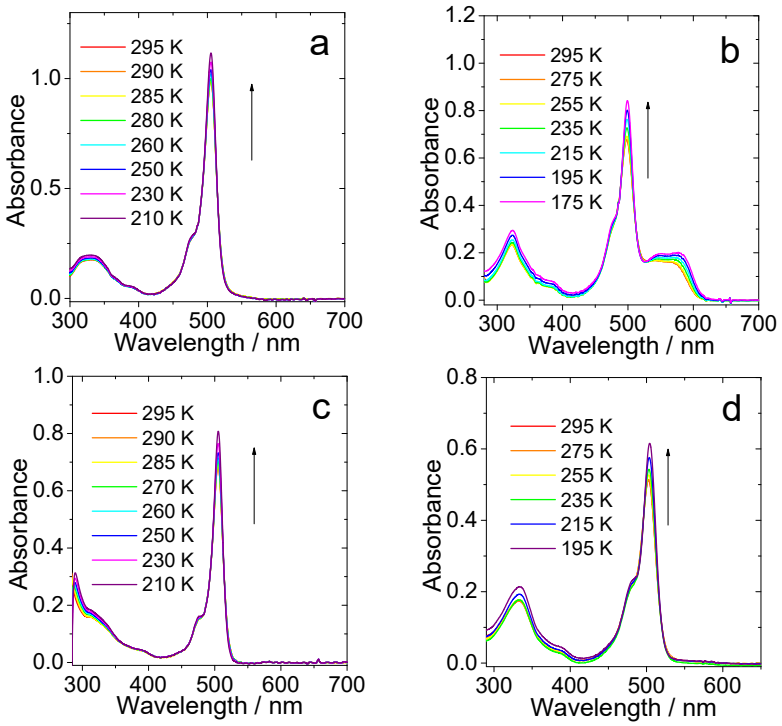

Figure S38. Temperature-dependent UV−Vis absorption spectra of (a) **BDP-PXZ-1**; (b) **BDP-PXZ-2**; (c) **BDP-PXZ-5** and (d) **BDP-PXZ-6**. (a) and (c) in toluene, (b) and (d) in *n*-hexane. $c = 1.0 \times 10^{-5}$ M.

4.0 Fluorescence Spectra and Triplet State Properties.

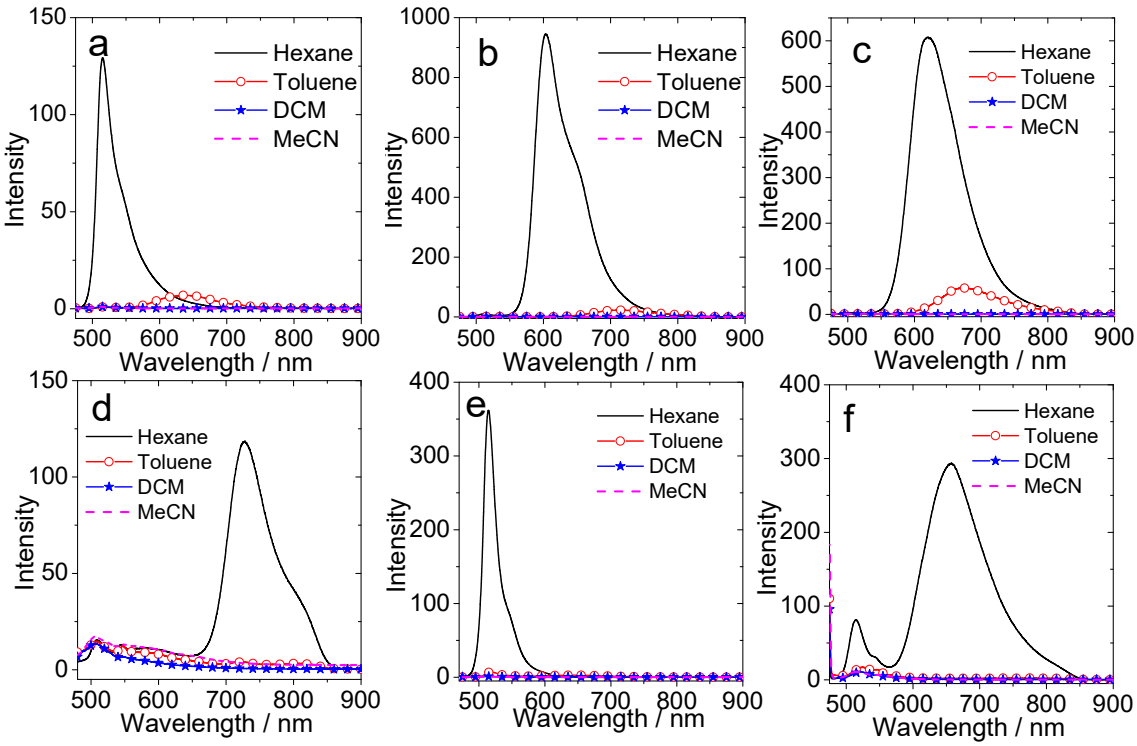

Figure S39. Comparison of the fluorescence emission spectra of the compounds in different solvents. (a) **BDP-PXZ-1**; (b) **BDP-PXZ-2**; (c) **BDP-PXZ-3**; (d) **BDP-PXZ-4**; (e) **BDP-PXZ-5** and (f) **BDP-PXZ-6**. λ_{ex} = 470 nm, Optically matched solutions were used (A = 0.186) so that the emission intensity can be compared. 20 °C.

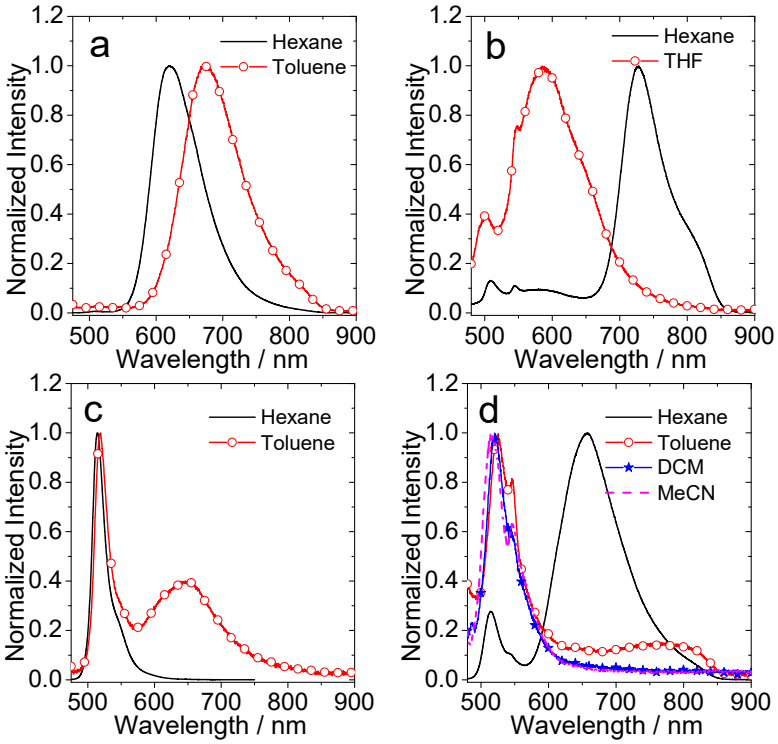

Figure S40. Normalized fluorescence emission spectra of the compounds in different solvents. (a) **BDP-PXZ-3**; (b) **BDP-PXZ-4**; (c) **BDP-PXZ-5**; (d) **BDP-PXZ-6**. λ_{ex} = 470 nm. Optically matched solutions were used (A = 0.186). 20 °C.

Table S1. The Parameters of Compounds in non-polar solvents

	solvent	λ_F [a]	Φ_F [b]	τ_F [c] (χ^2)	M_{fl} [d]
BDP-PXZ-1	HEX	515 [e]	15.5 [e]	3.4 [e] (1.18)	– [g]
	TOL	517 [e]/638 [f]	0.13 [e]/4.7 [f]	4.2 [e] (1.27)/4.9 [f] (1.14)	1.55
BDP-PXZ-2	HEX	515 [e]/604 [f]	0.08 [e]/16.4 [f]	2.3 [e] (1.24)/3.4 [f] (1.05)	3.62
	TOL	516 [e]/710 [f]	0.2 [e]/1.8 [f]	0.6 [e] (1.22)/1.4 [f] (1.59)	2.03
BDP-PXZ-3	HEX	620 [f]	16.0 [f]	3.1 [f] (1.19)	3.89
	TOL	675 [f]	3.3 [f]	1.5 [f] (1.31)	2.57
BDP-PXZ-4	HEX	509 [e]/727 [f]	0.05 [e]/0.2 [f]	2.4 [e] (2.41)/0.7 [f] (1.39)	1.06
	TOL	509 [e]	0.04 [e]	3.6 [e] (1.23)	– [g]
BDP-PXZ-5	HEX	515 [e]	30.3 [e]	2.6 [e] (1.13)	– [g]
	TOL	517 [e]/650 [f]	0.7 [e]/1.9 [f]	7.1 [e] (1.18)/9.5 [f] (1.15)	0.76
BDP-PXZ-6	HEX	515 [e]/655 [h]	0.03 [e]/1.0 [h]	2.5 [e] (1.15)/3.8 [f] (1.32)	0.94
	TOL	523 [e]	0.08 [e]	3.2 [e] (1.18)	– [g]
BDP-1	HEX	512 [e]	61.9 [e]	3.2 [e] (1.22)	– [g]
	TOL	515 [e]	83.0 [e]	3.7 [e] (1.16)	– [g]
BDP-2	HEX	515 [e]	2.2 [e]	0.3 [e] (1.18)	– [g]
	TOL	515 [e]	4.4 [e]	0.4 [e] (1.38)	– [g]

[a] In nm. [b] Fluorescence quantum yields, **BDP-2** in toluene (Φ_F = 4.4%) as reference. [c] Fluorescence lifetimes (λ_{ex} = 510 nm), in ns, $c = 1.0 \times 10^{-5}$ M. [d] The transition dipole moment of $^1CT \rightarrow S_0$ transition in *n*-hexane, in Debye. [e] The transition of $^1LE \rightarrow S_0$. [f] The transition of $^1CT \rightarrow S_0$. [g] Not observed.

Table S2. Fluorescence Properties of the Compounds in polar solvents

	solvent	λ_F [a]	Φ_F [b]	τ_F [c] (χ^2)
BDP-PXZ-1	DCM	513	0.1	5.6 (1.06)
	MeCN	507	0.1	5.4 (1.06)
BDP-PXZ-2	DCM	– [f]	– [f]	– [f]
	MeCN	– [f]	– [f]	– [f]
BDP-PXZ-3	DCM	– [f]	– [f]	– [f]
	MeCN	– [f]	– [f]	– [f]
BDP-PXZ-4	DCM	507	0.03	4.7 (1.42)
	MeCN	506	0.08	4.1 (1.13)
BDP-PXZ-5	DCM	516	0.2	2.9 (1.55)
	MeCN	512	0.1	1.8 (1.18)
BDP-PXZ-6	DCM	520	0.01	2.9
	MeCN	518	0.03	2.3

[a] In nm. [b] Fluorescence quantum yields, **BDP-2** (Φ_F = 4.4% in toluene) as standard. [c] Fluorescence lifetimes (λ_{ex} = 510 nm), in ns, $c = 1.0 \times 10^{-5}$ M. [d] Radiative rate constant $k_r = \Phi/\tau$, in 10^7 s^{-1}. [e] Non-radiative rate constant $k_{nr} = (1-\Phi)/\tau$, in 10^7 s^{-1}. [f] Not observed.

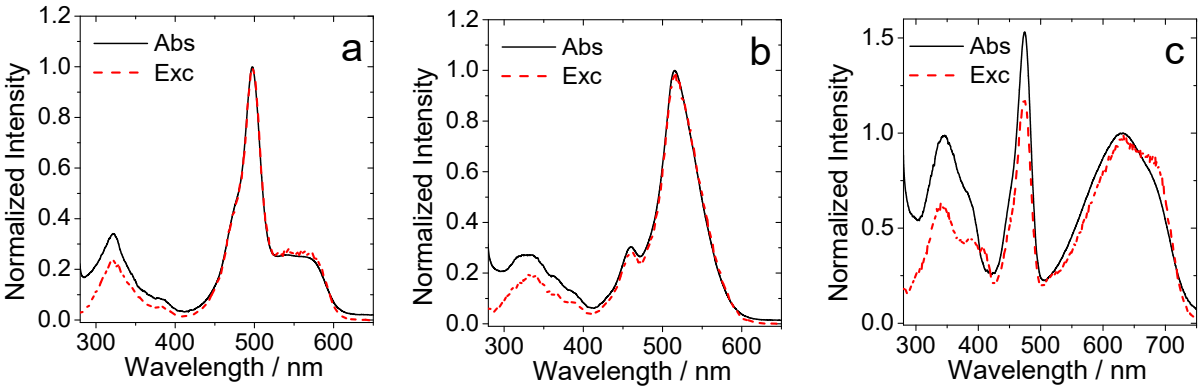

Figure S41. Normalized fluorescence excitation spectra and UV–Vis absorption spectra. (a) **BDP-PXZ-2**, λ_{em} = 650 nm; (b) **BDP-PXZ-3**, λ_{em} = 650 nm; (c) **BDP-PXZ-4**, λ_{em} = 775 nm. c = 1.0 × 10^{-6} M in *n*-hexane. 20 °C.

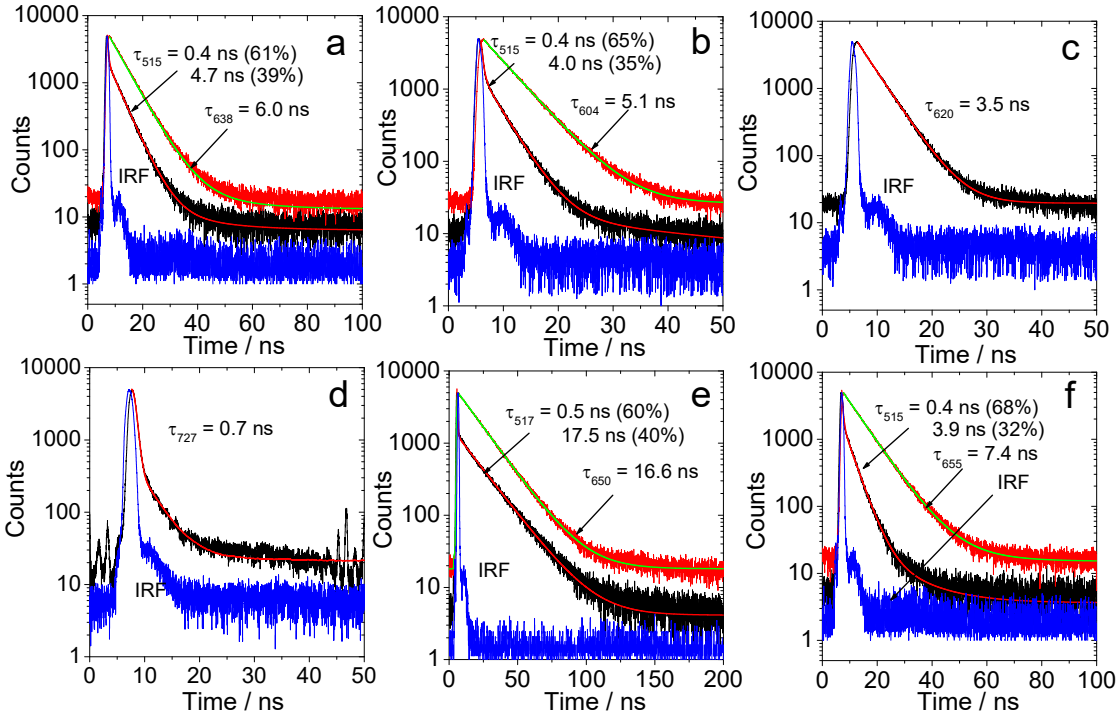

Figure S42. Fluorescence decay curves of (a) **BDP-PXZ-1** in toluene at 515 nm (χ^2 = 1.31) and 638 nm (χ^2 = 1.06), λ_{ex} = 510 nm; (b) **BDP-PXZ-2** in *n*-hexane at 515 nm (χ^2 = 1.24) and 604 nm (χ^2 = 1.05), λ_{ex} = 445 nm. (c) **BDP-PXZ-3** in *n*-hexane at 620 nm (χ^2 = 1.09), λ_{ex} = 510 nm; (d) **BDP-PXZ-4** in *n*-hexane at 727 nm (χ^2 = 2.59), λ_{ex} = 445 nm; (e) **BDP-PXZ-5** in toluene at 517 nm (χ^2 = 1.44) and 650 nm (χ^2 = 1.08), λ_{ex} = 510 nm; (f) **BDP-PXZ-6** in *n*-hexane at 515 nm (χ^2 = 1.51) and 655 nm (χ^2 = 1.05), λ_{ex} = 510 nm. The time resolution is 100 ps ~ 50 μs; Repetition rates of the EPL pulsed laser are 20 MHz for 50 ns time range, 10 MHz for 100 ns time range and 5 MHz for 200 ns time range. All the solvents were deaerated, c =1.0 × 10^{-5} M. 20 °C.

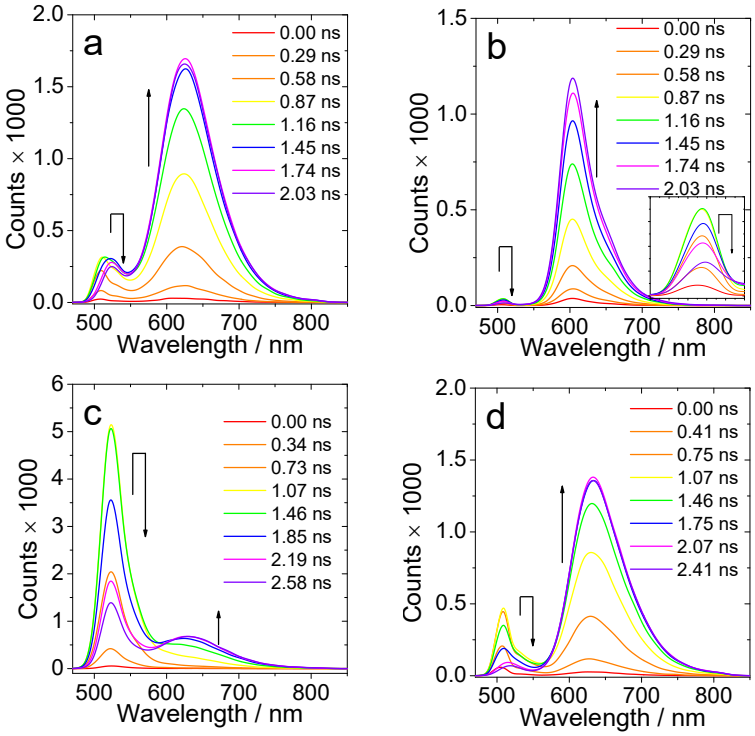

Figure S43. Time-resolved fluorescence emission spectra of (a) **BDP-PXZ-1**; (b) **BDP-PXZ-2**, insert: range 480–530 nm; (c) **BDP-PXZ-5** and (d) **BDP-PXZ-6**. (a) and (c) in deaerated toluene, (c) and (d) in deaerated *n*-hexane. $c = 1.0 \times 10^{-5}$ M, $\lambda_{ex} = 510$ nm. 20 °C.

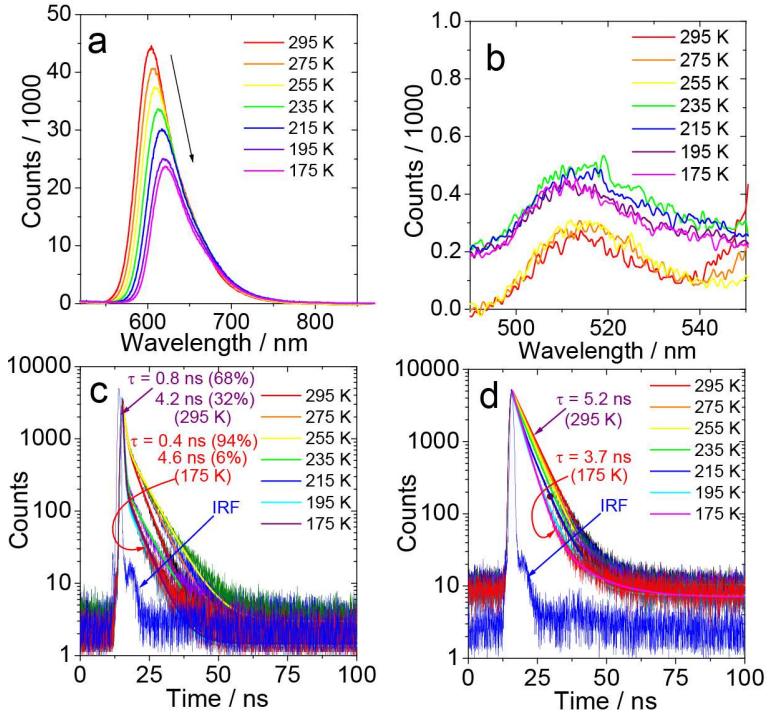

Figure S44. Temperature-dependent fluorescence emission spectra of the LE band of **BDP-PXZ-2** in deaerated *n*-hexane. (a) fluorescence spectra, (b) zoom in the region of 490 nm–550 nm, (c) decay kinetics at 517 nm (LE state) and (d) decay kinetics at 604 nm (CT emission). $c = 1.0 \times 10^{-5}$ M. The time resolution is 100 ps; Repetition rates are 10 MHz for 100 ns time range and 5 MHz for 200 ns time range.

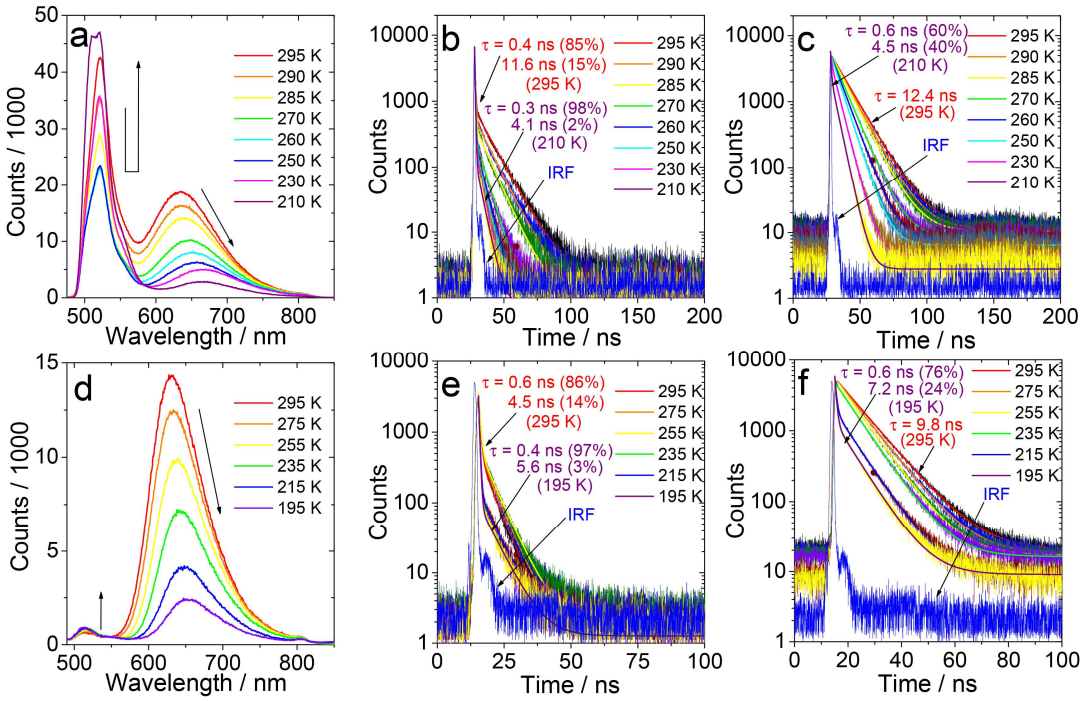

Figure S45. Temperature-dependent fluorescence emission spectra of **BDP-PXZ-5** and **BDP-PXZ-6**. **BDP-PXZ-5** in deaerated toluene, λ_{ex} = 510 nm (a) fluorescence spectra, (b) decay kinetics at 523 nm (LE state) and (c) decay kinetics at 634 nm (CT state). **BDP-PXZ-6** in deaerated *n*-hexane, λ_{ex} = 445 nm (d) fluorescence spectra, (e) decay kinetics at 517 nm (LE state) and (f) decay kinetics at 630 nm (CT state). $c = 1.0 \times 10^{-5}$ M. The time resolution is 100 ps; Repetition rates are 10 MHz for 100 ns time range and 5 MHz for 200 ns time range.

Table S3. The Single Oxygen Quantum Yields (Φ_Δ) and Triplet Quantum Yields (Φ_T) of Compounds in Different Solvents

	BDP-PXZ-1	BDP-PXZ-2	BDP-PXZ-3	BDP-PXZ-4	BDP-PXZ-5	BDP-PXZ-6
HEX	10.5 [a]/27.9 [b]	27.8 [a]/27.7 [b]	2.3 [a]/2.7 [a]	0 [a]/0 [a]	0 [a]/0.7 [b]	23.3 [a]/24.6 [b]
TOL	41.9 [a]/53.8 [b]	7.4 [a]/5.9 [b]	4.4 [a]/0.9 [a]	2.3 [a] /- [a]	31.5 [a]/26.5 [b]	– [c] /– [c]
DCM	0.7 [a]	– [c]	– [c]	– [c]	– [c]	– [c]
ACN	– [c]	– [c]	– [c]	– [c]	– [c]	– [c]

[a] Singlet oxygen quantum yield, **diiodo-BDP-1** as standard (Φ_Δ = 0.85 in toluene). [b] Triplet quantum yield **diiodo-BDP-1** as standard (Φ_T = 0.88 in toluene). [c] Not observed.

5.0 Nanosecond Time-Resolved Transient Absorption Spectra and the Kinetic Model.

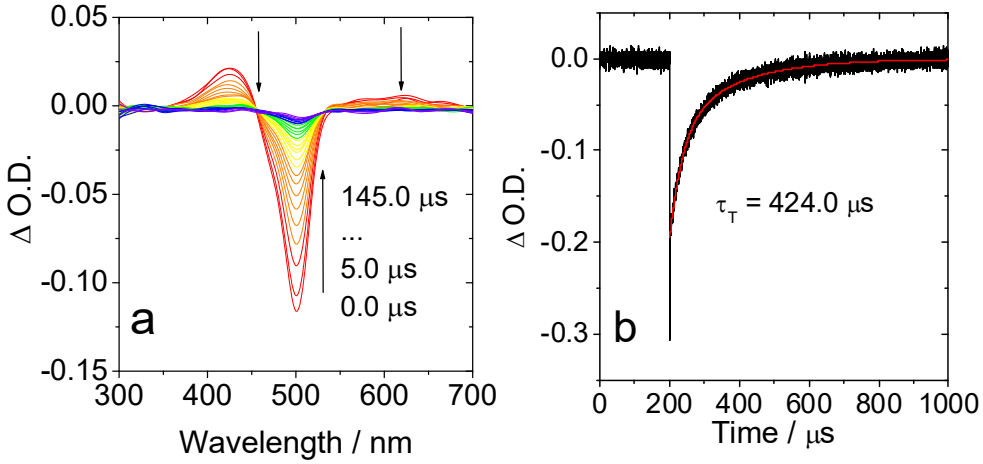

Figure S46. Nanosecond transient absorption spectra of **BDP-PXZ-1**. (a) transient absorption spectra and (b) Decay trace at 501 nm. λ_{ex} = 495 nm, c = 1.0 × 10^{-5} M, in deaerated *n*-hexane, 20 °C. The τ_T is the intrinsic lifetime obtained by fitting τ_T in two different concentrations.

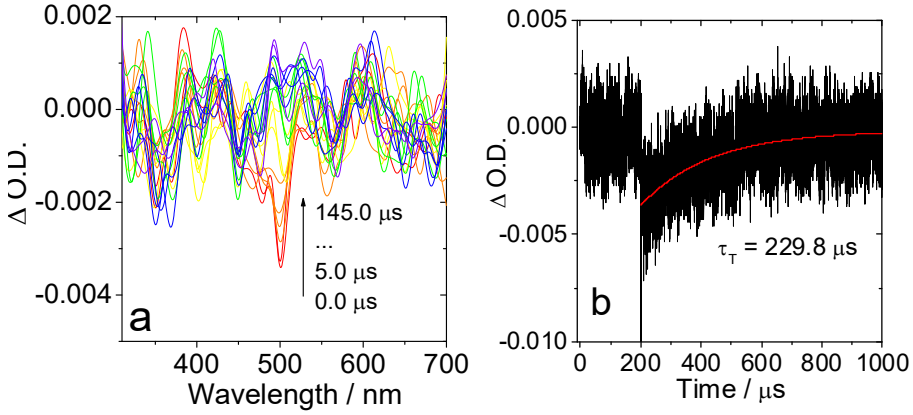

Figure S47. Nanosecond transient absorption spectra of **BDP-PXZ-1**. (a) transient absorption spectra and (b) Decay trace at 501 nm. λ_{ex} = 495 nm, c = 1.0 × 10^{-5} M, in deaerated DCM, 20 °C.

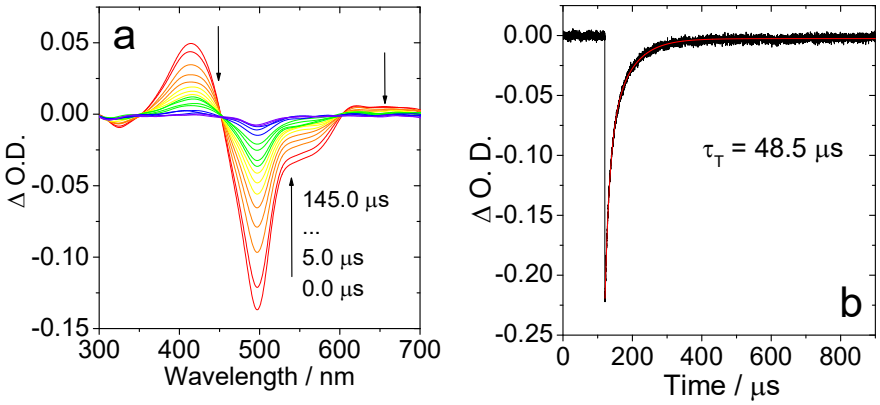

Figure S48. Nanosecond transient absorption spectra of **BDP-PXZ-2**. (a) Transient absorption spectra and (b) Decay trace at 497 nm. λ_{ex} = 560 nm, in deaerated *n*-hexane, $c = 1.0 \times 10^{-5}$ M, 20 °C.

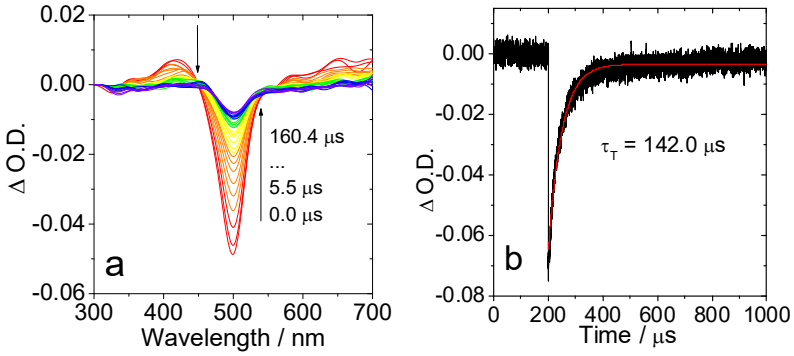

Figure S49. Nanosecond transient absorption spectra of **BDP-PXZ-2**. (a) transient absorption spectra and (b) decay trace at 497 nm. In deaerated toluene, λ_{ex} = 493 nm, $c = 1.0 \times 10^{-5}$ M, 20 °C. The τ_T is the intrinsic lifetime obtained by fitting τ_T in two different concentrations.

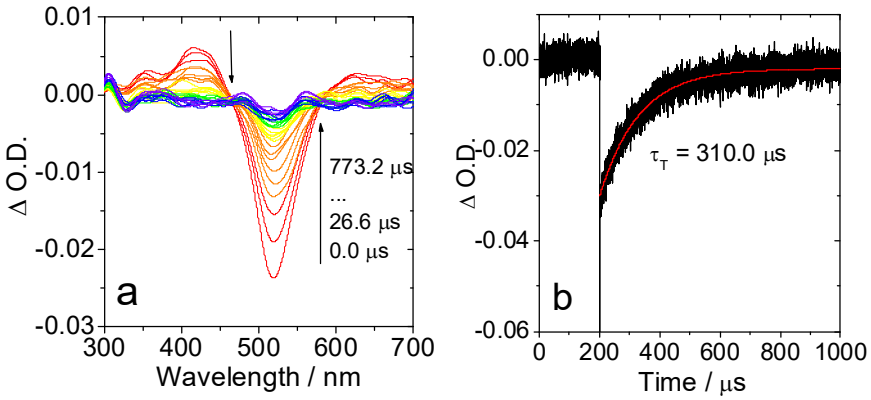

Figure S50. Nanosecond transient absorption spectra of **BDP-PXZ-3**. (a) Transient absorption spectra and (b) Decay trace at 515 nm. In deaerated *n*-hexane, λ_{ex} = 510 nm, c = 1.0 × 10^{-5} M, 20 °C. The τ_T is the intrinsic lifetime obtained by fitting τ_T in two different concentrations.

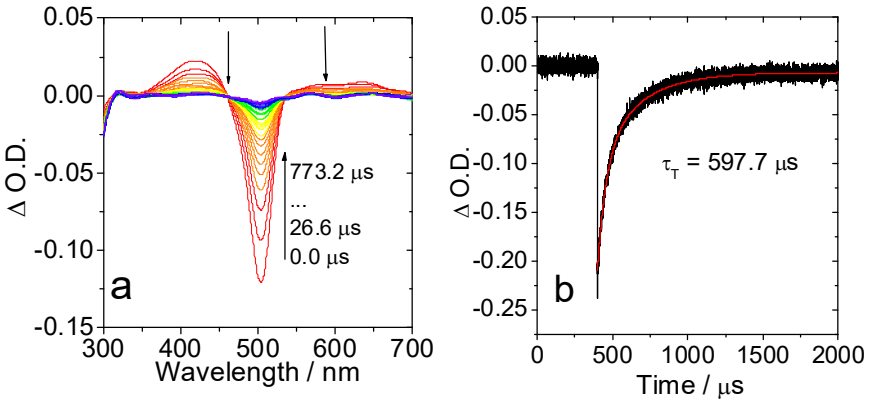

Figure S51. Nanosecond transient absorption spectra of **BDP-PXZ-5**. (a) Transient absorption spectra and (b) Decay trace at 503 nm. In deaerated toluene, λ_{ex} = 495 nm, c = 1.0 × 10^{-5} M, 20 °C. The τ_T is the intrinsic lifetime obtained by fitting τ_T in two different concentrations.

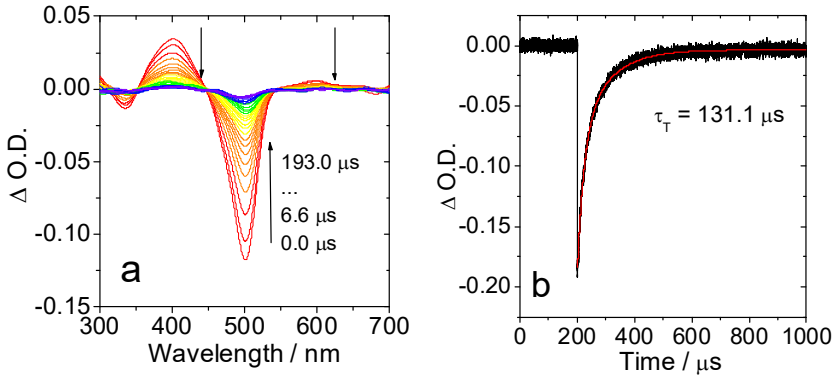

Figure S52. Nanosecond transient absorption spectra of **BDP-PXZ-6**. (a) Transient absorption spectra and (b) Decay trace at 503 nm. In deaerated *n*-hexane, λ_{ex} = 495 nm, c = 1.0 × 10^{-5} M, 20 °C. The τ_T is the intrinsic lifetime obtained by fitting τ_T in two different concentrations.

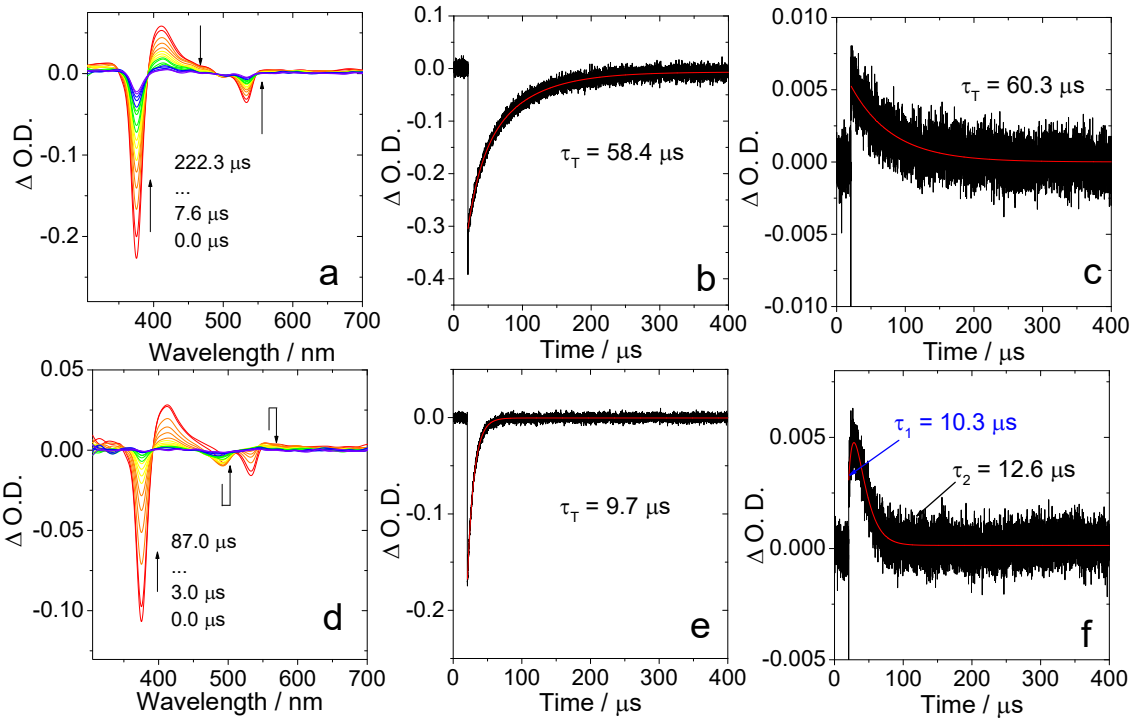

Figure S53. Intermolecular triplet−triplet energy transfer (TTET) from PtOEP to **BDP-PXZ-2**. (a) Transient absorption spectra; (b) Decay at 380 nm; (c) Decay at 550 nm; c (PtOEP) =2.5 × 10^{-6} M. And (d) Transient absorption spectra; (e) Decay at 380 nm; (f) Decay at 550 nm; c (PtOEP) =2.5 × 10^{-6} M, c (**BDP-PXZ-2**) =1.0 × 10^{-5} M. In acetonitrile. 20 °C.

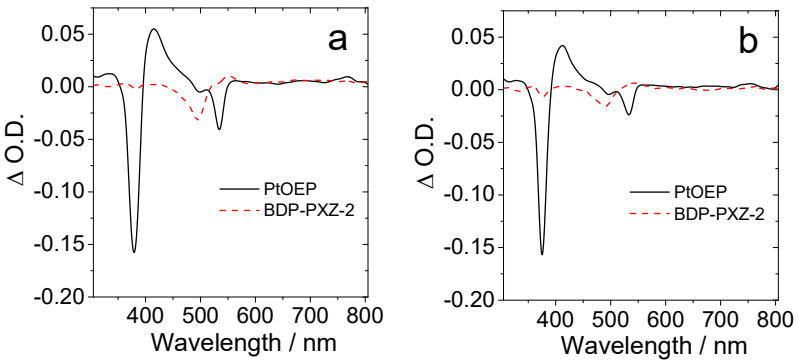

Figure S54. Species-associated difference spectra (SADS) of nanosecond transient absorption spectra of TTET (a) In DCM and (b) In acetonitrile. *c* (PtOEP) =2.5 × 10^{-6} M, *c* (**BDP-PXZ-2**) =1.0 × 10^{-5} M. 20 °C.

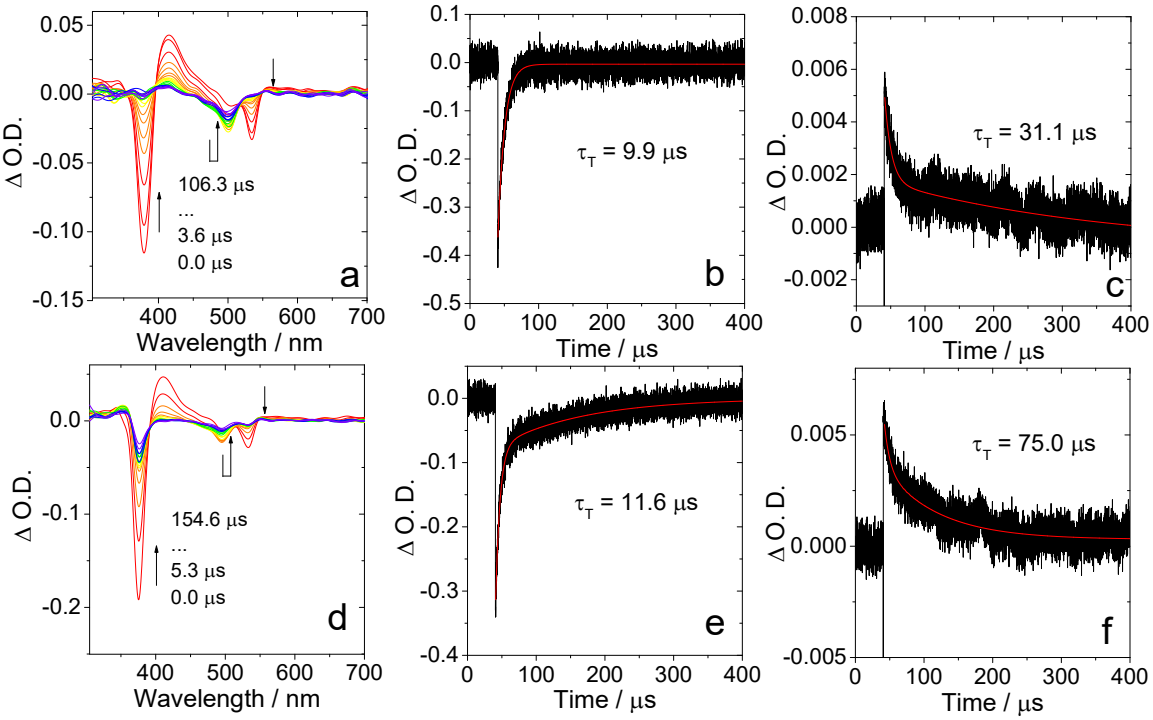

Figure S55. Intermolecular triplet−triplet energy transfer (TTET) from PtOEP to **BDP-2**. (a) Transient absorption spectra in DCM; (b) Decay at 380 nm; (c) Decay at 550 nm and (d) Transient absorption spectra in acetonitrile; (e) Decay at 380 nm; (f) Decay at 550 nm. *c* (PtOEP) =2.5 × 10^{-6} M, *c* (**BDP-2**) =1.0 × 10^{-5} M. 20 °C.

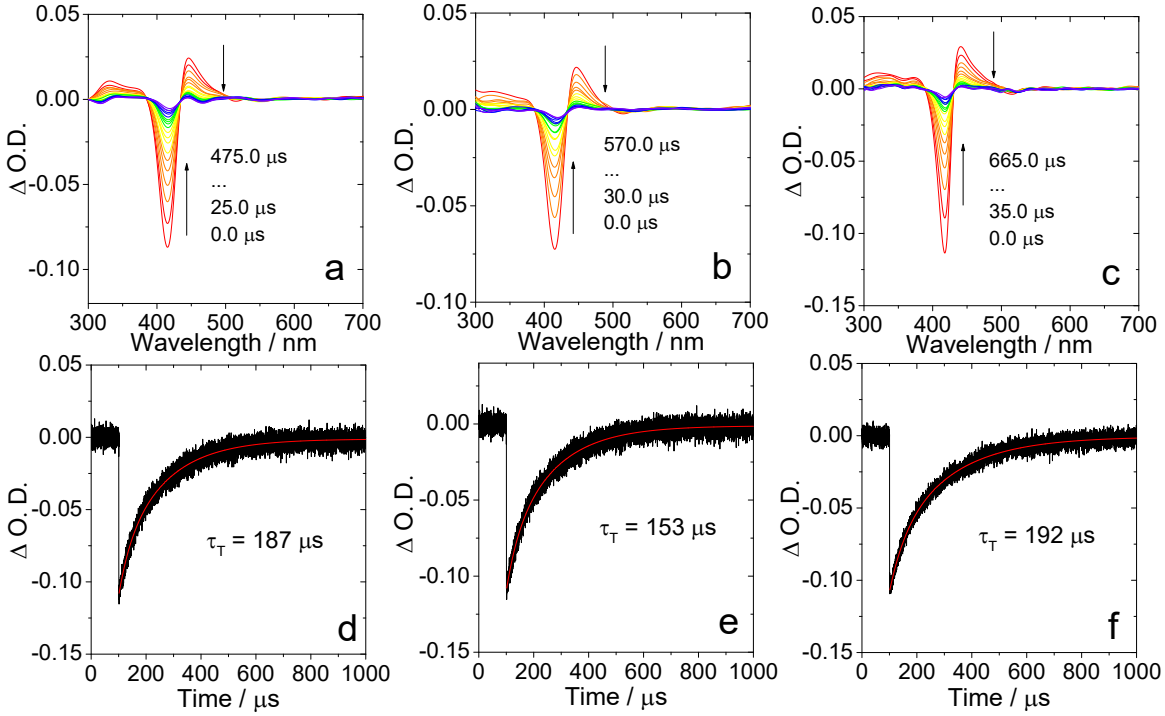

Figure S56. Intermolecular triplet−triplet energy transfer (TTET) from TPP to **BDP-PXZ-2** and **BDP-2** in DCM. Transient absorption spectra of (a) TPP; (b) TPP and **BDP-PXZ-2** and (c) TPP and **BDP-2**. Decay trace at 410 nm of (a) TPP; (e) TPP and **BDP-PXZ-2** and (f) TPP and **BDP-2**. *c* (TPP) =1 × 10^{-5} M, *c* (**BDP-2**) =2.0 × 10^{-5} M, *c* (**BDP-PXZ-2**) =2.0 × 10^{-5} M. 20 °C.

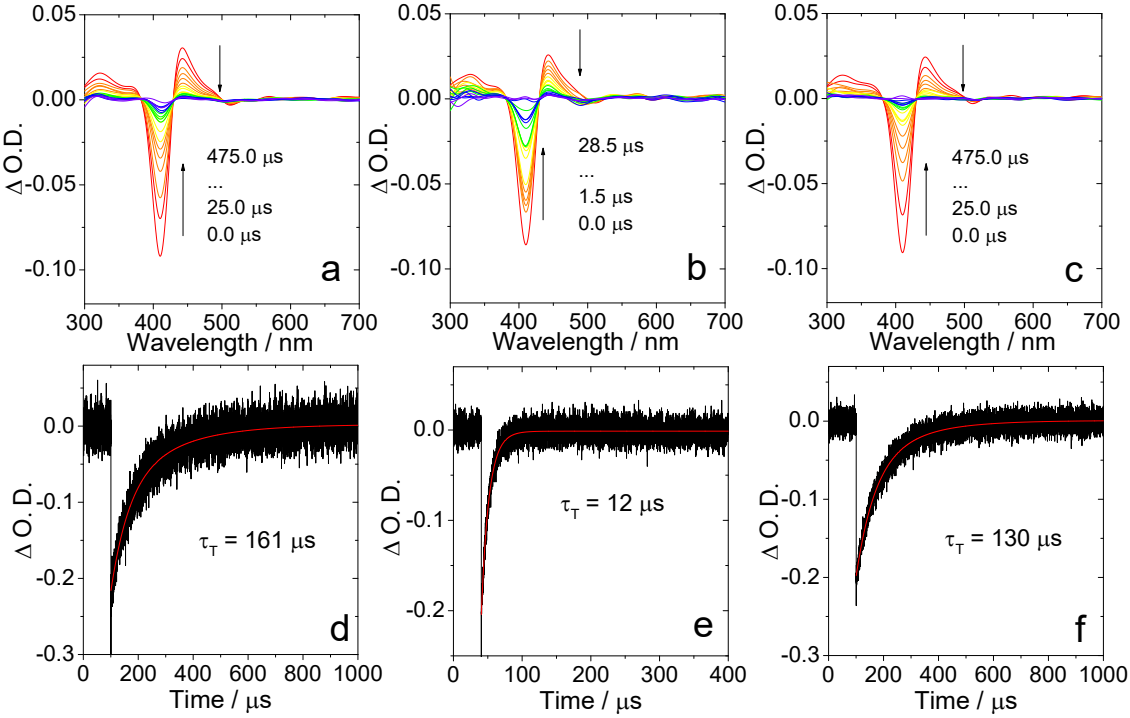

Figure S57. Intermolecular triplet−triplet energy transfer (TTET) from TPP to **BDP-PXZ-2** and **BDP-2** in ACN. Transient absorption spectra of (a) TPP; (b) TPP and **BDP-PXZ-2** and (c) TPP and **BDP-2**. Decay trace at 410 nm of (a) TPP; (e) TPP and **BDP-PXZ-2** and (f) TPP and **BDP-2**. *c* (TPP) =1 × 10^{-5} M, *c* (**BDP-2**) =2.0 × 10^{-5} M, *c* (**BDP-PXZ-2**) =2.0 × 10^{-5} M. 20 °C.

Intrinsic triplet state lifetime fitting:[S6]

When the intrinsic triplet state lifetime is long and the triplet state quantum yield is high, the triplet-triplet annihilation will contribute additional lifetime quenching factor to the decay of the transient absorption. Then triplet state lifetime will be quenched significantly and the experimental values will be shorter than the intrinsic lifetime. The corresponding differential equation for the triplet concentration

$$\frac{dc_T}{dt} = -k_1 c_T - k_2 c_T^2 \qquad \text{(Eq. S1a)}$$

has the solution

$$c_{\mathrm{T}}(t) = \frac{c_0 k_1}{\exp(k_1 t) \cdot (c_0 k_2 + k_1) - c_0 k_2} \qquad \text{(Eq. S1b)}$$

Where c_0 is the initial triplet concentration. This leads to the following expression for the transient absorption

$$A(t) = \frac{A_0 \tau_2/\tau_1}{\exp(t/\tau_1) \cdot (1 + \tau_2/\tau_1) - 1} \qquad \text{(Eq. S1c)}$$

Where A_0 is the initial transient absorption, $\tau_1 = 1/k_1$ is the intrinsic (unimolecular) lifetime of the triplet, and $\tau_2 = 1/c_0 k_2$. We fitted the data sets of **BDP-PXZ-1**, **BDP-PXZ-2**, **BDP-PXZ-3**, **BDP-PXZ-5** and **BDP-PXZ-6** triplet state lifetime values simultaneously by Eq. S1c, with variation of all parameters (A_0, τ_1, τ_2), but with the intrinsic triplet lifetime constrained to the same value in all data sets.

6.0 Femtosecond Transient Absorption Spectroscopy.

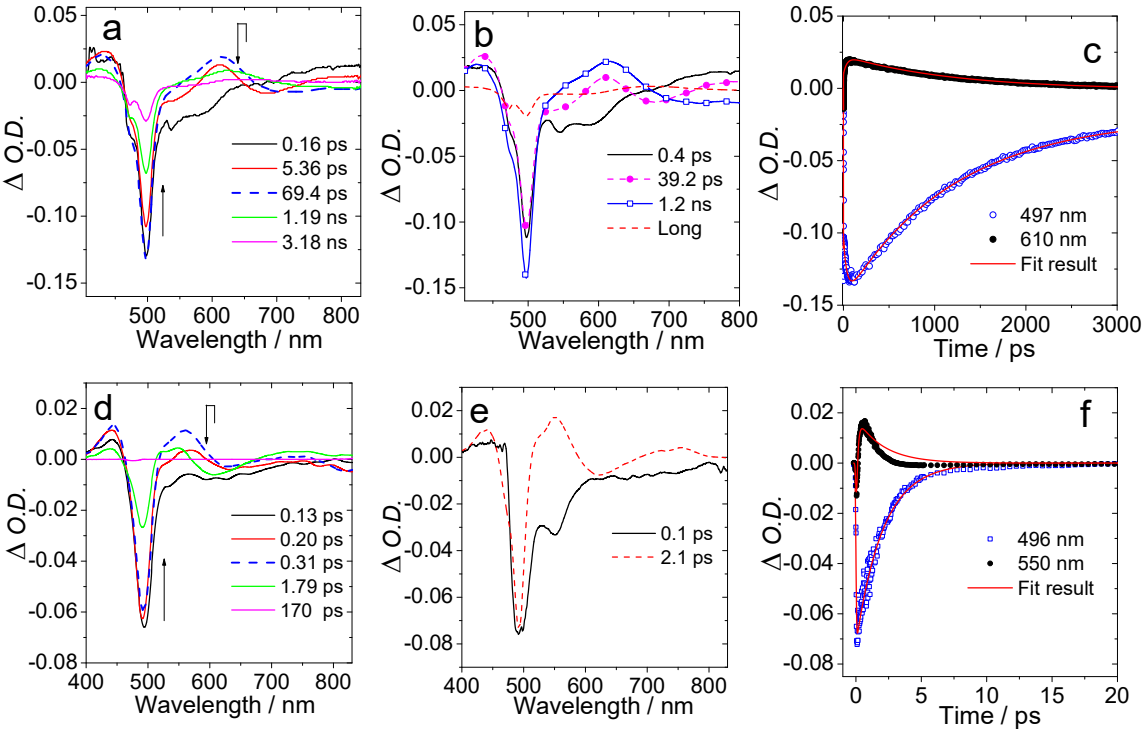

Figure S58. Femtosecond transient absorption spectra recorded for compound **BDP-PXZ-2** (a) Transient absorption spectra in *n*-hexane. λ_{ex} = 475 nm, $c = 1 \times 10^{-5}$ M. (b) Species-associated difference spectra (SADS) and (c) Kinetic traces at selected wavelengths. (d) Transient absorption spectra in ACN. λ_{ex} = 480 nm, $c = 1 \times 10^{-5}$ M. (e) Species-associated difference spectra (SADS) and (f) Kinetic traces at selected wavelengths. SADS were obtained by global fitting in sequential order. 20 °C.

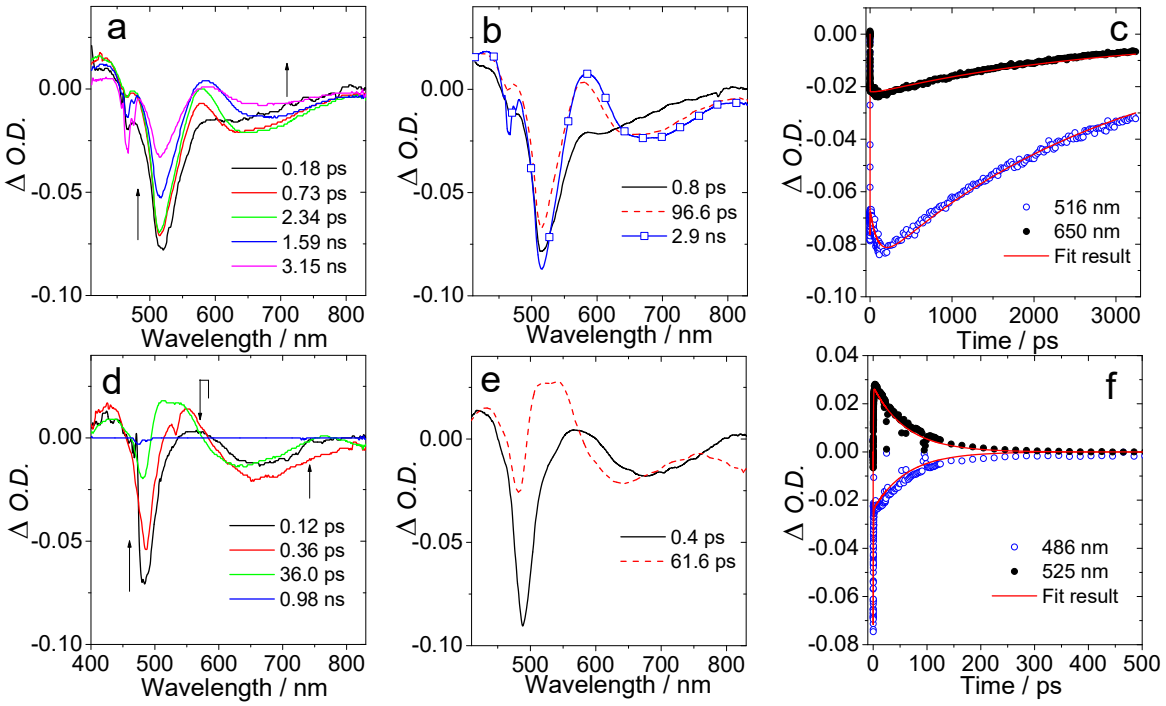

Figure S59. Femtosecond transient absorption spectra recorded for **BDP-PXZ-3** (a) Transient absorption spectra in *n*-hexane. λ_{ex} = 460 nm, c = 1 × 10^{-5} M. (b) Species-associated difference spectra (SADS) and (c) Kinetic traces at selected wavelengths. Femtosecond transient data recorded for **BDP-PXZ-4** (d) Transient absorption spectra in toluene. λ_{ex} = 480 nm, c = 1 × 10^{-5} M. (e) Species-associated difference spectra (SADS) and (f) Kinetic traces at selected wavelengths. SADS were obtained by global fitting in sequential order. 20 °C.

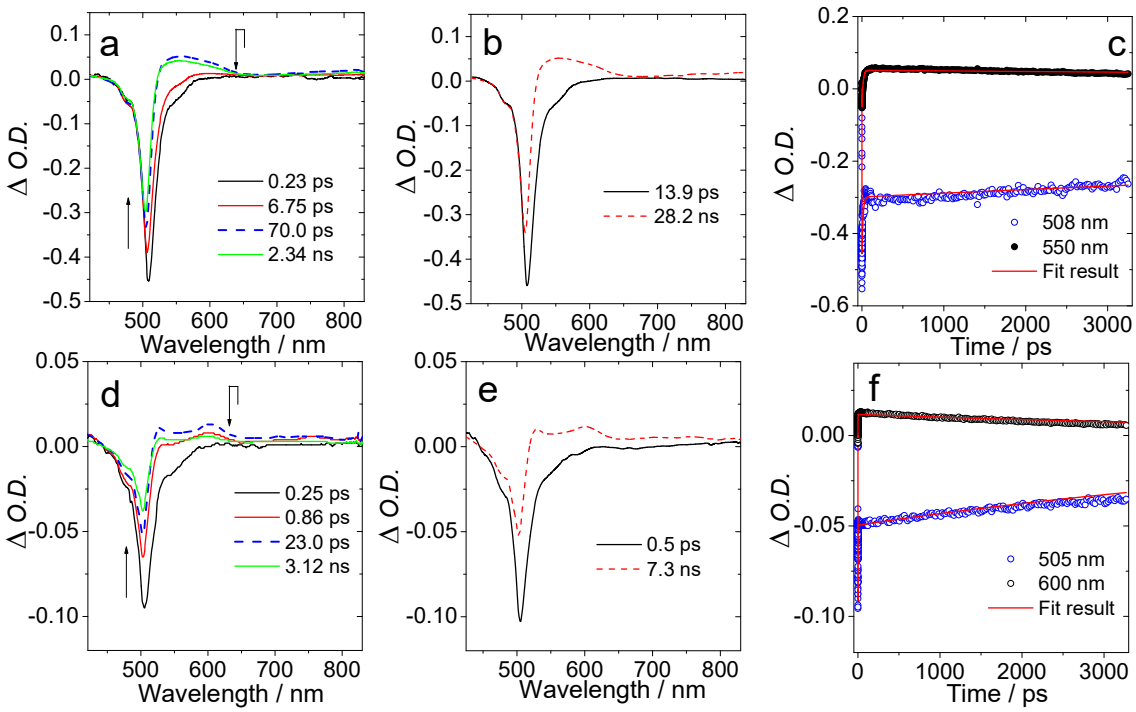

Figure S60. Femtosecond transient absorption spectra recorded for **BDP-PXZ-5** (a) Transient absorption spectra in toluene. λ_{ex} = 505 nm, $c = 1 \times 10^{-5}$ M. (b) Species-associated difference spectra (SADS) and (c) Kinetic traces at selected wavelengths. Femtosecond transient data recorded for **BDP-PXZ-6** (d) Transient absorption spectra in *n*-hexane. λ_{ex} = 500 nm, $c = 1 \times 10^{-5}$ M. (e) Species-associated difference spectra (SADS) and (f) Kinetic traces at selected wavelengths. SADS were obtained by global fitting in sequential order. 20 °C.

7.0 Electrochemical Characterization

Table S4. Redox Potentials of the Reference Compounds [a]

	***E*(ox)** [c]/ **V**	***E*(red)** [c]/ **V**
BDP-1	+0.79	–1.65
BDP-2	– [b]	–1.22
Phenoxazine	+0.22	– [b]
***N*-butylphenoxazine**	+0.27	– [b]

[a] Cyclic voltammetry in N_2 saturated DCM containing a 0.10 M Bu_4NPF_6 supporting electrolyte; Counter electrode is Pt electrode; working electrode is glassy carbon electrode; $Ag/AgNO_3$ couple as the reference electrode. [b] Not observed. [c] The value is obtained by setting the oxidation potential of Fc^+/Fc as 0.

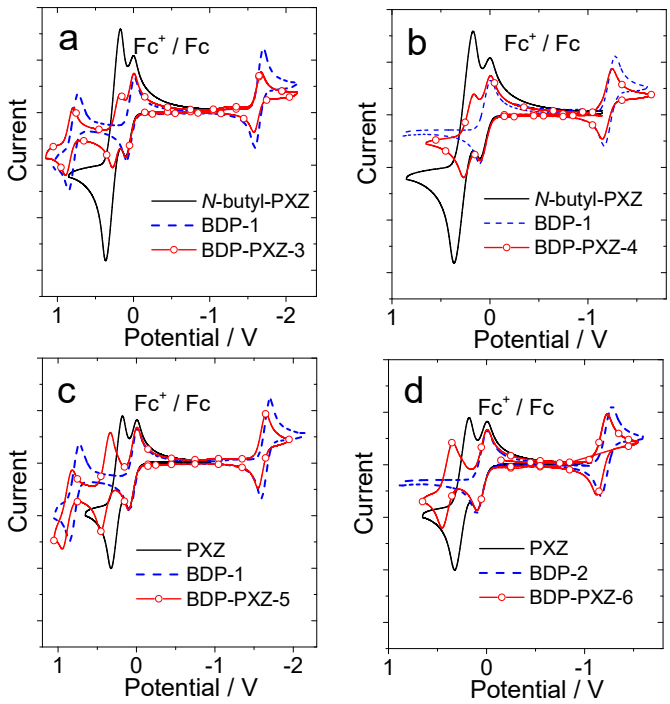

Figure S61. Cyclic voltammogram of the compounds. (a) ***N*-butyl-PXZ**, **BDP-1** and **BDP-PXZ-3**, (b) ***N*-butyl-PXZ**, **BDP-2** and **BDP-PXZ-4**, (c) **PXZ**, **BDP-1** and **BDP-PXZ-5**, (d) **PXZ**, **BDP-2** and **BDP-PXZ-6**. Ferrocene (Fc) was used as internal reference. In deaerated CH_2Cl_2 containing 0.10 M $Bu_4N[PF_6]$ as supporting electrolyte, $Ag/AgNO_3$ as reference electrode. Scan rates: 50 mV/s. $c = 1.0 \times 10^{-3}$ M, 20 °C.

8.0 Spectroelectrochemistry Data

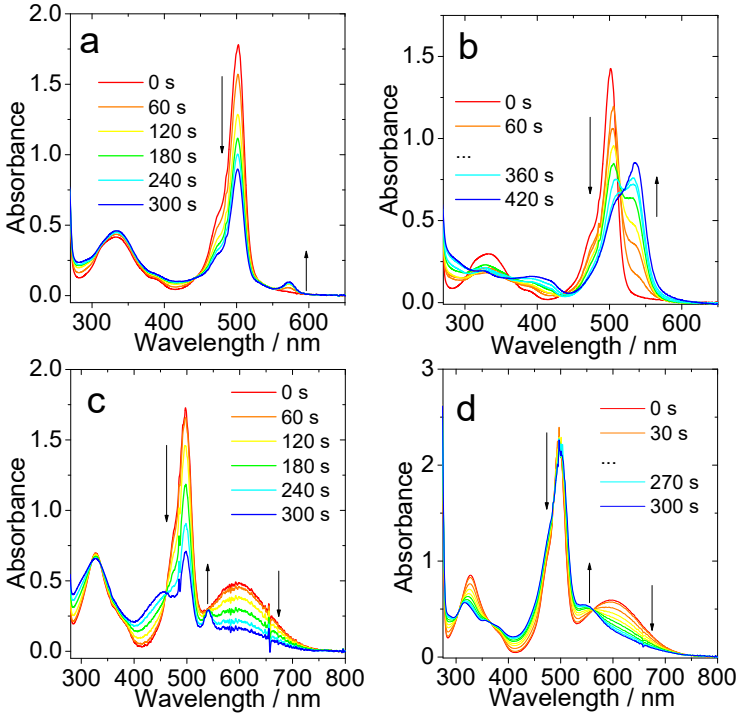

Figure S62. Spectroelectrochemistry traces of the UV-Vis absorption spectra observed at controlled-potential. (a) **BDP-PXZ-1** at −1.65 V. (b) **BDP-PXZ-1** at +0.60 V. (c) **BDP-PXZ-2** at −1.26 V and (d) **BDP-PXZ-2** at +0.67 V. In solution of 0.10 M of $Bu_4N[PF_6]$ in DCM. $Ag/AgNO_3$ as reference electrode. 20 °C.

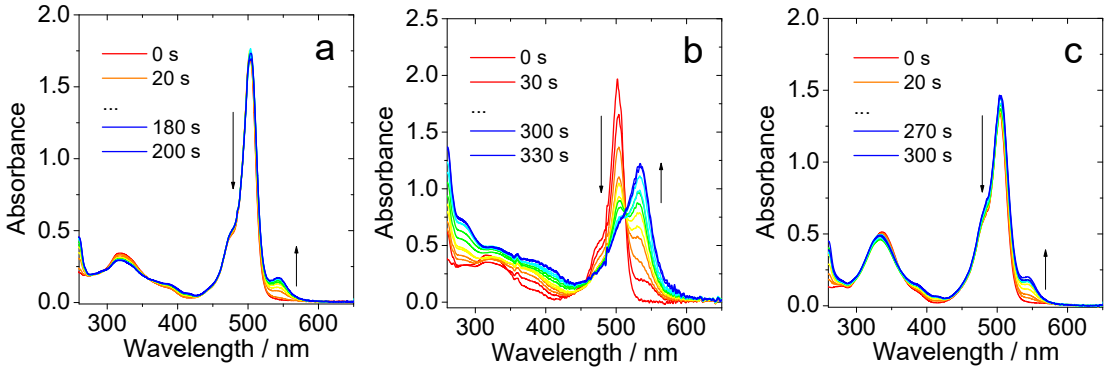

Figure S63. Spectroelectrochemistry traces of the UV-Vis absorption spectra observed at controlled-potential. (a) **BDP-PXZ-5** at −1.42 V (b) **BDP-PXZ-5** at +0.59 V and (c) **BDP-PXZ-6** at +0.60 V. In solution of 0.10 M $Bu_4N[PF_6]$ in DCM. $Ag/AgNO_3$ as reference electrode. 20 °C.

9.0 TREPR Spectroscopy.

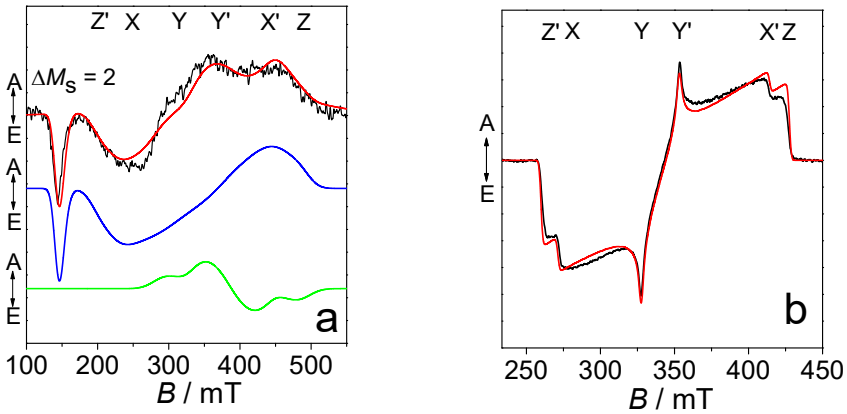

Figure S64. Experimental TREPR spectra (black line) and simulations (red line) of the compound (a) **BDP-PXZ-5** and (b) **BDP-PXZ-6**. The blue line and green line in (a) represent LE triplet state and ^{3}CT state, respectively. and Samples were excited by pulsed laser at 532 nm with energy 10 mJ per pulse. Solvent: isopropanol/toluene (1:1 = v/v). $c = 3.0 \times 10^{-4}$ M. $T = 80$ K.

10.0 TTA Upconversion.

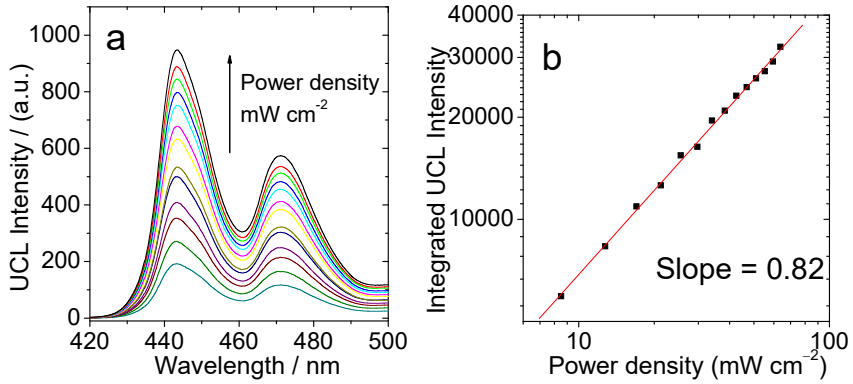

Figure S65. TTA upconversion with **BDP-PXZ-1** as the triplet photosensitizer and perylene (Py) as the acceptor, λ_{ex} = 510 nm. (a) Upconverted luminescence spectra at different incident laser power densities. (b) Integrated upconversion emission intensity data from (a) plotted as a function of incident laser power density. Upconversion was performed upon excitation of the solution with a 510 nm continuous wave (cw) laser. c (photosensitizer) = 1.0×10^{-5} M, c (acceptor) = 8.0×10^{-6} M, in deaerated toluene, 20 °C.

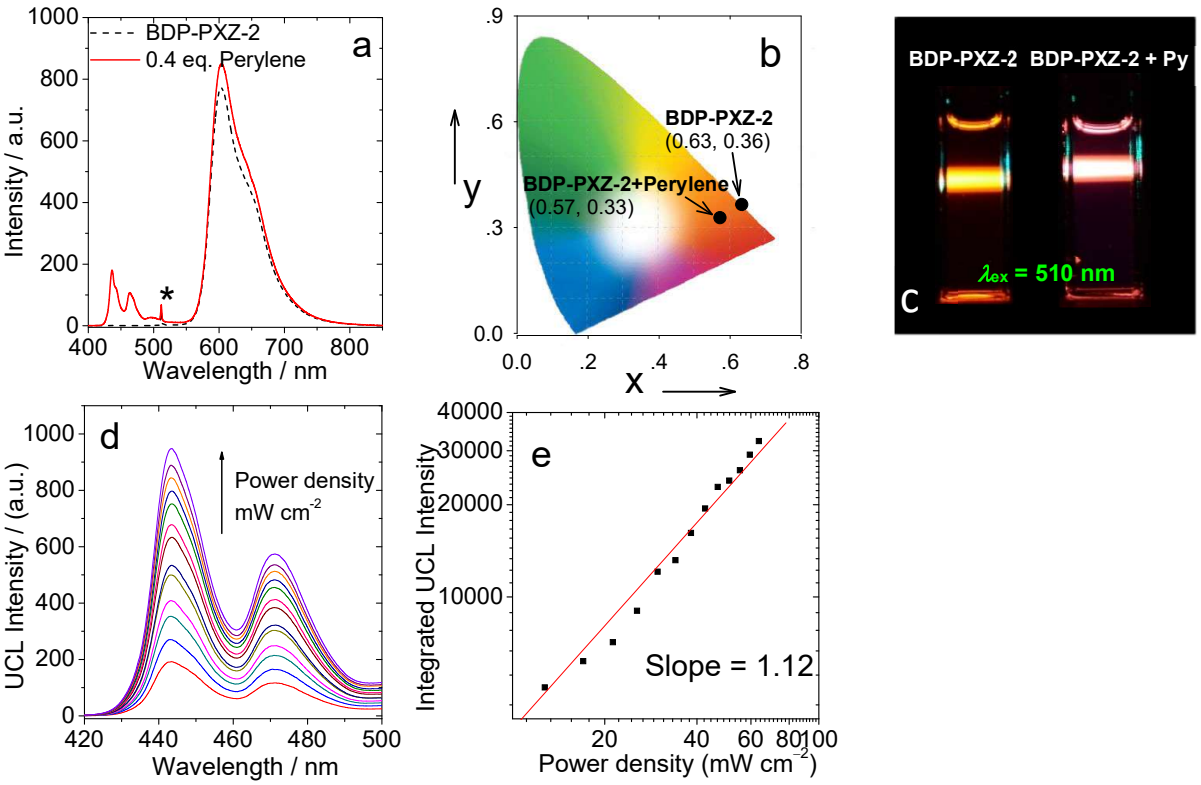

Figure S66. TTA upconversion with **BDP-PXZ-2** as the triplet photosensitizer and perylene (Py) as the acceptor, λ_{ex} = 510 nm. (a) Upconversion spectra, Φ_{UC} = 2.7%. (b) CIE diagram of **BDP-PXZ-2**. (c) The photographs of triplet photosensitizer alone and the upconversion. (d) Upconverted luminescence spectra at different incident power densities. (e) Integrated upconversion emission intensity data from part a plotted as a function of incident power density. Upconversion was performed upon excitation of the solution with 510 nm continuous laser (power density: 53.2 mW/cm^2). The asterisks indicate the scattered laser. *c* (photosensitizer) = 1.0×10^{-5} M, *c* (acceptor) = 4×10^{-6} M, in *n*-hexane, 20 °C.

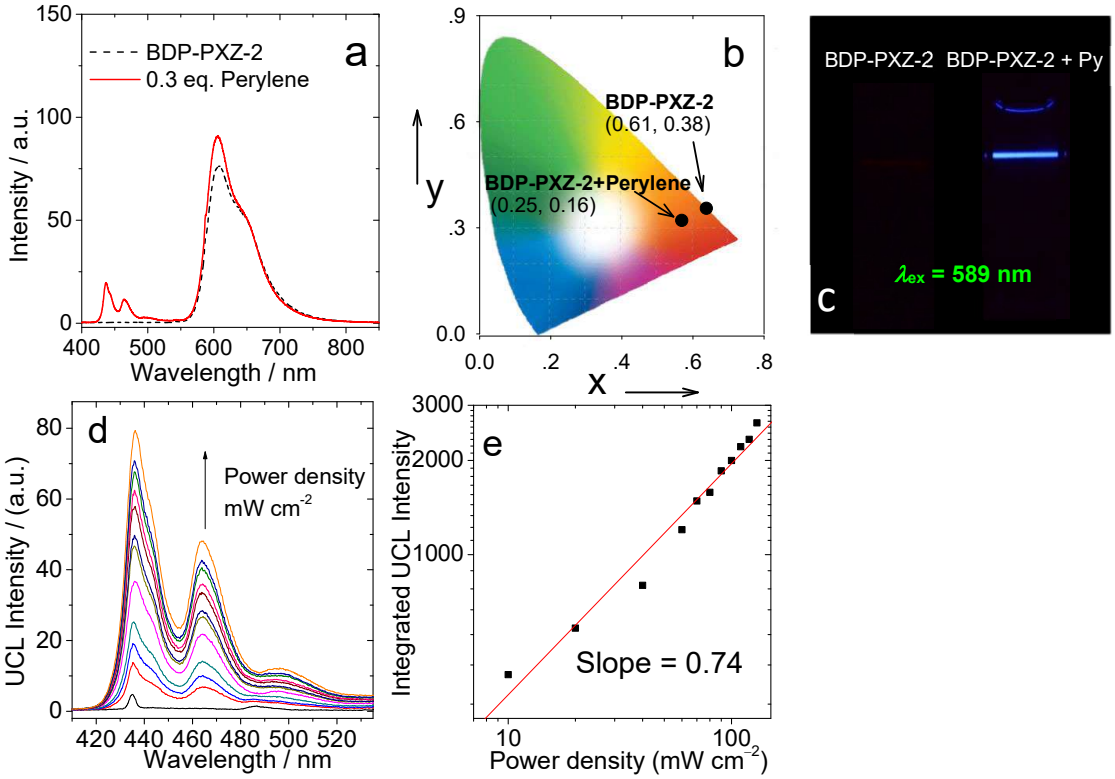

Figure S67. TTA upconversion with **BDP-PXZ-2** as the triplet photosensitizer and perylene (Py) as the acceptor, λ_{ex} = 589 nm. (a) Upconversion emission spectra and the corresponding (b) CIE diagram of **BDP-PXZ-2**. (c) The photographs of triplet photosensitizer alone and the upconversion, laser and CT emission are filtered by blue band pass filter (pass band: 380–520 nm). (d) Upconverted luminescence spectra at different incident power densities. (e) Integrated upconversion emission intensity data from part a plotted as a function of incident power density. Upconversion was performed upon excitation of the solution with a 589 nm continuous laser (power density: 125 mW/cm^2). *c* (photosensitizer) = 1.0 × 10^{-5} M, *c* (acceptor) = 3 × 10^{-6} M, in *n*-hexane, 20 °C.

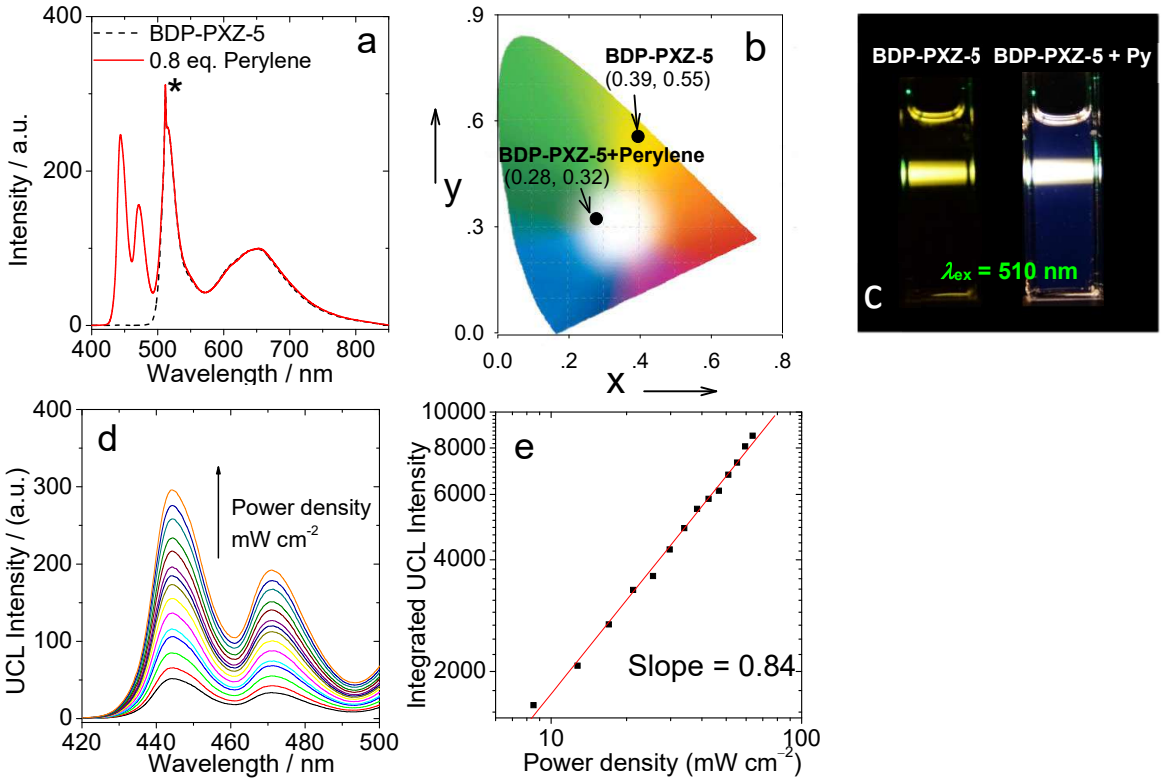

Figure S68. TTA upconversion with **BDP-PXZ-5** as the triplet photosensitizer and perylene (Py) as the acceptor, λ_{ex} = 510 nm. (a) Upconversion spectra, Φ_{UC} = 3.7%. (b) CIE diagram of **BDP-PXZ-5**. (c) The photographs of triplet photosensitizer alone and the upconversion. (d) Upconverted luminescence spectra at different incident power densities. (e) Integrated upconversion emission intensity data from part a plotted as a function of incident power density. Upconversion was performed upon excitation of the solution with 510 nm continuous laser (power density: 53.2 mW/cm^2). The asterisks indicate the scattered laser. *c* (photosensitizer) = 1.0×10^{-5} M, *c* (acceptor) = 8×10^{-6} M, in *n*-hexane, 20 °C.

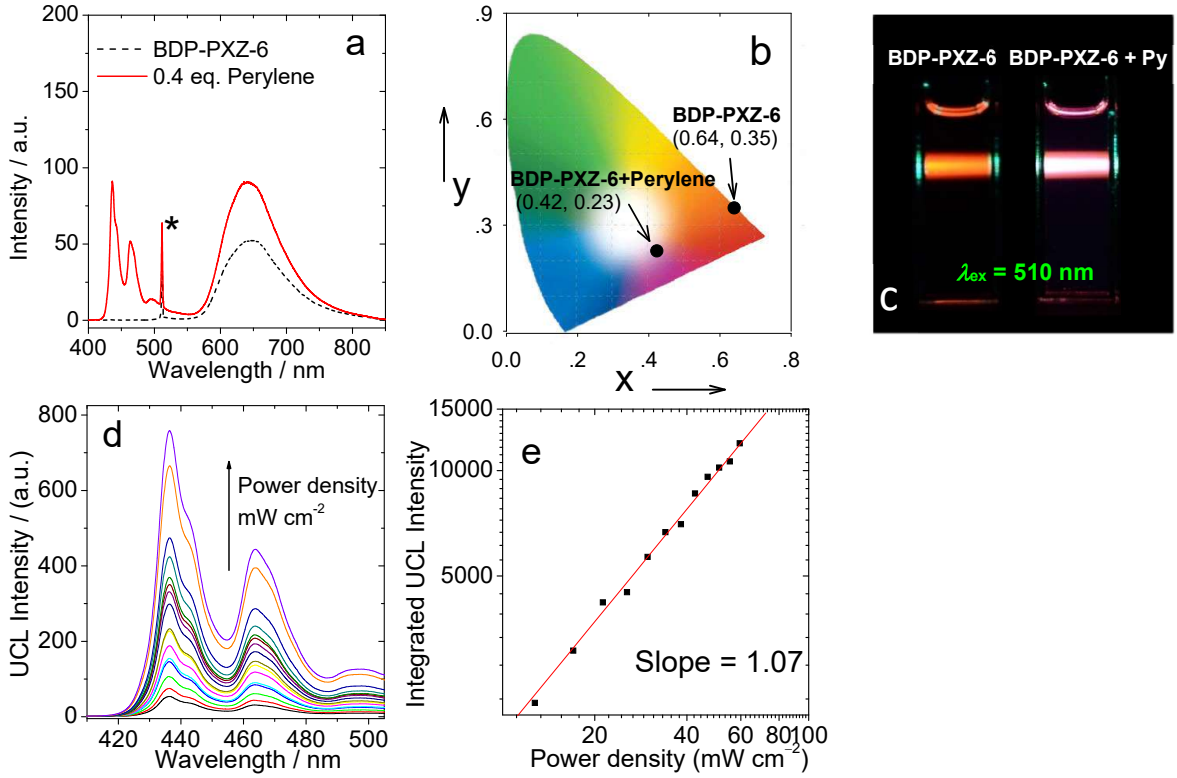

Figure S69. TTA upconversion with **BDP-PXZ-6** as the triplet photosensitizer and perylene (Py) as the acceptor, λ_{ex} = 510 nm. (a) Upconversion spectra, Φ_{UC} = 1.3%. (b) CIE diagram of **BDP-PXZ-6**. (c) The photographs of triplet photosensitizer alone and the upconversion. (d) Upconverted luminescence spectra at different incident power densities. (e) Integrated upconversion emission intensity data from part a plotted as a function of incident power density. Upconversion was performed upon excitation of the solution with 510 nm continuous laser (power density: 53.2 mW/cm^2). The asterisks indicate the scattered laser. *c* (photosensitizer) = 1.0 × 10^{-5} M, *c* (acceptor) = 4 × 10^{-6} M, in *n*-hexane, 20 °C.

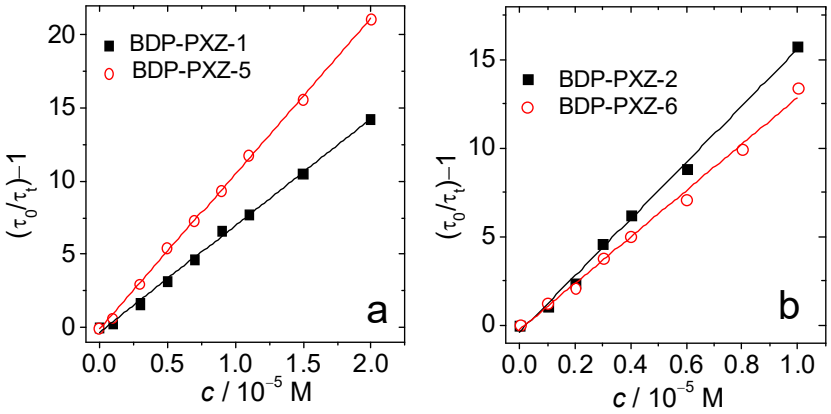

Figure S70. Stern−Volmer plot of quenching of the triplet state of compounds with perylene as the triplet acceptor (a) **BDP-PXZ-1** and **BDP-PXZ-5** in deaerated toluene; (b) **BDP-PXZ-2** and **BDP-PXZ-6** in deaerated *n*-hexane. *c* [triplet photosensitizer] = 1.0×10^{-5} M, 20 °C.

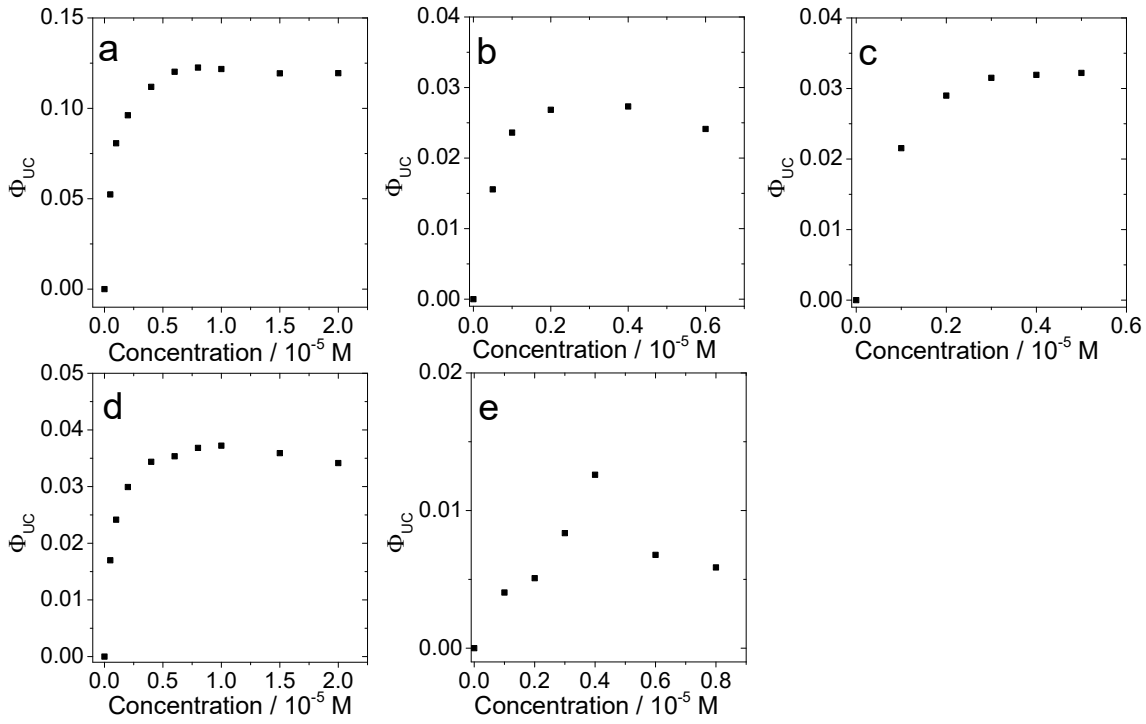

Figure S71. TTA upconversion quantum yield at different acceptor concentration. (a) **BDP-PXZ-1**, λ_{ex} = 510 nm, in toluene. Power density: 53.2 mW/cm^2 (b) **BDP-PXZ-2**, λ_{ex} = 510 nm, in *n*-hexane. Power density: 53.2 mW/cm^2. (c) **BDP-PXZ-2**, λ_{ex} = 589 nm, in *n*-hexane. (d) **BDP-PXZ-5**, λ_{ex} = 510 nm, in toluene. (e) **BDP-PXZ-6**, λ_{ex} = 510 nm, in *n*-hexane. *c* [triplet photosensitizer] = 1.0 × 10^{-5} M, 20 °C.

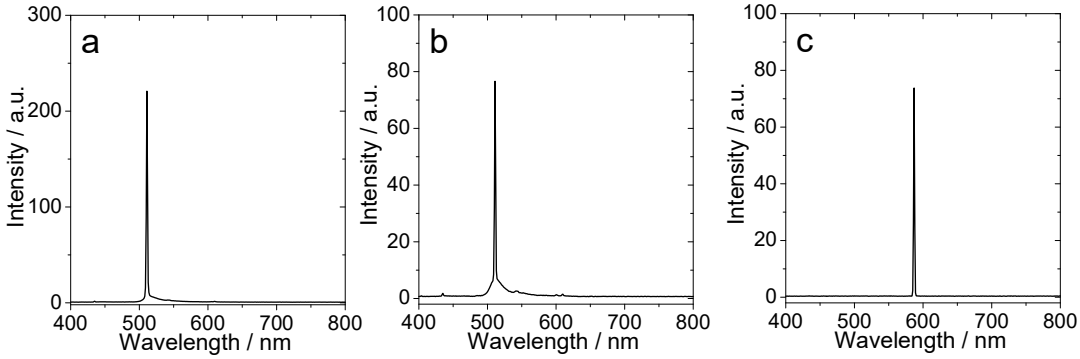

Figure S72. Emission of TTA-UC with only perylene. (a) 0.8×10^{-5} M, λ_{ex} = 510 nm, in toluene. (b) 0.4×10^{-5} M, λ_{ex} = 510 nm, in *n*-hexane and (c) 0.3×10^{-5} M, λ_{ex} = 589 nm, in *n*-hexane. Power density: 125 mW/cm^2. 20 °C.

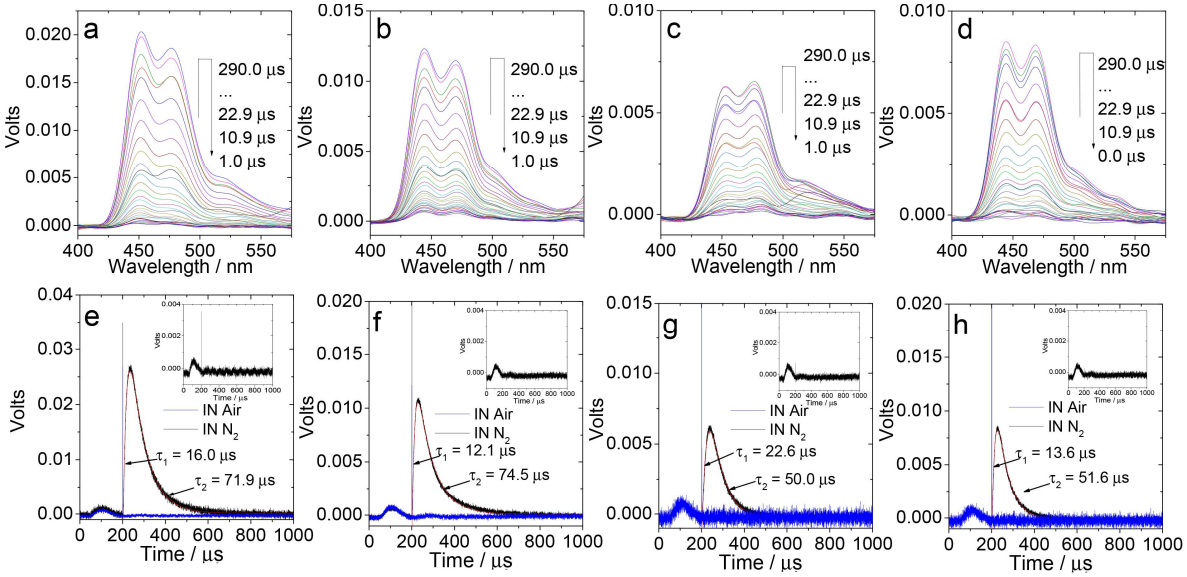

Figure S73. Delayed fluorescence observed in the TTA upconversion (perylene as the triplet acceptor). Excited at 510 nm (nanosecond pulsed OPO laser). (a) **BDP-PXZ-1** in toluene, (b) **BDP-PXZ-2** in *n*-hexane, (c) **BDP-PXZ-5** in toluene, (d) **BDP-PXZ-6** in *n*-hexane. Decay trace (e) at 445 nm of **BDP-PXZ-1** in toluene, (f) at 435 nm of **BDP-PXZ-2** in *n*-hexane, (g) at 445 nm of **BDP-PXZ-5** in toluene, (h) at 436 nm of **BDP-PXZ-6** in *n*-hexane. Insert: solvent decay trace. *c* (photosensitizer) = 1.0×10^{-5} M, 20 °C.

11.0 DFT Calculation.

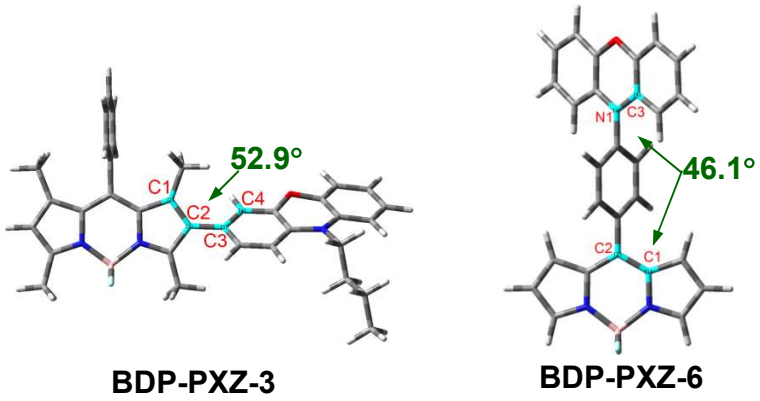

Figure S74. Optimized conformations and the dihedral angles of selected atoms of compounds **BDP-PXZ-3** and **BDP-PXZ-6** calculated by DFT at the B3LYP/6-31G(d) level with Gaussian 09W, based on the optimized ground state.

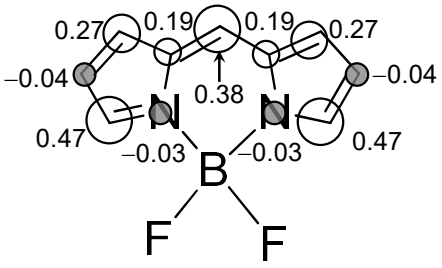

Figure S75. Isosurfaces of spin density of **BDP-2** at the optimized triplet state geometries. Calculation was performed at B3LYP/6-31G(d) level with Gaussian 09W. The numbers in the figure indicate the contribution of each atom to the total spin density.

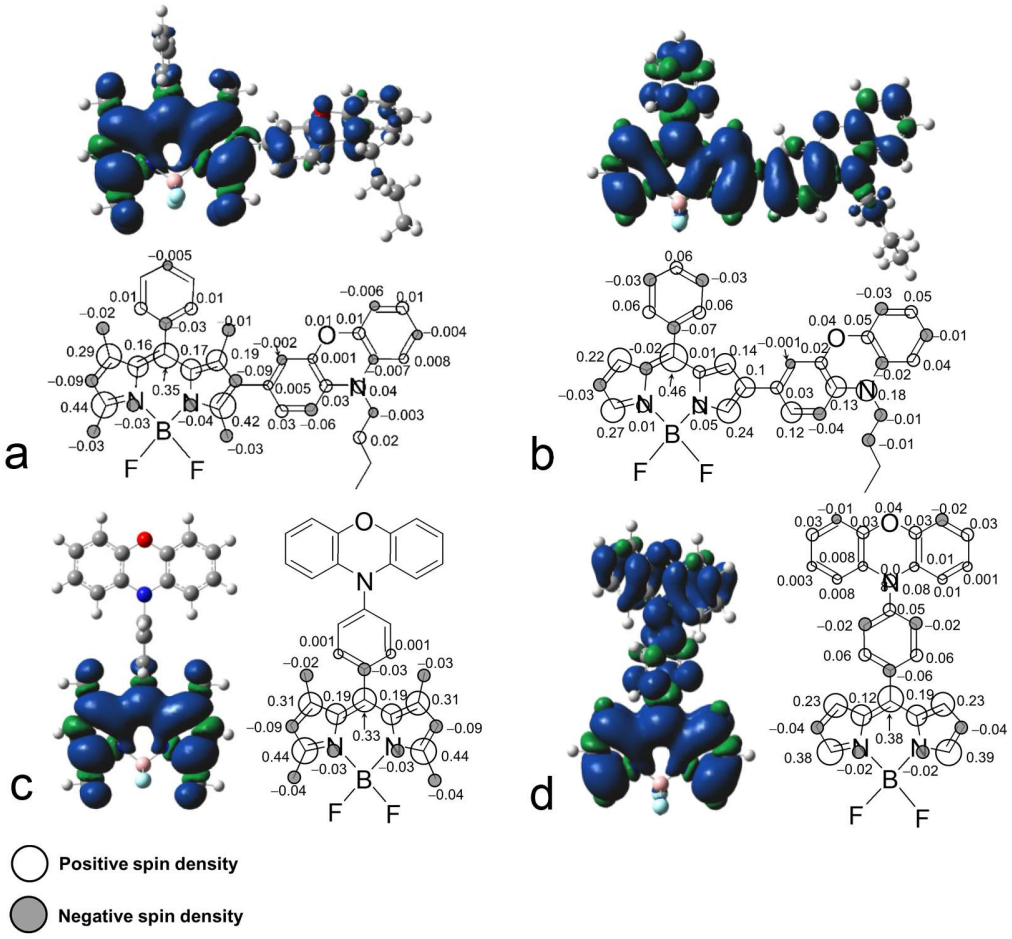

Figure S76. Isosurfaces of spin density of compounds at the optimized triplet state geometries. Calculation was performed at B3LYP/6-31G(d) level with Gaussian 09W. The numbers in the figure indicate the contribution of each atom to the total spin density. (a) **BDP-PXZ-3**; (b) **BDP-PXZ-4**; (c) **BDP-PXZ-5** and (d) **BDP-PXZ-6**.

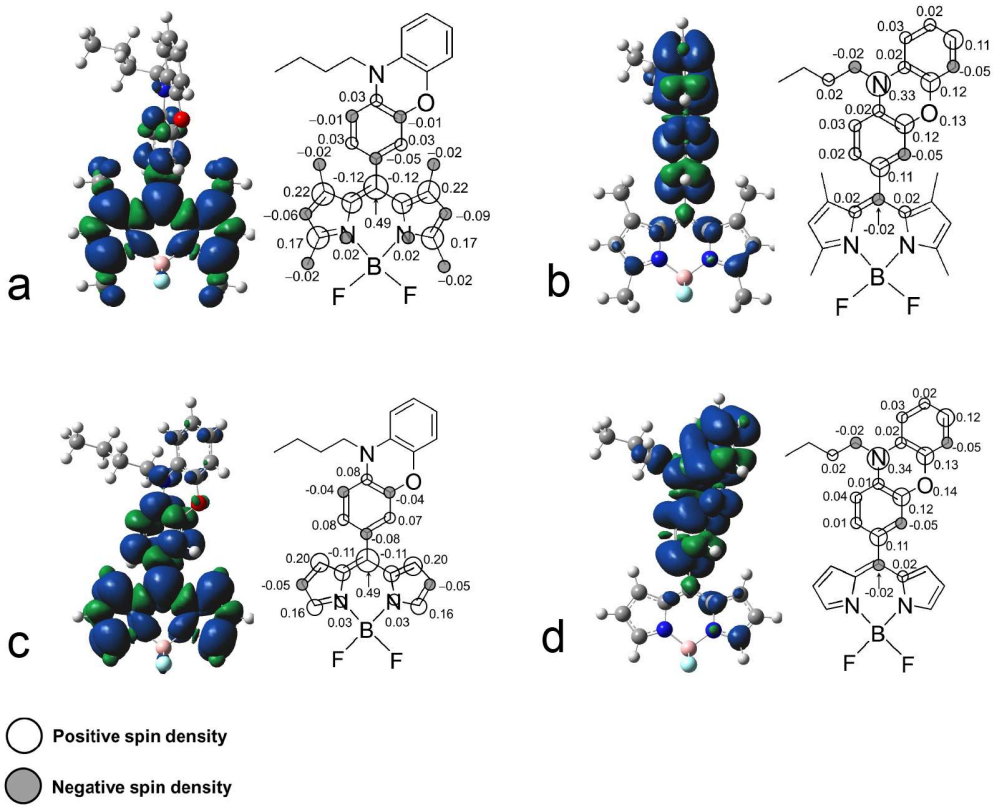

Figure S77. Isosurfaces of spin density of compounds at the optimized radical anion and radical cation geometries. Calculation was performed at B3LYP/6-31G(d) level with Gaussian 09W. The numbers in the figure indicate the contribution of each atom to the total spin density. **BDP-PXZ-1** (a) radical anion and (b) radical cation. **BDP-PXZ-2** (c) radical anion and (d) radical cation.

12.0 Photophysical Process Diagram.

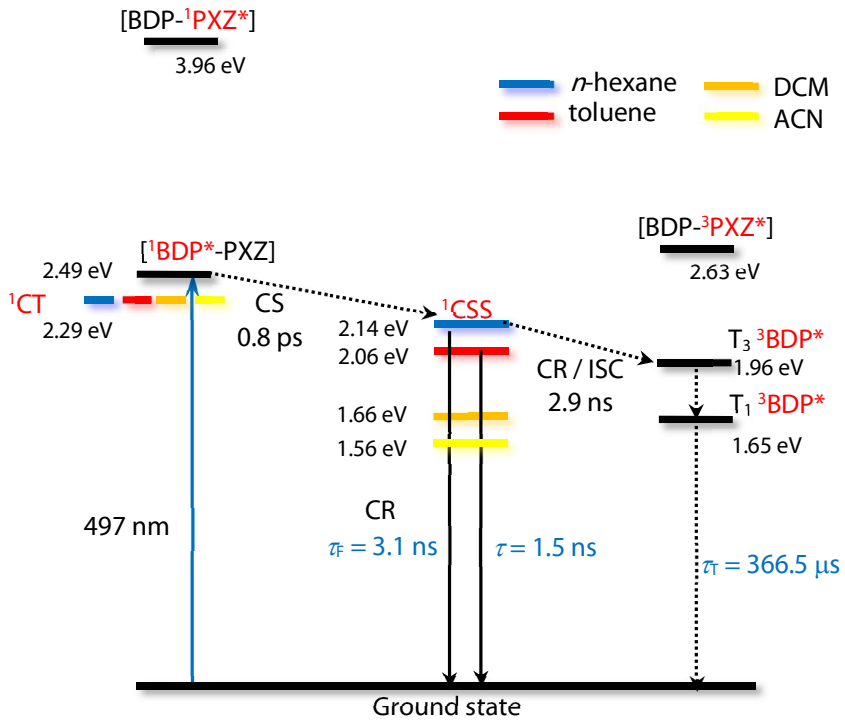

Figure S78. Photophysical processes of **BDP-PXZ-3**. ^{1}CT energy levels was determined by CT absorption band, ^{1}CSS energy levels were determined by electrochemical calculations. Triplet state lifetime is the intrinsic lifetime, obtained by fitting with kinetic model.

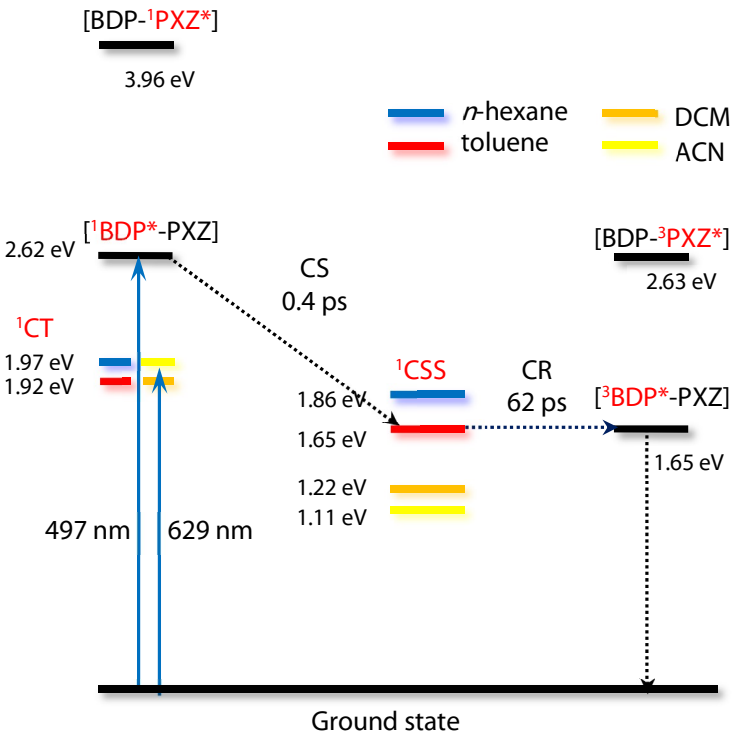

Figure S79. Photophysical processes of **BDP-PXZ-4**. ^{1}CT energy levels was determined by CT absorption band, ^{1}CSS energy levels were determined by electrochemical calculations.

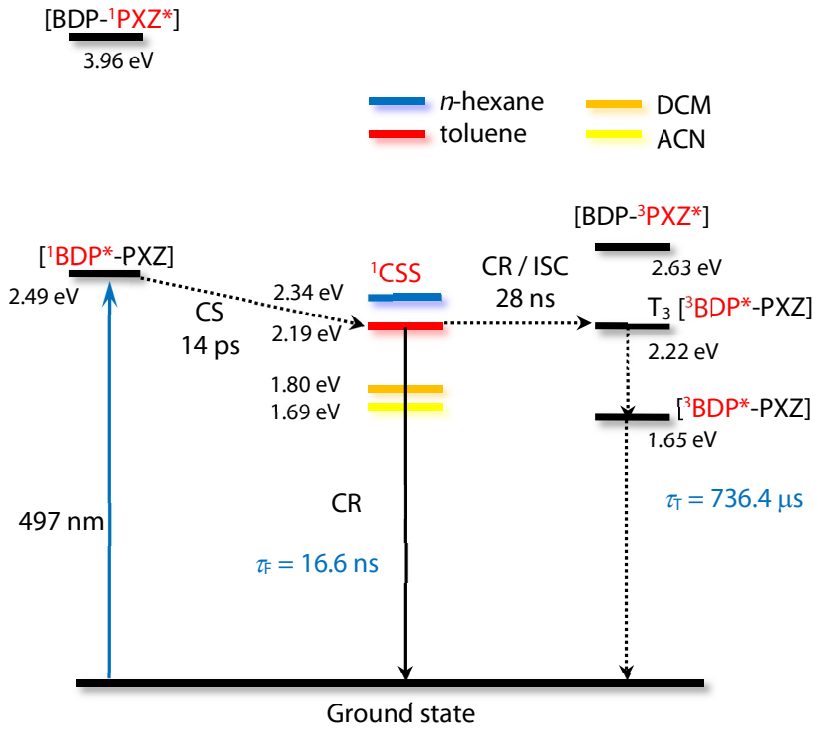

Figure S80. Photophysical processes of **BDP-PXZ-5**. ^{1}CSS energy levels were determined by electrochemical calculations. Triplet state lifetime is the intrinsic lifetime, obtained by fitting with kinetic model.

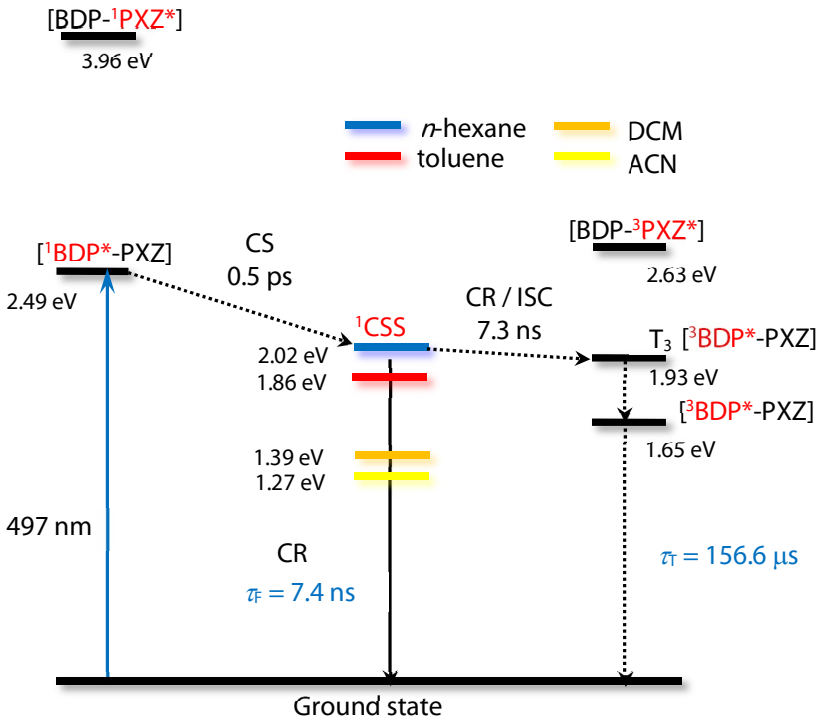

Figure S81. Photophysical processes of **BDP-PXZ-6**. ^{1}CSS energy levels were determined by electrochemical calculations. Triplet state lifetime is the intrinsic lifetime, obtained by fitting with kinetic model.

13.0 Coordinates of the Optimized Geometries of the Compounds.

BDP-PXZ-1

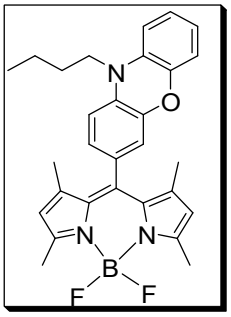

C	-4.20152800	2.17417100	1.55607400
C	-1.93252000	2.10626200	1.43985100
C	-2.49807200	1.04680300	0.65352700
C	-1.90562600	0.03266700	-0.11805500
C	-2.69079000	-0.92004600	-0.78839800
C	-2.34143500	-2.02523700	-1.63530400
C	-4.60032600	-1.88720100	-1.42415600
N	-3.89158000	1.13232600	0.76081500
N	-4.08702000	-0.87867800	-0.69401600
B	-4.92195800	0.17496000	0.09253500
F	-5.69173000	-0.45588500	1.06850100
F	-5.73820500	0.88687500	-0.78519500
C	-0.49309700	2.45946100	1.67529500
H	0.08256900	1.61319700	2.06405100
H	0.00867000	2.78386800	0.75692000
H	-0.42806400	3.27664100	2.40075000
C	-6.06968800	-2.13069600	-1.54081500
H	-6.26508600	-3.00854600	-2.16200000
H	-6.51324700	-2.28144700	-0.55107400
H	-6.56966900	-1.26029200	-1.97914800
C	-0.98803600	-2.50721700	-2.06822800
H	-0.38577300	-2.86205700	-1.22460800
H	-1.10041100	-3.33730300	-2.77293400
H	-0.40650300	-1.72011400	-2.55954500

C	-5.61033500	2.54672200	1.88542000
H	-6.11475200	1.72349100	2.40268200
H	-5.63300500	3.43692500	2.51928400
H	-6.18125900	2.73973600	0.97105300
C	-3.01030200	2.79201300	1.98800600
C	-3.54390700	-2.61013000	-2.01493600
H	-3.66196400	-3.47404300	-2.65682800
H	-2.95659700	3.65416900	2.64079500
C	-0.41678900	-0.03435100	-0.22345900
C	0.32103800	-0.85342700	0.64622400
C	1.70153500	-0.92345700	0.54786400
C	2.41504100	-0.17727300	-0.41376800
C	1.66919900	0.64779500	-1.26623600
C	0.27455700	0.71208200	-1.17648200
C	4.47510000	-0.93481300	0.59392000
C	3.71870600	-1.66456300	1.53131100
C	4.31573500	-2.32017100	2.59640900
H	3.67888900	-2.86905300	3.28298100
C	5.70450800	-2.27623400	2.75630900
C	6.47076900	-1.55729600	1.84602400
C	5.86261500	-0.88481600	0.78000700
H	2.17001900	1.25520200	-2.01040500
H	-0.27177600	1.35796500	-1.85748000
H	6.17055300	-2.79757800	3.58663100
H	7.54997000	-1.50425200	1.95607200
H	6.48217200	-0.31702800	0.09605700
N	3.80950200	-0.30873800	-0.47776000

C	4.56445000	0.30482800	-1.56492600
C	4.97617400	1.76759100	-1.32666600
H	3.96068100	0.22708800	-2.47589700
H	5.45199300	-0.31215900	-1.74206700
C	5.76472600	2.35016700	-2.50655200
H	4.07854700	2.37284900	-1.14443800
H	5.57612600	1.83126000	-0.40966800
C	6.17942100	3.80865000	-2.28770600
H	6.66053400	1.73788100	-2.68447400
H	5.16026000	2.27501200	-3.42199400
H	6.74063900	4.19551000	-3.14542200
H	5.30321300	4.45236100	-2.14417300
H	6.81430800	3.91098900	-1.39940700
H	-0.17223800	-1.45429100	1.40379700
O	2.34591900	-1.78347100	1.41018400

Calculation Type = FREQ

Calculation Method = RB3LYP

Basis Set = 6-31G(d)

Charge = 0

Spin = Singlet

E(RB3LYP) = –1587.38105579 a.u.

RMS Gradient Norm = 0.00000365 a.u.

Imaginary Freq = 0

Dipole Moment = 6.5666 Debye

Point Group = C1

BDP-PXZ-2

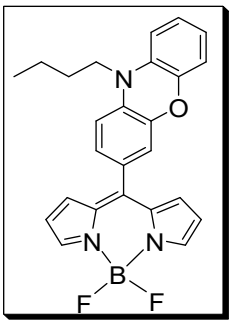

C	-4.72036100	2.28942100	1.39006700
C	-2.47921100	2.25387900	1.29044700
C	-3.00856200	1.14773500	0.57272000
C	-2.36555600	0.06405300	-0.06122700
C	-3.13417900	-1.00760500	-0.56025800
C	-2.75688200	-2.19617900	-1.24107000
C	-4.98651800	-2.13901500	-0.99789400
N	-4.39701500	1.20747200	0.66549200
N	-4.52321400	-1.01050800	-0.43949700
B	-5.40814700	0.19144100	0.03792400
F	-6.31597300	-0.22447100	0.99345800
F	-6.04377600	0.76067700	-1.05238900
C	-3.55717800	2.97232100	1.79384100
C	-3.92091800	-2.90866200	-1.50254200
H	-4.00875800	-3.86472100	-2.00004100
H	-3.52607600	3.86931000	2.39697200
C	-0.89492900	0.05472500	-0.18163700
C	-0.13623200	-1.07245300	0.19415300
C	1.24015300	-1.07515100	0.06628700
C	1.94234800	0.03958900	-0.44365000
C	1.18216400	1.16151400	-0.80747800
C	-0.20636400	1.16928400	-0.67801000
C	4.01499300	-1.08681100	0.06833800
C	3.27271800	-2.17290600	0.56979100
C	3.88744300	-3.24719400	1.19383100

H	3.26175300	-4.05632900	1.55695400
C	5.27873100	-3.27459300	1.33035800
C	6.03107500	-2.20938100	0.84806600
C	5.40573100	-1.12084900	0.23043300
H	1.67045700	2.04556200	-1.19855200
H	-0.76187200	2.04485200	-0.99619300
H	5.75832900	-4.12070400	1.81245800
H	7.11212900	-2.20776300	0.95128200
H	6.01471400	-0.29587700	-0.11941700
N	3.33126100	-0.03191600	-0.57154800
C	4.07321000	1.04064200	-1.22933000
C	4.47527200	2.20422400	-0.30782600
H	3.46163400	1.40901500	-2.05958600
H	4.96150100	0.59576400	-1.68936300
C	5.24255300	3.30234100	-1.05574300
H	3.57409700	2.62875100	0.15368000
H	5.08648100	1.81857400	0.51818800
C	5.64999800	4.46877500	-0.14990800
H	6.13990700	2.86904300	-1.52043200
H	4.62491900	3.67957700	-1.88336700
H	6.19564400	5.23542800	-0.71083500
H	4.77167500	4.94638600	0.30063700
H	6.29737400	4.12829300	0.66706100
H	-0.61277800	-1.95222700	0.61168300
O	1.89828000	-2.22813700	0.43486400
H	-6.04956600	-2.33801900	-1.02527800
H	-1.74733600	-2.47465500	-1.50620100

H	-1.42883000	2.46131800	1.43500000
H	-5.75737200	2.51891600	1.59551700

Calculation Type = FREQ

Calculation Method = RB3LYP

Basis Set = 6-31G(d)

Charge = 0

Spin = Singlet

E(RB3LYP) = –1430.10311828 a.u.

RMS Gradient Norm = 0.00000265 a.u.

Imaginary Freq = 0

Dipole Moment = 8.3514 Debye

Point Group = C1

BDP-PXZ-3

C	1.07495700	-0.24996400	0.20668600
C	1.76567000	0.78253200	-0.45702300
C	3.13837700	0.91784800	-0.33844200
C	3.90871300	0.02110400	0.42824200
C	3.22386200	-1.01929200	1.06935200
C	1.83547400	-1.14295700	0.96992100
C	5.90715800	1.11633200	-0.37377800
C	5.09468100	1.99017900	-1.12408300
C	5.63925000	2.91270300	-2.00379900
H	4.96093300	3.56039400	-2.55037800
C	7.02651200	3.00142600	-2.15946000
C	7.84666100	2.14484100	-1.43431700

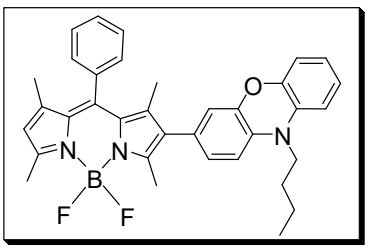

C	7.29356000	1.20512700	-0.55709700
H	3.76875900	-1.74556300	1.66073000
H	1.34125200	-1.94553400	1.50905600
H	7.44939700	3.73045900	-2.84378400
H	8.92617200	2.19086400	-1.54553100
H	7.95605500	0.53818600	-0.01839800
N	5.29603000	0.21893800	0.52093600
C	6.10263300	-0.59981300	1.41800600
C	6.59047000	-1.92938200	0.81762800
H	5.51085000	-0.78888200	2.32025800
H	6.95685700	0.00362500	1.74363500
C	7.43284900	-2.74378800	1.80789700
H	5.72373300	-2.51956600	0.49275200
H	7.17555200	-1.72485800	-0.08839300
C	7.92824400	-4.07019100	1.22287100
H	8.29430000	-2.14320500	2.13401100
H	6.84167400	-2.94152900	2.71372000
H	8.52683700	-4.62800700	1.95162100
H	7.08890700	-4.70845500	0.92159300
H	8.55166700	-3.90337200	0.33615700
H	1.23731900	1.49360100	-1.08359800
O	3.71940800	1.98651300	-0.99198800
C	-1.07835200	-1.56931300	-0.29917800
C	-1.36162800	0.59832300	0.33000000
C	-2.63317300	-0.01353700	0.07843300
C	-3.94754000	0.47690300	0.16517000
C	-5.05252500	-0.34648700	-0.11333100

C	-6.46489300	-0.08771500	-0.11859700
C	-6.06584300	-2.24885400	-0.69943600
N	-2.40229900	-1.33968800	-0.30249500
N	-4.86291200	-1.68425100	-0.47816600
B	-3.49196100	-2.39649300	-0.65926300
F	-3.34629400	-2.81002000	-1.98356000
F	-3.39533400	-3.48412400	0.20503600
C	-1.07445700	1.99264600	0.80694800
H	-1.25665400	2.74297700	0.02807900
H	-1.69970900	2.27066200	1.65995700
H	-0.02712800	2.07545500	1.10820000
C	-6.22413200	-3.67573800	-1.11279400
H	-7.28151800	-3.92326400	-1.23676200
H	-5.69716100	-3.86314300	-2.05444300
H	-5.78207100	-4.34518100	-0.36720500
C	-7.21039400	1.17916400	0.18455400
H	-6.86992800	2.01843700	-0.43061000
H	-8.27836300	1.03121900	-0.00453100
H	-7.09443400	1.48925900	1.22881000
C	-0.50556500	-2.89388700	-0.68887900
H	-0.97343600	-3.24791700	-1.61180300
H	0.57456900	-2.82028200	-0.82849900
H	-0.71441900	-3.64784900	0.07932600
C	-4.18353000	1.90024400	0.55772500
C	-4.45531600	2.23268100	1.89178300
C	-4.14273700	2.91792500	-0.40443100
C	-4.67827300	3.56101400	2.25754000

C	-4.37183800	4.24537900	-0.03824800
H	-3.93404600	2.66469900	-1.44035400
H	-4.88417900	3.80655000	3.29592600
H	-4.34017600	5.02551600	-0.79409400
C	-4.63861700	4.57009900	1.29311300
H	-4.48759300	1.44648600	2.64129500
C	-0.39147300	-0.38472100	0.08997500
C	-7.07077400	-1.28494300	-0.48275800
H	-4.81433400	5.60385800	1.57777200
H	-8.13427000	-1.45830300	-0.58868000

Calculation Type = FREQ

Calculation Method = RB3LYP

Basis Set = 6-31G(d)

Charge = 0

Spin = Singlet

E(RB3LYP) = –1818.43636894 a.u.

RMS Gradient Norm = 0.00000857 a.u.

Imaginary Freq = 0

Dipole Moment = 3.6752 Debye

Point Group = C1

BDP-PXZ-4

C	0.61353900	-0.48730600	0.16938200
C	1.24944100	0.75013100	-0.05131900
C	2.61948700	0.88310100	0.07589500
C	3.44413500	-0.21031900	0.41337400
C	2.81208700	-1.44510200	0.61097300

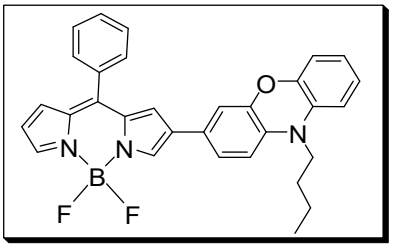

C	1.42689000	-1.57693900	0.50186000
C	5.37898500	1.19456700	0.07059100
C	4.51533700	2.25713600	-0.26257600
C	5.00177800	3.47357500	-0.71568700
H	4.28623100	4.25475800	-0.95249000
C	6.37984100	3.67512000	-0.84439900
C	7.25003800	2.63856300	-0.52681900
C	6.75564200	1.40735000	-0.08222500
H	3.39754800	-2.32253300	0.85808100
H	0.98346500	-2.54894800	0.69525700
H	6.75707400	4.63176700	-1.19241300
H	8.32349200	2.77086300	-0.62640400
H	7.45610400	0.61157900	0.14146000
N	4.82585200	-0.00849600	0.54580500
C	5.68544000	-1.07132500	1.05435000
C	6.20908500	-2.04852000	-0.01214400
H	5.12405300	-1.61626300	1.82092700
H	6.52403300	-0.59997800	1.57807600
C	7.10838400	-3.13660900	0.58741400
H	5.35825400	-2.51083200	-0.52932000
H	6.76151400	-1.48798000	-0.77740900
C	7.64113700	-4.11903200	-0.46065900
H	7.95337800	-2.66462400	1.10937600
H	6.54923300	-3.68990000	1.35576000
H	8.27783300	-4.88352200	-0.00168200
H	6.82037000	-4.63308400	-0.97512800
H	8.23671500	-3.60165100	-1.22239500

H	0.68149800	1.63125900	-0.33147700
O	3.14558700	2.14334800	-0.12301700
C	-1.56477500	-1.82619900	-0.12899900
C	-1.81148300	0.38846300	0.10912800
C	-3.08149200	-0.22182000	-0.04769500
C	-4.37979100	0.31430000	-0.00160200
C	-5.49753900	-0.53956500	-0.07253800
C	-6.88924300	-0.25590100	-0.07833400
C	-6.56638700	-2.47006900	-0.24659700
N	-2.87876900	-1.59514300	-0.18996300
N	-5.34326500	-1.92027300	-0.18477900
B	-3.99127000	-2.68752000	-0.37195000
F	-3.92644100	-3.22304800	-1.64524000
F	-3.84827100	-3.66258600	0.59690200
C	-4.56913700	1.77910900	0.13505900
C	-5.36683800	2.30703600	1.16480000
C	-3.95010100	2.66469600	-0.76376000
C	-5.53627500	3.68478100	1.29273400
C	-4.13188300	4.04116000	-0.63936000
H	-3.34631100	2.26548500	-1.57285500
H	-6.14531100	4.07798400	2.10204000
H	-3.65693500	4.71193200	-1.34996200
C	-4.92272800	4.55543300	0.38997700
H	-5.83084500	1.63265500	1.87776700
C	-0.84242000	-0.61626000	0.05513300
C	-7.55620600	-1.47121300	-0.17808300
H	-5.05935300	5.62877200	0.48866800

H	-8.62464900	-1.63503700	-0.20599700
H	-7.32714500	0.73041700	-0.02521700
H	-6.68009200	-3.54131000	-0.34659400
H	-1.64639400	1.44166200	0.28458200
H	-1.18609900	-2.83461700	-0.22840600

Calculation Type = FREQ

Calculation Method = RB3LYP

Basis Set = 6-31G(d)

Charge = 0

Spin = Singlet

E(RB3LYP) = –1661.16148022 a.u.

RMS Gradient Norm = 0.00000219 a.u.

Imaginary Freq = 0

Dipole Moment = 4.0653 Debye

Point Group = C1

BDP-PXZ-5

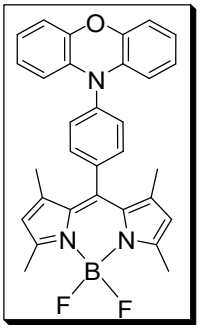

C	4.69267700	2.52669000	0.00005100
C	2.42050400	2.58516800	0.00027900
C	2.87924600	1.22413900	0.00019000
C	2.19076900	0.00002700	0.00030500
C	2.87919400	-1.22410800	0.00016400
C	2.42037900	-2.58510600	0.00042400
C	4.69255500	-2.52674900	-0.00028000
N	4.27898700	1.24539500	0.00006000
N	4.27893200	-1.24543200	-0.00023600

B	5.21551500	-0.00004000	-0.00065700
F	6.00853900	0.00010800	-1.14595400
F	6.00989200	-0.00022200	1.14371000
C	1.01957200	3.12401200	0.00043200
H	0.45116600	2.79996300	-0.87825300
H	0.45245400	2.80253300	0.88092500
H	1.04602600	4.21807400	-0.00114500
C	6.13663000	-2.90857100	-0.00062200
H	6.24547000	-3.99603400	-0.00099100
H	6.64304300	-2.49462000	-0.87904500
H	6.64331000	-2.49519900	0.87792200
C	1.01941100	-3.12385700	0.00107400
H	0.45156900	-2.80186300	-0.87875300
H	1.04579000	-4.21792100	0.00206100
H	0.45177100	-2.80024000	0.88042700
C	6.13677100	2.90843500	-0.00030100
H	6.64288100	2.49543300	-0.87935800
H	6.24567000	3.99589200	0.00045400
H	6.64371000	2.49405900	0.87760800
C	3.56459500	3.37328300	0.00021500
C	3.56442800	-3.37328400	0.00011100
H	3.59736800	-4.45541600	0.00024900
H	3.59759300	4.45541400	0.00019200
C	0.69508500	0.00003600	0.00045500
C	-0.01591300	-0.00117200	-1.20717600
C	-1.41094200	-0.00112900	-1.20818300
C	-2.11496000	0.00001400	0.00070400

C	-1.41072600	0.00115500	1.20945900
C	-0.01569000	0.00121000	1.20821400
H	-1.96226600	0.00199800	2.14491100
H	0.52738000	0.00211200	2.14915100
H	0.52699100	-0.00207900	-2.14821000
C	-5.76578900	3.60017000	-0.00077200
C	-6.40858800	2.35818500	-0.00124200
C	-5.66542500	1.18682600	-0.00076200
C	-4.25805500	1.21755500	0.00027800
C	-3.62725200	2.46613200	0.00070100
C	-4.37577500	3.64766700	0.00018000
C	-4.25804900	-1.21754600	0.00041200
C	-5.66541900	-1.18682400	-0.00066400
C	-6.40857400	-2.35818900	-0.00102100
H	-7.49103900	-2.27659100	-0.00187900
C	-5.76576700	-3.60017000	-0.00030800
C	-4.37575300	-3.64766000	0.00080300
C	-3.62723900	-2.46611900	0.00119500
H	-2.54421700	2.51430500	0.00142300
H	-3.85729600	4.60207100	0.00052200
H	-6.35361300	-4.51290500	-0.00061600
H	-3.85726900	-4.60206000	0.00140100
H	-2.54420300	-2.51428100	0.00210200
N	-3.54577700	0.00000500	0.00086300
H	-7.49105200	2.27657900	-0.00204000
O	-6.37185100	-0.00000100	-0.00144600
H	-1.96262700	-0.00198600	-2.14355000

H	-6.35363900	4.51290200	-0.00116200

Calculation Type = FREQ

Calculation Method = RB3LYP

Basis Set = 6-31G(d)

Charge = 0

Spin = Singlet

E(RB3LYP) = –1661.17447840 a.u.

RMS Gradient Norm = 0.00000209 a.u.

Imaginary Freq = 0

Dipole Moment = 1.7683 Debye

Point Group = C1

BDP-PXZ-6

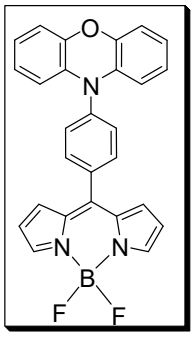

C	5.15525400	2.26163500	-1.13912500
C	2.91152100	2.30221700	-1.12147500
C	3.37653800	1.07890600	-0.56517900
C	2.67958500	0.00670100	0.01866000
C	3.38622300	-1.05257300	0.61423100
C	2.93313000	-2.24180000	1.24870400
C	5.17631500	-2.18022600	1.25972200
N	4.76980100	1.09954800	-0.59351600
N	4.78018600	-1.06064000	0.63804200
B	5.72450400	-0.03429700	-0.08173900
F	6.34877800	-0.64841000	-1.15151800
F	6.63844600	0.48652500	0.81270000
C	4.03053600	3.03825600	-1.48580400

C	4.05914800	-2.94132400	1.66045700
H	4.09189100	-3.88777600	2.18217600
H	4.05433900	4.02138300	-1.93517100
C	1.19558400	0.00373600	0.01727500
C	0.48355400	0.14329000	-1.18616900
C	-0.90960000	0.13958900	-1.19122400
C	-1.61886200	-0.00108900	0.00675800
C	-0.91796900	-0.13791600	1.21013000
C	0.47517800	-0.13611700	1.21562000
H	-1.47193800	-0.24018800	2.13831900
H	1.01187500	-0.22563200	2.15473200
H	1.02745600	0.23778600	-2.12069600
C	-5.28264400	3.44167800	1.01505400
C	-5.92010600	2.24800700	0.66333500
C	-5.17204500	1.12731400	0.33269200
C	-3.76504800	1.16138700	0.34686600
C	-3.13940000	2.36416500	0.69209200
C	-3.89274400	3.49427500	1.02575000
C	-3.75667500	-1.17250400	-0.35416100
C	-5.16383500	-1.14397000	-0.35514300
C	-5.90387400	-2.26689400	-0.69610200
H	-6.98649600	-2.18902900	-0.68148300
C	-5.25792200	-3.45740000	-1.04300300
C	-3.86778800	-3.50457800	-1.03857700
C	-3.12254600	-2.37216700	-0.69470500
H	-2.05675800	2.41789900	0.69958700
H	-3.37819300	4.41317800	1.29116100

H	-5.84326000	-4.33210000	-1.30923600
H	-3.34675400	-4.42095000	-1.30003600
H	-2.03969000	-2.42174200	-0.69052600
N	-3.04771700	-0.00452500	0.00155600
H	-7.00219300	2.16589100	0.63700700
O	-5.87410300	-0.01013000	-0.01359600
H	-1.45691000	0.24106500	-2.12343800
H	6.20650700	2.49133500	-1.25149100
H	1.87530900	2.59496600	-1.21327400
H	1.89971600	-2.53295400	1.37111800
H	6.22971100	-2.39447100	1.38223200
H	-5.87427200	4.31457000	1.27319700

Calculation Type = FREQ

Calculation Method = RB3LYP

Basis Set = 6-31G(d)

Charge = 0

Spin = Singlet

E(RB3LYP) = –1503.89452192 a.u.

RMS Gradient Norm = 0.00000198 a.u.

Imaginary Freq = 0

Dipole Moment = 2.9560 Debye

Point Group = C1

References:

(S1) Lee, W.; Yuk, S. B.; Choi, J.; Kim, H. J.; Kim, H. W.; Kim, S. H.; Kim, B.; Min, J. K.; Kim, J. P. The Effects of the Number of Anchoring Groups and *N*-Substitution on the Performance of Phenoxazine Dyes in Dye-Sensitized Solar Cells. *Dyes Pigments* **2014**, *102*, 13–21.

(S2) Mao, M.; Li, Q.-S.; Zhang, X.-L.; Wu, G.-H.; Dai, C.-G.; Ding, Y.; Dai, S.-Y.; Song, Q.-H. Effects of Donors of Bodipy Dyes on the Performance of Dye-Sensitized Solar Cells. *Dyes Pigments* **2017**, *141*, 148–160.

(S3) Wang, Z.; Zhao, J. Bodipy-Anthracene Dyads as Triplet Photosensitizers: Effect of Chromophore Orientation on Triplet-State Formation Efficiency and Application in Triplet-Triplet Annihilation Upconversion. *Org. Lett.* **2017**, *19*, 4492–4495.

(S4) Zhang, L.; Huang, X.; Zhen, S.; Zhao, J.; Li, H.; Yuan, B.; Yang, G. Pd-Catalyzed Double *N*-Arylation of Primary Amines to Synthesize Phenoxazines and Phenothiazines. *Org. Biomol. Chem.* **2017**, *15*, 6306–6309.

(S5) Cai, H; Du, M. Thermally Activated Delayed Fluorescent Material Based on Pyranypropyl Acetonitrile Derivative and Organic Light Emitting Device. CN107298676A, 2017 [*Chem. Abstr*. **2017**, *167*, 587030].

(S6) Wang, Z.; Sukhanov, A. A.; Toffoletti, A.; Sadiq, F.; Zhao, J.; Barbon, A.; Voronkova, V. K.; Dick, B. Insights into the Efficient Intersystem Crossing of Bodipy-Anthracene Compact Dyads with Steady-State and Time-Resolved Optical/Magnetic Spectroscopies and Observation of the Delayed Fluorescence. *J Phys Chem C* **2019**, *123*, 265–274.

The Complete Author List of Abbreviated References in the Main Text of Manuscript:

(12) Suzuki, S.; Matsumoto, Y.; Tsubamoto, M.; Sugimura, R.; Kozaki, M.; Kimoto, K.; Iwamura, M.; Nozaki, K.; Senju, N.; Uragami, C.; Hashimoto, H.; Muramatsu, Y.; Konno, A.; Okada, K. Photoinduced Electron Transfer of Platinum(II) Bipyridine Diacetylides Linked by Triphenylamine- and Naphthaleneimide-Derivatives and Their Application to Photoelectric Conversion Systems. *Phys. Chem. Chem. Phys.* **2013**, *15*, 8088–8094.

(50) Filatov, M. A.; Karuthedath, S.; Polestshuk, P. M.; Savoie, H.; Flanagan, K. J.; Sy, C.; Sitte, E.; Telitchko, M.; Laquai, F.; Boyle, R. W.; Senge, M. O. Generation of Triplet Excited States via Photoinduced Electron Transfer in meso-Anthra-BODIPY: Fluorogenic Response toward Singlet Oxygen in Solution and in Vitro. *J. Am. Chem. Soc.* **2017**, *139*, 6282–6285.

(61) Frisch, M. J.; Trucks, G. W.; Schlegel, H. B.; Scuseria, G. E.; Robb, M. A.; Cheeseman, J. R.; Scalmani, G.; Barone, V.; Mennucci, B.; Petersson, G. A.; Nakatsuji, H.; Caricato, M.; Li, X.; Hratchian, H. P.; Izmaylov, A. F.; Bloino, J.; Zheng, G.; Sonnenberg, J. L.; Hada, M.; Ehara, M.; Toyota, K.; Fukuda, R.; Hasegawa, J.; Ishida, M.; Nakajima, T.; Honda, Y.; Kitao, O.; Nakai, H.; Vreven, T.; Montgomery, J. A., Jr.; Peralta, J. E.; Ogliaro, F.; Bearpark, M.; Heyd, J. J.; Brothers, E.; Kudin, K. N.; Staroverov, V. N.; Kobayashi, R.; Normand, J.; Raghavachari, K.; Rendell, A.; Burant, J. C.; Iyengar, S. S.; Tomasi, J.; Cossi, M.; Rega, N.; Millam, J. M.; Klene, M.; Knox, J. E.; Cross, J. B.; Bakken, V.; Adamo, C.; Jaramillo, J.; Gomperts, R.; Stratmann, R. E.; Yazyev, O.; Austin, A. J.; Cammi, R.; Pomelli, C.; Ochterski, J. W.; Martin, R. L.; Morokuma, K.; Zakrzewski, V. G.; Voth, G. A.; Salvador, P.; Dannenberg, J. J.; Dapprich, S.; Daniels, A. D.; Farkas, Ö .; Foresman, J. B.; Ortiz, J. V.; Cioslowski, J.; Fox, D. J. *Gaussian 09W* (Revision A.1), Gaussian Inc.: Wallingford, CT, **2009**.

(75) Akasaka, T.; Nakata, A.; Rudolf, M.; Wang, W.-W.; Yamada, M.; Suzuki, M.; Maeda, Y.; Aoyama, R.; Tsuchiya, T.; Nagase, S.; Guldi, D. M. Synthesis and Photoinduced Electron-Transfer Reactions in a $La_2@I_h$-C_{80}–Phenoxazine Conjugate. *ChemPlusChem* **2017***, 82,* 1067−1072.